

Anacostia Sediment Models:

Phase 3 Anacostia HSPF Watershed Model

and

Version 3 TAM/WASP Water Clarity Model

**Cherie Schultz
Sunghee Kim
Ross Mandel
Andrea Nagel**

**Interstate Commission on the Potomac River Basin
51 Monroe Street, Suite PE-08
Rockville, MD 20850**

March 2007

ICPRB Report 07-10

TABLE OF CONTENTS

| | | |
|-------|--|----|
| 1 | INTRODUCTION | 1 |
| 1.1 | Background | 1 |
| 1.2 | Setting | 1 |
| 1.3 | Water quality parameters | 2 |
| 1.4 | Hydrologic conditions | 3 |
| 2 | PHASE 3 ANACOSTIA HSPF WATERSHED MODEL | 6 |
| 2.1 | General Overview of the HSPF Model | 6 |
| 2.2 | Segmentation | 7 |
| 2.3 | Model Land Use | 8 |
| 2.3.1 | Original Sources of Land Use Data | 8 |
| 2.3.2 | Determination of Impervious Area | 14 |
| 2.3.3 | Effective Impervious Area | 14 |
| 2.4 | Hydrology Calibration | 14 |
| 2.4.1 | Meteorological Input Data | 15 |
| 2.4.2 | Calibration Methodology | 15 |
| 2.4.3 | Hydrology Calibration Results | 16 |
| 2.5 | Sediment Calibration | 27 |
| 2.5.1 | Edge-of-Field and Edge-of-Stream Calibration Targets and Calibration Results | 27 |
| 2.5.2 | Streambank Erosion Targets and Calibration Results | 33 |
| 3 | VERSION 3 TAM/WASP TIDAL WATER CLARITY MODEL | 46 |
| 3.1 | Overview | 46 |
| 3.2 | Model inputs | 50 |
| 3.2.1 | Model geometry | 50 |
| 3.2.2 | Tide data | 53 |
| 3.2.3 | Tributary, separate storm sewer system, and CSO flows | 54 |
| 3.2.4 | Sediment load inputs | 58 |
| 3.2.5 | Load inputs to the TAM/WASP eutrophication model | 61 |
| 3.3 | Data Support for model calibration | 61 |
| 3.3.1 | Sediment transport model | 61 |
| 3.3.2 | Eutrophication model | 63 |
| 3.3.3 | Characterization of water clarity in the tidal Anacostia | 63 |
| 3.4 | Description of TAM/WASP water quality model components | 66 |
| 3.4.1 | Sediment transport model | 67 |
| 3.4.2 | Eutrophication model | 70 |
| 3.5 | Water clarity model calibration/verification | 73 |
| 3.5.1 | Sediment transport component: configuration and input parameters | 73 |
| 3.5.2 | Sediment transport component: calibration | 73 |
| 3.5.3 | Eutrophication component: configuration and input parameters | 84 |
| 3.5.4 | Eutrophication component: calibration/verification | 84 |
| 4 | CONCLUSIONS | 93 |
| 5 | REFERENCES | 94 |

Appendix A – ESTIMATOR Results

TABLES

| | |
|--|----|
| Table 1-1. Summary statistics for Anacostia basin hydrology, with probabilities of exceedances | 5 |
| Table 2-1. Phase III HSPF Model Land Use Acreage By Segment (acres) | 9 |
| Table 2-2. Model Classification for Maryland's Land Use | 10 |
| Table 2-3. Crop Acres at Beltsville Agricultural Research Center..... | 10 |
| Table 2-4. Model Classification for District of Columbia's Land Use..... | 11 |
| Table 2-5. Key Hydrology Calibration Parameters | 17 |
| Table 2-6. Ratio of Cropland Parameters to Those for Other Land Uses..... | 17 |
| Table 2-7. Monthly Hydrology Parameters | 17 |
| Table 2-8. Hydrology Calibration Parameter Values | 18 |
| Table 2-9. Hydrology Calibration Results | 18 |
| Table 2-10. Edge-of-Field Erosion Yield Targets (tons/acre/year) | 29 |
| Table 2-11. Sediment Delivery Ratios (SDR) and Segment Physiographic Provinces | 29 |
| Table 2-12. Calibration Target EOS TSS Concentrations for Developed Land Uses | 29 |
| Table 2-13. Urban BMP Types and Efficiencies | 30 |
| Table 2-14. BMP Acres By Segment and Land Use | 31 |
| Table 2-15. Sediment BMP Reduction By Segment and Land Use | 32 |
| Table 2-16. Calibrated Sediment Removal Rates (tons/inches/hour) By Segment and Land Use | 32 |
| Table 2-17. Watershed Factors Used in the AVGWLF Streambank Erosion Algorithm..... | 39 |
| Table 2-18. AVGWLF Streambank Erosion Rates and HSPF Subwatershed Erosion Targets .. | 40 |
| Table 2-19. Scour Calibration Parameters | 40 |
| Table 2-20. Comparison of Average Annual TSS Load Estimates from Anacostia Models (tons/yr)..... | 41 |
| Table 3-1. Sediment transport model geometry..... | 52 |
| Table 3-2. Vertical datum for NOAA tide station, 8594900, located in the Washington Shipping Channel | 53 |
| Table 3-3. Sub-basins of the tidal drainage area of the Anacostia Watershed | 55 |
| Table 3-4. Mean annual and growing season sediment loads by tributary and land use (1995-1997) | 59 |
| Table 3-5. Mean annual sediment loads for TAM/WASP Version 3 | 61 |
| Table 3-6. Main channel water quality data sets - solids and water clarity-related parameter values | 62 |
| Table 3-7. Calibration values of parameters governing erosion and depostion of cohesive sediments..... | 76 |
| Table 3-8. TAM/WASP Version 3 eutrophication component parameter values | 86 |

FIGURES

| | |
|---|----|
| Figure 1-1. Anacostia watershed..... | 4 |
| Figure 2-1. Model Segmentation and USGS Gages | 12 |
| Figure 2-2. Aggregated Land Use in the Anacostia Watershed..... | 13 |
| Figure 2-3. Time Series. Simulated and Observed Daily Average Flow. Northeast Branch. | 19 |
| Figure 2-4. Scatter Plot. Simulated and Observed Daily Average Flow. Northeast Branch | 19 |
| Figure 2-5. Cumulative Distribution Function. Simulated and Observed Daily Average Flow. Northeast Branch | 20 |
| Figure 2-6. Scatter Plot. Simulated and Observed Monthly Average Flow, Northeast Branch. . | 20 |
| Figure 2-7. Time Series. Simulated and Observed Daily Average Flow. Northwest Branch at Riverdale. | 21 |
| Figure 2-8. Scatter Plot. Simulated and Observed Daily Average Flow. Northwest Branch at Riverdale | 21 |
| Figure 2-9. Cumulative Distribution Function. Simulated and Observed Daily Average Flow. Northwest Branch at Riverdale. | 22 |
| Figure 2-10. Scatter Plot. Simulated and Observed Monthly Average Flow. Northwest Branch at Riverdale. | 22 |
| Figure 2-11. Time Series. Simulated and Observed Daily Average Flow. Watts Branch..... | 23 |
| Figure 2-12. Scatter Plot. Simulated and Observed Daily Average Flow. Watts Branch | 23 |
| Figure 2-13. Cumulative Distribution Function. Simulated and Observed Daily Average Flow. Watts Branch..... | 24 |
| Figure 2-14. Scatter Plot. Simulated and Observed Monthly Average Flow. Watts Branch. | 24 |
| Figure 2-15. Time Series. Simulated and Observed Daily Average Flow. Northwest Branch at Colesville | 25 |
| Figure 2-16. Scatter Plot. Simulated and Observed Daily Average Flow. Northwest Branch at Colesville | 25 |
| Figure 2-17. Cumulative Distribution Function. Simulated and Observed Daily Average Flow. Northwest Branch at Colesville | 26 |
| Figure 2-18. Scatter Plot. Simulated and Observed Monthly Average Flow. Northwest Branch at Colesville. | 26 |
| Figure 2-19. Time Series. ESTIMATOR and HSPF Monthly TSS Load. Northeast Branch. ... | 42 |
| Figure 2-20. Time Series. ESTIMATOR and HSPF Monthly TSS Load. Northwest Branch ... | 42 |
| Figure 2-21. Scatter Plot. ESTIMATOR and HSPF Monthly TSS Load. Northeast Branch. | 43 |
| Figure 2-22. Scatter Plot. ESTIMATOR and HSPF Monthly TSS Load. Northwest Branch. ... | 43 |
| Figure 2-23. Cumulative Distribution Function. ESTIMATOR and HSPF Monthly TSS Load. Northeast Branch. | 44 |
| Figure 2-24. Cumulative Distribution Function. ESTIMATOR and HSPF Monthly TSS Load. Northwest Branch. | 44 |
| Figure 2-25. Observed and Simulated Daily Maximum TSS Concentrations, Lower Beaverdam Creek | 45 |
| Figure 3-1. Schematic diagram of TAM/WASP water clarity model components | 48 |
| Figure 3-2. TAM/WASP V3 segmentation, with locations of main routine monitoring stations | 49 |
| Figure 3-3. Schematic diagram of sediment transport model geometry..... | 51 |
| Figure 3-4. Long-term Growing Season Medians of Water Quality Parameters in the Tidal Anacostia River..... | 64 |

| | |
|---|----|
| Figure 3-5. Long-term Growing Season Medians of Secchi Depth in the Tidal Anacostia River..... | 65 |
| Figure 3-6. Conceptual model of impact of suspended sediment/algae interaction..... | 66 |
| Figure 3-7. Daily TSS predictions versus observations at segments 1, 2, and 8 | 77 |
| Figure 3-8. Daily TSS predictions versus observations at segments 16, 23, and 30 | 78 |
| Figure 3-9. Cumulative distribution functions for predicted and observed TSS values..... | 79 |
| Figure 3-10. Longitudinal profiles of predicted (calibration run) and observed TSS values | 80 |
| Figure 3-11. Longitudinal profiles of predicted TSS percentile values for calibration and "no erosion" run..... | 81 |
| Figure 3-12. Longitudinal profiles of predicted TSS percentile values for calibration and "no erosion" run..... | 82 |
| Figure 3-13. Longitudinal profiles of predicted TSS percentile values for calibration and "no loads" runs..... | 83 |
| Figure 3-14. Predicted vs. observed concentrations at segment 2 (ANA0082 - Bladensburg Rd)..... | 87 |
| Figure 3-15. Predicted vs. observed concentrations at segment 8 (ANA01 - New York Ave).... | 88 |
| Figure 3-16. Predicted vs. observed concentrations at segment 16 (ANA08 - Benning Rd)..... | 89 |
| Figure 3-17. Predicted vs. observed concentrations at segment 23 (ANA14 - Pennsylvania Ave)..... | 90 |
| Figure 3-18. Predicted vs. observed concentrations at segment 30 (ANA24 - South Capitol St)..... | 91 |
| Figure 3-19. Longitudinal profiles of predicted and observed median Secchi depths..... | 92 |

ACKNOWLEDGEMENTS

The authors would like to thank the following persons who provided data and other information used in model development and model calibration: Brenda Majedi of the U.S. Geological Survey – MD-DE-DC Water Science Center; Meo Curtis and Keith Van Ness of the Montgomery County Department of Environmental Protection; Dr. M. Cheng, Dawn Hawkins-Nixon, Sharon Meigs, and Donna Wilson, Director, Prince George’s County Department of Environmental Resources. The authors would also like to thank Nauth Panday, Miao-Li Chang, Lee Currey, and Tom Thornton of the Maryland Department of Environment for their valuable input and assistance, and for their encouragement and patience throughout this project.

The opinions expressed in this report are those of the authors and should not be construed as representing the several states of the signatories or Commissioners to the Interstate Commission on the Potomac River Basin: Maryland, Pennsylvania, Virginia, West Virginia, or the District of Columbia.

Funding for this project was provided by the Maryland Department of the Environment and the signatories to the Interstate Commission on the Potomac River Basin.

1 INTRODUCTION

1.1 Background

This study was undertaken to support the Maryland Department of Environment (MDE) in their determination of Total Maximum Daily Load (TMDL) allocations for sediment in the Anacostia River watershed. The Anacostia is an interstate watershed, and includes portions of the District of Columbia, and Montgomery County and Prince George's County in Maryland (see Figure 1-1). The Anacostia River is actually a freshwater estuary. Its four largest tributaries are the Northeast Branch (NEB), the Northwest Branch (NWB), Lower Beaverdam Creek (LBC), and Watts Branch. Waters in the Maryland portion of the Anacostia watershed were identified as impaired due to sediment in 1996, with the publication of Maryland's 1996 303(d) list. The District of Columbia's portion of the tidal river, along with the Watts Branch tributary, were also designated as impaired due to sediment on the District's 1996 303(d) list.

This report describes the construction and calibration of two computer models which simulate water quality conditions related to sediment in the Anacostia and its tributaries. The Phase 3 Anacostia HSPF watershed model of the non-tidal tributaries simulates loads of sediment from land surface areas, erosion of sediment from stream channels, and transport of sediment by non-tidal streams. The TAM/WASP Version 3 water clarity model of the tidal river simulates the transport of suspended sediment by the river's current, sediment settling and re-suspension, light conditions, and the growth of algae. These models can be used together to simulate the existing daily sediment loads entering the tidal river and their impact on daily water clarity conditions. The TAM/WASP model can be also used to predict changes in water clarity due to hypothetical sediment load reduction scenarios.

The models described in this report are upgraded versions of those used in previous studies of the Anacostia River watershed. These most recent versions take advantage of an extensive new set of NEB and NWB automated sampler data collected by the U.S. Geological Survey (USGS) in 2003 and 2004, with funding from MDE and Prince George's County. The previous version of the TAM/WASP sediment transport model, Version 2, was used by the U.S. Environmental Protection Agency (USEPA) Region 3 to compute TMDL allocations for sediment for the Anacostia (USEPA, 2002a). Version 2 of the TAM/WASP water clarity model (consisting of the sediment transport model coupled to the eutrophication model) was used by the DC Department of Health (DCDOH) in its draft TMDL for sediment in the Anacostia River (DCDOH, 2002). The previous version of the Anacostia HSPF model, Phase 2 (Mandel *et al.*, 2003), was constructed for MDE to estimate sediment loads to the tidal river from the NEB and NWB tributaries.

1.2 Setting

The Anacostia River watershed covers an area of approximately 174 square miles (mi²), with 17% of the watershed lying within the boundaries of District of Columbia, and 83% in the State of Maryland. The main channel of the Anacostia River begins in Bladensburg, Maryland, at the confluence of its two largest tributaries, the Northeast Branch and the Northwest Branch, and flows a distance of approximately 8.4 miles before it discharges into the Potomac River in

Washington, DC (see Figure 1-1). The drainage areas of the Northeast and Northwest Branch tributaries, 53 mi² and 72 mi², respectively, comprise approximately 72% of the total area of the watershed.

Because of its location in the Washington metropolitan area, the majority of the watershed is highly urbanized, with a population of 804,500 in 1990 and a projected population of 838,100 by the year 2010 (Warner *et al.*, 1997). Land use in the watershed is approximately 75% urban, 5% agricultural, and 20% forest or wetlands, with 23% of the area of the watershed covered by impervious surfaces.

The Anacostia River is actually an estuary, with tidal influence extending some distance into the Northeast and the Northwest Branch tributaries. The variation in the river's water surface elevation over a tidal cycle is approximately 3 feet. However, water in the tidal portion of the river is fresh, with negligible values of salinity. From an analysis by the National Oceanographic and Atmospheric Administration (NOAA) of sounding data taken by the US Army Corps of Engineers prior to a 1999 dredging project combined with additional bathymetry data taken by the Navy in the summer of 2000, the volume of the tidal portion of the river at mean tide is approximately 10,000,000 cubic meters (m³), with a surface area of approximately 3,300,000 square meters (m²). The width of the river varies from approximately 60 meters (m) in some upstream reaches to approximately 500 m near the confluence with the Potomac, and average depths across channel transects vary from approximately 1.2 m upstream of Bladensburg to about 5.6 m just downstream of the South Capital Street Bridge. During non-storm conditions, measured flow velocities during the tidal cycle have been in the range of 0 to 0.3 m/sec (Katz *et al.*, 2000; Schultz and Velinsky, 2001).

1.3 Water quality parameters

Water quality data related to sediment and water clarity for Anacostia non-tidal tributaries and for the tidal river are available from a variety of monitoring programs and special studies, described in Appendix A and in Section 3.3 of this report. Data are available for the following water quality parameters used in this study: total suspended solids (TSS), suspended sediment concentration (SSC), chlorophyll *a* (Chla), and Secchi depth. TSS and SSC are two measures of the dry weight of particulate matter suspended in the water column, per unit volume of water, based on two different laboratory analytical methods (see Appendix A). Both parameters are generally reported in units of milligrams per liter (mg/L). The Chla concentration of a water sample, typically reported in units of micrograms per liter (µg/L), is a measure of the amount of phytoplankton, that is, algae, which is present. Phytoplankton concentrations (PHYT), given in units of mg C/L, are assumed to be related to Chla concentration by a simple multiplicative constant, the "carbon-chlorophyll ratio", Θ_c . Secchi depth is a simple measure of water clarity based on the visibility of a "Secchi disk", an eight-inch diameter disk with black and white quadrants. Secchi depth, usually reported in units of meters (m), is defined as the depth at which a submerged Secchi disk is no longer visible. Data are also available for a fourth water quality parameter, turbidity, a commonly available measure of water clarity that can be correlated with TSS and the inverse of Secchi depth. At the time this report was prepared, routine monitoring data for the tidal Anacostia were available through 2002.

Data are also available for a number of other secondary constituents used in the TAM/WASP water clarity model, including dissolved oxygen (DO), biochemical oxygen demand (BOD), ammonia (NH₃), nitrate + nitrite (NO₃), organic nitrogen (ON), and total phosphorus (TP).

1.4 Hydrologic conditions

The primary study period is 1995 through 2004, the most recent ten-year time period for which data were available at the time this project was initiated. The Phase 3 Anacostia HSPF watershed model was calibrated for this ten-year study period. The TAM/WASP, Version 3, water clarity model was calibrated for the eight year time period, 1995 through 2002, where 2002 was the latest year for which tidal Anacostia water column data were available at the time this study was initiated. Because pollutant loads can vary dramatically depending on hydrologic conditions, Table 1-1 provides a comparison of several summary statistics for Anacostia basin hydrology, for the years 1963 through 2004. This table gives annual total precipitation, annual mean upstream flow (from the sum of annual NEB and NWB flows), and growing season mean upstream flow (where the growing season is defined here to be the seven-month time period, April 1 through October 31, consistent with DC water quality standards, applicable to most portions of the tidal river). Annual values were computed for the calendar year, January 1 through December 31. The table also gives percentile values, as probabilities of exceedance, where the percentiles for annual precipitation were computed from available annual totals for Washington, DC from the National Climatic Data Center for the available period of record, 1963 through 2005. Percentiles for flow were computed from USGS gage data for the available period of record, 1939 through 2004. Comparisons of estimated annual sediment loads for these two time periods are given in Section 3.2 of this report.

The study period represents a wide range of hydrologic conditions. The years 1996 and 2003 were extremely wet, with 2003 having the highest combined upstream tributary flow for the period of record, 1939-2004. The time period, 1998-2002, was a period of prolonged drought throughout the eastern portion of the United States. A significant hydrologic event, Hurricane Floyd, occurred on September 16, 1999.

The three-year time period, 1995 through 1997, is used in this study to compute baseline sediment loads by drainage area and by landuse type. This time period was chosen to represent a range of hydrologic conditions, containing a reasonably average year, 1995, a very wet year, 1996, and a somewhat dry year, 1997. For Version 2 of the TAM/WASP models (Mandel and Schultz, 2000; Schultz, 2003), used to support the District of Columbia's TMDL for sediment in the tidal Anacostia River (DCDOH, 2002; USEPA, 2002a; 2002b) the three year time period, 1988-1990, was used for model calibration and for computing baseline loads.

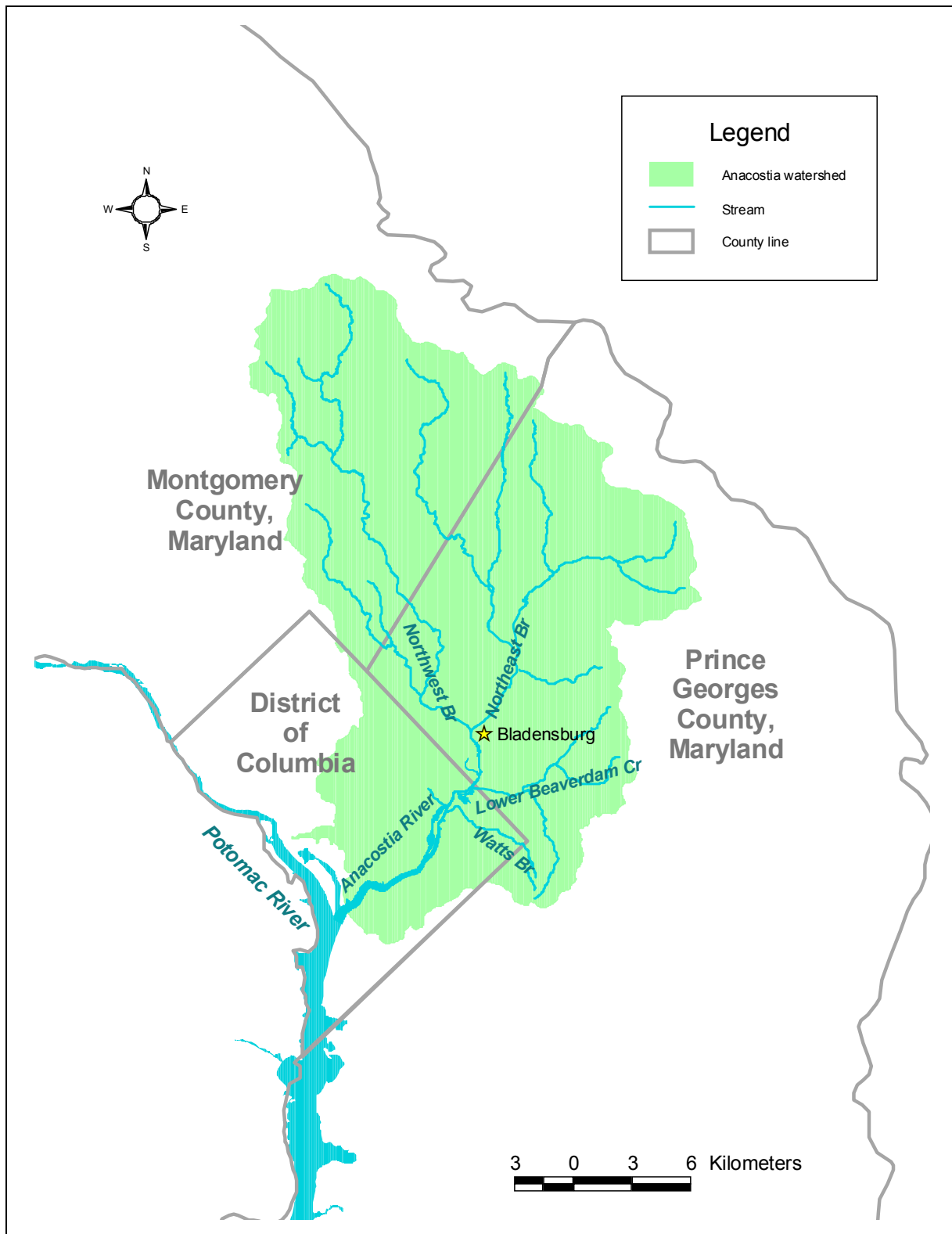


Figure 1-1. Anacostia watershed

Table 1-1. Summary statistics for Anacostia basin hydrology, with probabilities of exceedances

| Calendar Year | Annual Precipitation, Washington, DC ¹ (in) | Annual Precipitation, Washington, DC (%) | Annual Mean Combined (NEB+NWB) Flow (cfs) | Annual Mean Combined (NEB+NWB) Flow (%) | Growing Season Mean (NEB+NWB) Flow (cfs) | Growing Season Mean (NEB+NWB) Flow (%) |
|---------------|--|--|---|---|--|--|
| 2004 | 39.1 | 50.0% | 165.7 | 21.6% | 165.2 | 15.4% |
| 2003 | 64.8 | 0.0% | 303.2 | 0.0% | 302.9 | 0.0% |
| 2002 | 38.4 | 62.0% | 93.6 | 89.3% | 75.6 | 80.0% |
| 2001 | 35.0 | 85.8% | 111.2 | 66.2% | 117.9 | 41.6% |
| 2000 | 36.0 | 78.6% | 130 | 44.7% | 118.7 | 38.5% |
| 1999 | 43.6 | 33.4% | 128.9 | 49.3% | 119.9 | 35.4% |
| 1998 | 37.4 | 71.5% | 159.2 | 26.2% | 102.2 | 60.0% |
| 1997 | 36.5 | 73.9% | 139.7 | 33.9% | 98.2 | 61.6% |
| 1996 | 58.1 | 4.8% | 240.7 | 4.7% | 196.9 | 7.7% |
| 1995 | 40.2 | 40.5% | 126.6 | 50.8% | 103.0 | 58.5% |
| 1994 | 44.3 | 28.6% | 170.7 | 20.0% | 116.5 | 44.7% |
| 1993 | 47.0 | 12.0% | 184.6 | 13.9% | 114.1 | 49.3% |
| 1992 | 44.4 | 23.9% | 133.8 | 37.0% | 115.1 | 47.7% |
| 1991 | 34.0 | 88.1% | 108.1 | 69.3% | 72.9 | 83.1% |
| 1990 | 45.3 | 21.5% | 153.6 | 29.3% | 150.2 | 20.0% |
| 1989 | 44.3 | 26.2% | 178.3 | 17.0% | 206.0 | 6.2% |
| 1988 | 39.8 | 45.3% | 116.3 | 60.0% | 97.4 | 63.1% |
| 1987 | 40.8 | 38.1% | 118.4 | 55.4% | 105.7 | 55.4% |
| 1986 | 30.4 | 97.7% | 97.3 | 83.1% | 59.7 | 95.4% |
| 1985 | 32.9 | 92.9% | 93.9 | 87.7% | 75.3 | 81.6% |
| 1984 | 44.1 | 31.0% | 152.4 | 30.8% | 127.2 | 30.8% |
| 1983 | 46.2 | 16.7% | 199.6 | 9.3% | 185.0 | 10.8% |
| 1982 | 38.6 | 57.2% | 100.8 | 78.5% | 85.7 | 69.3% |
| 1981 | 32.1 | 95.3% | 76.1 | 97.0% | 80.2 | 73.9% |
| 1980 | 33.8 | 90.5% | 125.5 | 52.4% | 117.0 | 43.1% |
| 1979 | 55.4 | 7.2% | 269.2 | 1.6% | 258.3 | 3.1% |
| 1978 | 37.7 | 69.1% | 176.7 | 18.5% | 137.7 | 24.7% |
| 1977 | 35.9 | 83.4% | 112.7 | 61.6% | 77.2 | 77.0% |
| 1976 | 36.2 | 76.2% | 155.8 | 27.7% | 147.0 | 23.1% |
| 1975 | 52.6 | 9.6% | 232.6 | 6.2% | 274.5 | 1.6% |
| 1974 | 38.1 | 66.7% | 131.3 | 41.6% | 112.2 | 52.4% |
| 1973 | 41.5 | 35.8% | 187.9 | 10.8% | 181.9 | 12.4% |
| 1972 | 59.1 | 2.4% | 253.3 | 3.1% | 227.3 | 4.7% |
| 1971 | 46.6 | 14.3% | 199.7 | 7.7% | 186.5 | 9.3% |
| 1970 | 38.9 | 52.4% | 130.6 | 43.1% | 120.8 | 33.9% |
| 1969 | 38.2 | 64.3% | 117.6 | 58.5% | 118.9 | 37.0% |
| 1968 | 38.5 | 59.6% | 111.9 | 64.7% | 93.5 | 64.7% |
| 1967 | 39.4 | 47.7% | 129.8 | 46.2% | 113.2 | 50.8% |
| 1966 | 40.1 | 42.9% | 101.3 | 75.4% | 104.6 | 57.0% |
| 1965 | 28.9 | 100.0% | 82.4 | 95.4% | 59.0 | 97.0% |
| 1964 | 36.0 | 81.0% | 109.6 | 67.7% | 71.5 | 84.7% |
| 1963 | 38.7 | 54.8% | 112.6 | 63.1% | 78.7 | 75.4% |

¹ Annual totals for Washington, DC from National Climatic Data Center, NOAA Satellite and Information Service, <http://lwf.ncdc.noaa.gov/oa/climate/research/cag3/city.html>

2 PHASE 3 ANACOSTIA HSPF WATERSHED MODEL

The computer model Hydrological Simulation Program—Fortran (HSPF) was used to develop a computer simulation of the Northwest Branch, Northeast Branch, Lower Beaverdam Creek, Watts Branch, and other areas draining to the tidal Anacostia River. The model has three purposes. First, the model is used to quantify sediment loads by key source categories: forest, agriculture, developed land, and streambank erosion. Second, while the HSPF model is not used to provide sediment loads from the Northwest and Northeast Branches to the TAM/WASP model, it has been calibrated to agree with the sediment loads from ESTIMATOR for the tidal model's simulation period and used to provide sediment loads for the tidal model from Lower Beaverdam Creek, Watts Branch, and other areas contributing to the tidal Anacostia River (see Appendix A). Third, since Maryland currently has no numerical water quality criteria for sediment for non-tidal waters, the HSPF model is used with the “reference watershed” approach in the development of MDE's Anacostia sediment TMDL, as part of a heuristic argument to demonstrate that the reductions required to meet water quality standards in the tidal Anacostia would be protective of non-tidal water quality.

This is the third version HSPF Model of the Non-tidal Anacostia Watershed developed by ICPRB within the past decade. The Phase I Anacostia Model (Manchester and Mandel, 2001) was developed to confirm the nutrient, sediment, and BOD loading rates used in DC's sediment and BOD TMDLs. It simulated the period 1988-1995, coincident with the simulation period of the TAM/WASP model of the tidal Anacostia. It was calibrated primarily against water quality monitoring data collected by the Coordinated Anacostia Monitoring Program (CAMP). The Phase II Anacostia Model (Mandel *et al.*, 2003) was intended to update the Phase I Model. The simulation period was 1996-2000, and it was calibrated against water quality monitoring data collected by the Metropolitan Washington Council of Governments (MWWOG) for the DC combined sewer system overflow (CSO) Long-Term Control Plan (LTCP) 1999-2000. While the LTCP data was more up-to-date than the CAMP data, it was collected during a very dry period punctuated by an extreme event, Hurricane Floyd, in September 1999. The Phase III Anacostia Model fulfills the promise of the Phase II Model. The simulation period is 1995-2004, to cover the simulation period of the Tidal Anacostia Model used in Maryland's sediment TMDL. It is calibrated primarily against ESTIMATOR sediment loads, which are based on ten years of available water quality monitoring data, including the recent automated sampler data collected by the USGS at the Northwest and Northeast gages (see Appendix A).

2.1 General Overview of the HSPF Model

The HSPF Model simulates the fate and transport of pollutants over the entire hydrological cycle. Two distinct sets of processes are represented in HSPF: (1) processes that determine the fate and transport of pollutants at the surface or in the subsurface of a watershed, and (2) in-stream processes. The former will be referred to as land or watershed processes, the latter as in-stream or river reach processes.

Constituents can be represented at various levels of detail and simulated both on land and for in-stream environments. These choices are made in part by specifying the modules that are used, and thus the choices establish the model structure used for any one problem. In addition to the choice of modules, other types of information must be supplied for the HSPF calculations,

including model parameters and time-series of input data. Time-series of input data include meteorological data, point sources, reservoir information, and other types of continuous data as needed for model development.

A watershed is subdivided into model segments, which are defined as areas with similar hydrologic characteristics. Within a model segment, multiple land use types can be simulated, each using different modules and different model parameters. There are two general types of land uses represented in the model: pervious land, which uses the PERLND module, and impervious land, which uses the IMPLND module. More specific land uses, like forest, crop, or developed land, can be implemented using these two general types. In terms of simulation, all land processes are computed for a spatial unit of one acre. The number of acres of each land use in a given model segment is multiplied by the values (fluxes, concentrations, and other processes) computed for the corresponding acre. Although the model simulation is performed on a temporal basis, land use information does not change with time.

Within HSPF, the RCHRES module sections are used to simulate hydraulics of river reaches and the sediment transport, water temperature, and water quality processes that result in the delivery of flow and pollutant loading to a bay, reservoir, ocean or any other body of water. Flow through a reach is assumed to be unidirectional. In the solution technique of normal advection, it is assumed that simulated constituents are uniformly dispersed throughout the waters of the RCHRES; constituents move at the same horizontal velocity as the water, and the inflow and outflow of materials are based on a mass balance. HSPF primarily uses the “level pool” method of routing flow through a reach. Outflow from a free-flowing reach is a single-valued function of reach volume, specified by the user in an F-Table, although within a time step, the HSPF model uses a convex routing method to move mass flow and mass within the reach. Outflow may leave the reach through as many as five possible exits, which can represent water withdrawals or other diversions.

Bicknell *et al.* (2000) describe the HSPF model in greater detail.

2.2 Segmentation

Figure 2-1 shows the segmentation of subwatersheds used in the Phase III Model. It is based on the previous versions of the model, with the following exceptions:

- Segments 210 and 270, representing the upper portions of the Northwest Branch and Upper Paint Branch, were split off from Segments 10 and 70;
- Segment 150, representing the Watts Branch, was terminated at the USGS gaging station 01651800; and
- The remainder of the Watts Branch and other areas draining directly to the tidal Anacostia were collected together in a new Segment 160.

2.3 Model Land Use

The following eight land uses are represented in the HSPF model:

Developed Land:

- Low Density Residential
- Medium Density Residential
- High Density Residential
- Commercial
- Industrial

Undeveloped Land:

- Forest
- Pasture
- Cropland.

The developed land uses were further subdivided into pervious and impervious areas. Table 2-1 gives the model land use categories and the acreage of each category by model segment. Figure 2-2 represents the model land use by segment.

2.3.1 Original Sources of Land Use Data

Land use for the Maryland portion of the Anacostia watershed was based on Maryland Department of Planning (MDP)'s 2002 *Land Use/Land Cover for Maryland* GIS layer, which was originally developed from 1997 high altitude aerial photography and satellite imagery. MDP then refined the land cover types using 2002 aerial photography, and updated urban land use using parcel information from their 2002 Edition of MDPropertyView. Table 2-2 shows how MDP land use classifications were assigned to model land uses. Model land uses are, for the most part, more general classes of the MDP land uses, with a few exceptions. MDP forests and wetlands were both classified as forests in the model. Barren land was assigned to the low-density residential category, and extractive land to the impervious industrial category. The small number of acres of unpaved roadways was somewhat arbitrarily assigned to pervious commercial land.

Following the guidance from Montgomery County DEP, all cropland in Montgomery County was classified as pasture. Cropland in Prince George's County was limited to the Beltsville Agricultural Research Center (BARC). BARC personnel (K. Hummel, 2003, personal communication) provided acres of cropland for the Phase II Model. These are shown in Table 2-3. According to the BARC estimates, cropland is overestimated by the MDP land use layer. The additional acreage MDP classified as cropland was reclassified as pasture.

Land use for the District of Columbia portion of the watershed was derived from Anacostia Land Use/Land Cover GIS layer produced by MWCOC from the 1990 DC Planned Land Use layer and Maryland Office of Planning's 1990 Land Use/Land Cover data layer (Warner *et al.*, 1997). Table 2-4 shows the original land use codes and corresponding descriptions as well as the land use classification scheme used in the model.

Table 2-1. Phase III HSPF Model Land Use Acreage By Segment (acres)

| Segment | Pervious Low Density Residential | Impervious Low Density Residential | Pervious Medium Density Residential | Impervious Medium Density Residential | Pervious High Density Residential | Impervious High Density Residential | Pervious Commercial | Impervious Commercial | Pervious Industrial | Impervious Industrial | Forest | Pasture | Crop | Total |
|---------|----------------------------------|------------------------------------|-------------------------------------|---------------------------------------|-----------------------------------|-------------------------------------|---------------------|-----------------------|---------------------|-----------------------|--------|---------|-------|--------|
| 10 | 2,009 | 136 | 2,506 | 552 | 338 | 245 | 1,541 | 150 | 0 | 0 | 2,107 | 541 | 0 | 10,123 |
| 20 | 1,607 | 192 | 1,430 | 430 | 133 | 92 | 852 | 226 | 0 | 0 | 889 | 17 | 0 | 5,868 |
| 30 | 2,535 | 450 | 14 | 7 | 188 | 152 | 494 | 396 | 22 | 10 | 417 | 0 | 0 | 4,686 |
| 40 | 653 | 106 | 2,018 | 636 | 747 | 462 | 1,046 | 648 | 38 | 58 | 778 | 45 | 0 | 7,233 |
| 50 | 1,228 | 56 | 1,258 | 242 | 13 | 4 | 241 | 45 | 0 | 0 | 1,284 | 362 | 0 | 4,732 |
| 60 | 102 | 9 | 1,696 | 391 | 159 | 115 | 1,102 | 307 | 407 | 226 | 596 | 41 | 0 | 5,150 |
| 70 | 213 | 14 | 1,793 | 497 | 315 | 203 | 851 | 351 | 45 | 54 | 1,817 | 644 | 262 | 7,059 |
| 80 | 169 | 9 | 242 | 33 | 237 | 90 | 922 | 205 | 3 | 0 | 5,458 | 1,030 | 607 | 9,006 |
| 90 | 205 | 7 | 577 | 113 | 102 | 36 | 316 | 122 | 600 | 1,568 | 1,859 | 272 | 358 | 6,135 |
| 100 | 200 | 12 | 2,839 | 894 | 1,211 | 547 | 2,471 | 1,263 | 115 | 64 | 2,884 | 151 | 0 | 12,651 |
| 120 | 39 | 1 | 970 | 311 | 559 | 303 | 901 | 433 | 341 | 514 | 895 | 20 | 0 | 5,286 |
| 130 | 79 | 3 | 493 | 128 | 514 | 175 | 393 | 116 | 253 | 223 | 755 | 53 | 0 | 3,184 |
| 140 | 0 | 0 | 259 | 79 | 39 | 15 | 117 | 58 | 109 | 157 | 316 | 12 | 0 | 1,162 |
| 150 | 80 | 2 | 646 | 335 | 315 | 115 | 207 | 99 | 16 | 7 | 269 | 28 | 0 | 2,119 |
| 210 | 1,096 | 44 | 328 | 27 | 2 | 1 | 271 | 52 | 0 | 0 | 1,086 | 499 | 0 | 3,404 |
| 270 | 90 | 5 | 309 | 101 | 43 | 22 | 441 | 29 | 101 | 77 | 310 | 30 | 0 | 1,558 |
| NW | 7,900 | 927 | 6,297 | 1,651 | 1,408 | 951 | 4,204 | 1,471 | 60 | 68 | 5,276 | 1,102 | 0 | 31,314 |
| NE | 2,207 | 112 | 8,714 | 2,271 | 2,081 | 1,016 | 6,345 | 2,322 | 1,270 | 1,990 | 14,210 | 2,530 | 1,227 | 46,353 |
| LBC | 118 | 4 | 1,722 | 517 | 1,111 | 492 | 1,410 | 608 | 704 | 893 | 1,966 | 85 | 0 | 9,631 |
| Watts | 80 | 2 | 646 | 335 | 315 | 115 | 207 | 99 | 16 | 7 | 269 | 28 | 0 | 2,119 |

Table 2-2. Model Classification for Maryland's Land Use

| MDP Land Use Code | MDP Land Use Description | Model Land Use |
|--------------------------|--|----------------------------|
| 11 | Low Density Residential | Low Density Residential |
| 12 | Medium Density Residential | Medium Density Residential |
| 13 | High Density Residential | High Density Residential |
| 14 | Commercial | Commercial |
| 15 | Industrial | Industrial |
| 16 | Institutional | Commercial |
| 17 | Extractive | Industrial |
| 18 | Open Urban Land | Commercial |
| 21 | Cropland | Cropland |
| 22 | Pasture | Pasture |
| 23 | Orchards, Vineyards, Horticulture | Cropland |
| 25 | Row and Garden Crops | Cropland |
| 41 | Deciduous Forest | Forest |
| 42 | Evergreen Forest | Forest |
| 43 | Mixed Forest | Forest |
| 44 | Brush | Forest |
| 50 | Water | Water |
| 60 | Wetlands | Forest |
| 73 | Bare Ground | Low Density Residential |
| 80 | Transportation | Commercial |
| 241 | Feeding operations | Cropland |
| 242 | Agricultural Building, Breeding, and Training Facilities | Cropland |

Table 2-3. Crop Acres at Beltsville Agricultural Research Center

| Crop | Acres | Crop | Acres |
|----------------------------|--------------|---------------|--------------|
| Corn | 500 | Alfalfa | 150 |
| Small Grains (Barley, Rye) | 225 | Orchard Grass | 120 |
| Soybeans | 225 | Sudan Grass | 25 |

Table 2-4. Model Classification for District of Columbia's Land Use

| MWCOG Land Use Code | Description | Mean Percent Imperviousness | Model Land Use Classification |
|----------------------------|---|------------------------------------|--------------------------------------|
| RD2 | Low/Medium Density Residential: detached single family/duplex dwellings, attached single unit row housing. | 22.5 | MDR |
| RD3 | Medium Density Residential: row houses, garden apartments, and associated areas. | 40 | MDR |
| RD4 | Medium/High Density Residential: attached single unit row housing, mid-rise apartment, multiple-unit housing | 60 | HDR |
| RD5 | High Density Residential: high-rise apartments are the predominant land use | 75 | HDR |
| CM1 | Low Density Commercial and Commercially-dominant Mixed Land Use | 60 | Commercial |
| CM2 | Medium Density Commercial and Commercial-dominant Mixed Land Use | 75 | Commercial |
| CM3 | Medium/High Density Commercial and Commercially-dominant Mixed Land Use | 85 | Commercial |
| CM4 | High Density Commercial and Commercially-dominant Mixed Land Use; Central Business District | 95 | Commercial |
| FD | Federal Lands and Property (military installations included) | 60 | Commercial |
| IL2 | Elementary and Secondary Schools, Public and Private Colleges, and Churches | 75 | Commercial |
| L | Local Government Lands and Property | 60 | Commercial |
| PK | Parks and Open Space: includes golf courses, cemeteries, beaches, and bare ground. | 7.5 | Commercial |
| IY | Manufacturing and Industrial Parks: includes associated warehouses, parking areas, laboratories, and industrially-dominant Mixed Land Use | 75 | Industrial |

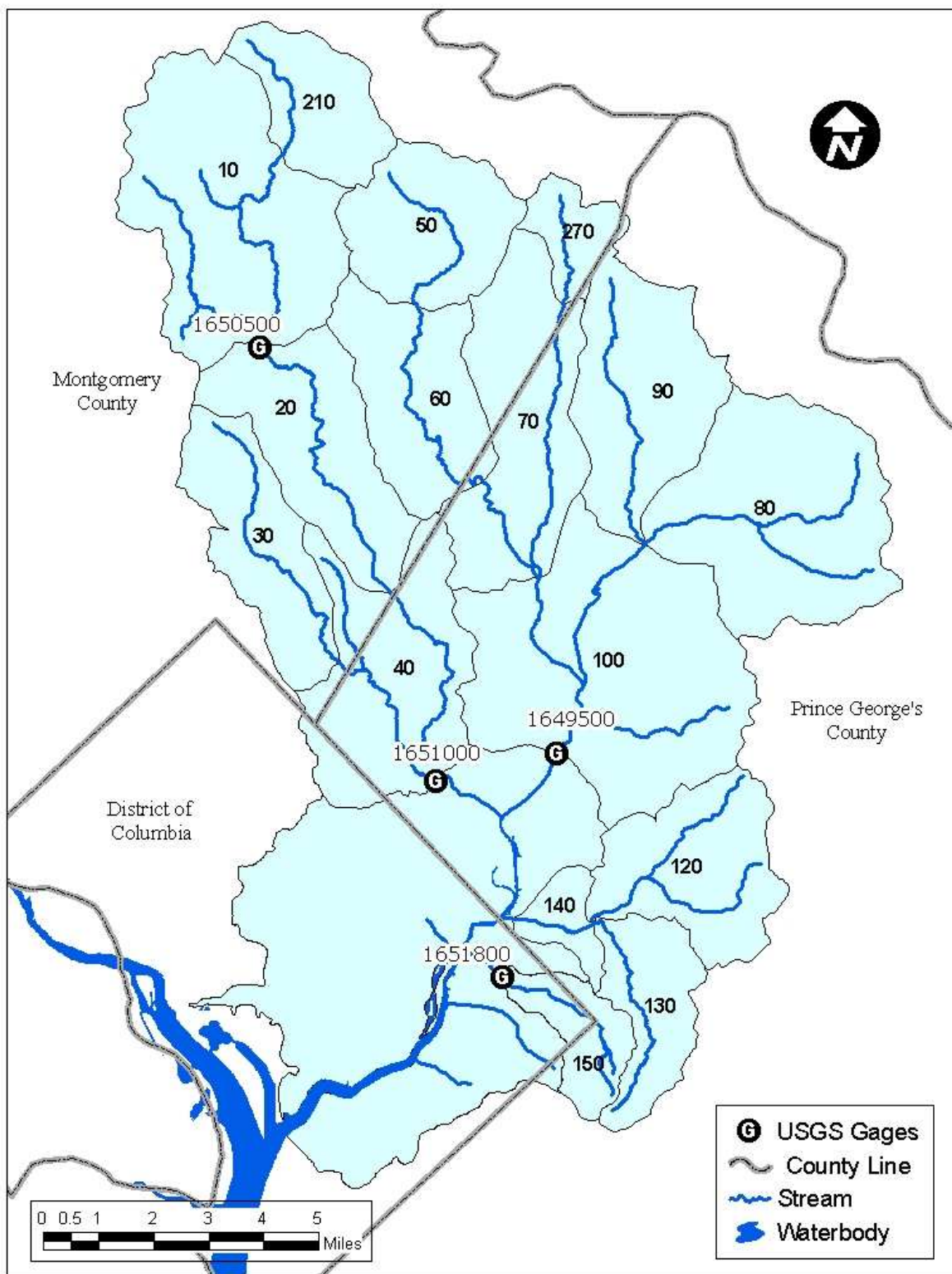


Figure 2-1. Model Segmentation and USGS Gages

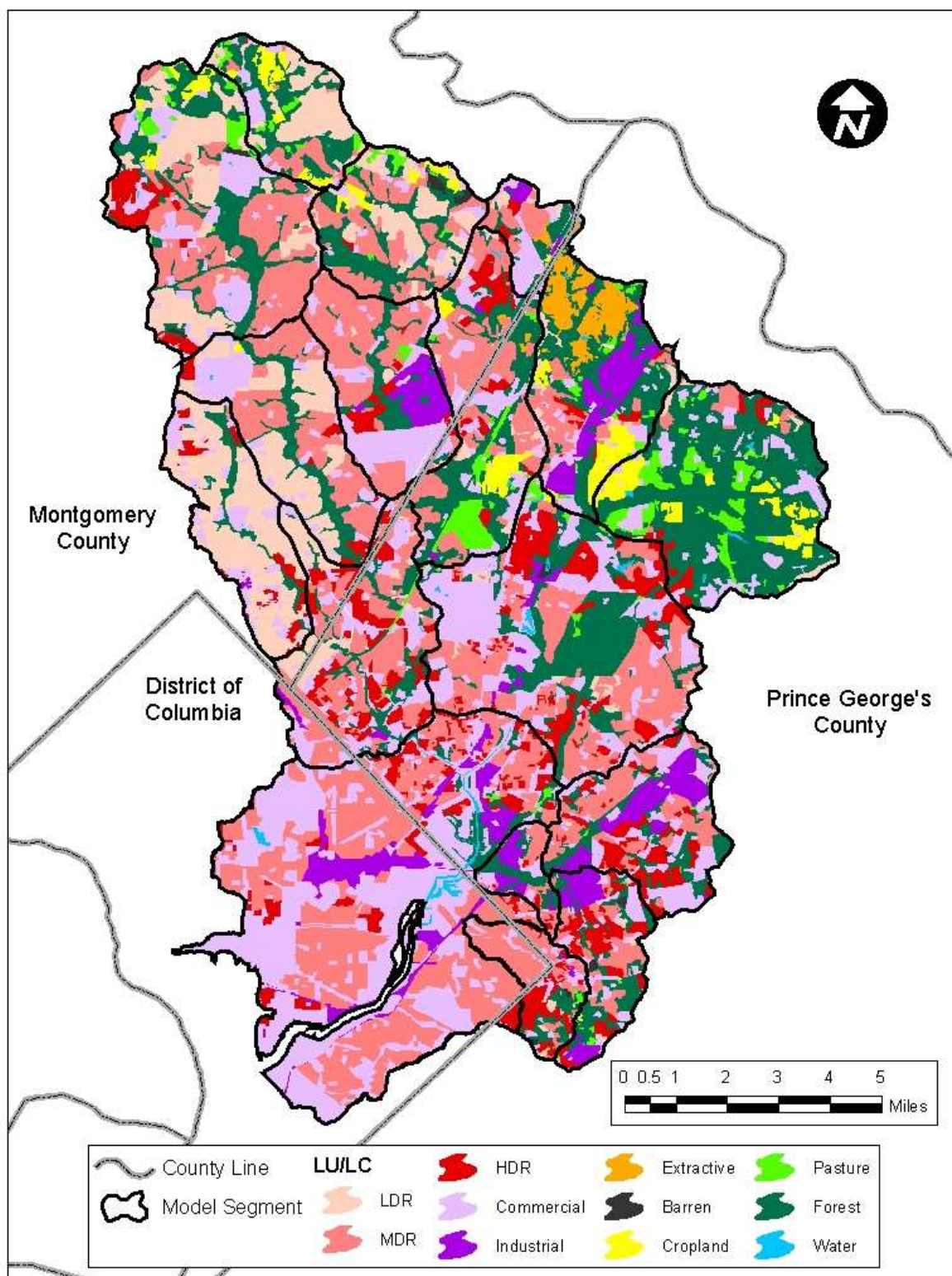


Figure 2-2. Aggregated Land Use in the Anacostia Watershed

2.3.2 Determination of Impervious Area

Impervious area in the Maryland portion of the Anacostia watershed was estimated from several planimetric GIS layers representing building footprints and paved areas in combination with two line layers representing sidewalks and street centerlines. The street centerline layer for Montgomery County was provided by the MC DEP. The other layers were obtained from the Montgomery County and the Prince George's County Planning Departments of the Maryland Capital Park and Planning Commission (M-NCPPC).

Montgomery County: Sidewalk area was calculated from the *Sidewalk* line layer, assuming that sidewalks had a width of four feet (L. Darr, personal communication). Acreage under pavement was determined from the *Parking* and *Roads* layers. The *Roads* layer was reconciled with the *Street Centerline* layer. The impervious area in buildings was obtained from the *Build* layer. The various layers were combined to obtain a representative layer of impervious area within the Montgomery County portion of the watershed, and then apportioned by land use according to the MDP land use classification.

Prince George's County: For Prince George's County, paved area was determined from the *Bridges* layer and the *Trans* layer, which contains various transportation-related features including roadways, parking lots and airports. The area in roads was checked against the *Road Centerline* layer and reconciled where necessary. GIS data were not readily available for paved area in sidewalks and private driveways. Impervious area attributed to buildings was determined from the *Build* layer, which provides building footprint information. These GIS layers were combined into a single layer to represent the total impervious area in the Prince George's County portion of the watershed, and then apportioned by land use according to the MDP land use classification.

District of Columbia: Building footprint and paved area data were not available for the District of Columbia portion of the Anacostia watershed. The MWCOG's Anacostia Land Use/Land Cover layer, however, gives information on mean imperviousness by land use category (see Table 2-4), and this information was used to calculate impervious area for the model.

2.3.3 Effective Impervious Area

The total impervious area in a watershed was modified to attempt to account for the net "effective" or connected impervious area. Not all impervious areas drain into storm sewers. Drainage from roofs in detached low-density single-family housing is often directed on lawns rather than on driveways or other areas hydraulically connected to storm sewers. Therefore impervious roof drainage from low-density residential land was transferred from the impervious category to the pervious category.

2.4 Hydrology Calibration

The simulation of hydrology was calibrated against daily flows observed at the USGS gages on the Northeast Branch (01649500), Northwest Branch (01651000), and the Watts Branch (01651800). The USGS gage on the Northwest Branch at Colesville (0160500), which was not operable over the entire simulation period, was used to help verify the calibration. Overall, the

simulation period was characterized by extreme flows. 1996 was a wet year in which a January snowmelt caused flooding. 1997 was the wettest December on record for both the Northeast Branch and the Watts Branch. It was also the wettest December on the Northwest Branch until 2003. 1998 and 1999 were dry years overall; 1999 was the driest July on record for the Northeast Branch. The drought of 1999 ended with Hurricane Floyd in September. On both Branches, the driest February occurred in 2002. Water Year 2002 was the driest year on the Northeast Branch, while Water Year 2003 was the wettest year on both the Northeast and Northwest Branches. Overall, however, the calibrated model was able to match the variability in observed flows.

2.4.1 Meteorological Input Data

HSPF requires hourly time series of precipitation, pan evaporation, air temperature, solar radiation, cloud cover, wind speed and dew point temperature. The latter five input time series are necessary only to simulate snowmelt or evaporation from the river reaches.

Hourly time series of precipitation, air temperature, dew point temperature, and wind speed were taken from Reagan National Airport (COOP Station 448906). Cloud cover was also taken from Reagan Airport, except for the period prior to May 1995, where it was taken from Dulles Airport. Pan evaporation and solar radiation were calculated on the basis of cloud cover and other inputs using the WDMUtil software. The Penman Method was used to calculate pan evaporation.

2.4.2 Calibration Methodology

The hydrology calibrations were performed using version 5 of PEST, the model-independent parameter estimation software developed by J. Doherty (Doherty, 2001). PEST determines the values of parameters that optimize a user-specified objective function. In these simulations, the objective function was the sum of the squares of the differences between daily observed and simulated flows. This is equivalent to maximizing the coefficient of determination (R^2) between observed and simulated flows.

Table 2-5 gives the key parameters adjusted in hydrology calibration. Each land use represented in HSPF has its own set of hydrology parameters. Comparing observed to simulated flows can help determine the best values of infiltration rates and baseflow recession coefficient, but cannot, by itself, help distinguish the infiltration rates for different land uses, like forest, pasture, or cropland. In the development of the Chesapeake Bay Program Phase 5 Watershed Model, a set of rules relating the values of calibration parameters on different land used was determined by best professional judgment. These rules were adopted for the calibration of the Anacostia Watershed HSPF Model. The rules can be formulated in terms of the values of parameters for cropland. Table 2-6 gives the ratio of cropland parameters to other land uses. The seasonal distribution of monthly UZSN values, shown in Table 2-7, was also adopted from the Phase 5 Model. The calibration of the Anacostia Watershed Model differed from the Phase 5 Model primarily in two respects. First, the ratio between UZSN and LZSN was allowed to vary; in the Phase 5 Model it had a fixed value for each land use. The rules specifying the variability of the ratio with land use, however, were adopted from the Phase 5 Model. These are given in Table 2-6. Second, the LZETP was also treated as a calibration parameter, varying monthly. Table 2-7 shows the monthly values of the LZETP as a function of the base rate for pasture and urban land.

The Phase II Model used different hydrology parameters for Piedmont and Coastal Plain subwatersheds. The Montgomery County-Prince George's County border approximates the division between the Piedmont and the Coastal Plain Physiographic Provinces. Soils in the Piedmont portion of the Anacostia watershed belong to the Glenelg-Gaila-Occoquan Association or the Wheaton-Glenelg Association, which are typically well-drained (NRCS, 1995). Soils in the Atlantic Coastal Plain, however, belong to either the Beltsville-Leonardstown-Chillum Association or the Christiana-Sunnyside-Beltsville Association. Soils in both these associations can have compact subsoils that inhibit drainage (SCS, 1967). A consistent set of parameters was therefore used for modeling Segments 10-60 and 210 in the Piedmont and Segments 70-150 and 270 in the Coastal Plain.

2.4.3 Hydrology Calibration Results

Table 2-8 gives the final hydrology simulation parameters used in the simulation. Table 2-9 shows the coefficient of determination for monthly flows, the overall bias, and storm flow and low flow volumes, as represented by the sum of flows greater than 90th percentile and less than the 50th percentile flows. Figure 2-3 through Figure 2-6, Figure 2-7 through Figure 2-10, Figure 2-11 through Figure 2-14, and Figure 2-15 through Figure 2-18 show, for the Northeast Branch, the Northwest Branch at Riverdale, Watts Branch, and the Northwest Branch at Colesville, respectively, (1) time series of simulated and observed daily flows, (2) scatter plots of daily flows, (3) scatter plots of monthly flows, and (4) comparative empirical cumulative distribution of flows over the simulation period.

Total flow volume is slightly undersimulated in the Northwest Branch; otherwise at the calibration stations there is a good agreement in the overall water volume and distribution of flow between high flows and low flows, as shown in Table 2-9. Generally, Hurricane Floyd (September, 1999) is undersimulated by the HSPF model. For calibration stations, however, the coefficient of determination (R^2) between simulated and observed daily average flows is about 0.8, which means that the HSPF model captures a good deal of the variability of the flows during the simulation period, which, as noted above, is characterized by both wet and dry extreme conditions.

The statistics comparing observed and simulated flows at the Colesville gaging station on the NW Branch are not quite as good as those for the calibration stations. The model tends to oversimulate low flows and undersimulate high flows. The trouble seems confined to the very wet year 2003. The coefficient of determination (R^2) between simulated and observed daily average flows is 0.76 for the period 1997-2002, comparable to the results for the calibration stations.

Table 2-5. Key Hydrology Calibration Parameters

| Parameter | Description |
|------------------|--|
| LAND_EVAP | PET adjustment (similar to pan evaporation coefficient) |
| INFILT | Base infiltration rate |
| LZSN | Lower zone soil moisture storage index |
| UZSN | Upper zone soil moisture storage index |
| AGWR | Baseflow recession coefficient |
| INTFW | Ratio of interflow to surface runoff |
| IRC | Interflow recession coefficient |
| LZETP | Evapotranspiration from lower zone storage |
| RETSC | Impervious surface retention storage |

Table 2-6. Ratio of Cropland Parameters to Those for Other Land Uses

| Land use | INFILT | LZSN | AGWR | INTFW | IRC | Max LZETP |
|-----------------|---------------|-------------|-------------|--------------|------------|------------------|
| Forest | 1.6 | 1.0 | 1.0 | 1.25 | 1.0 | 1.1 |
| Grasses | 1.0 | 1.0 | 1.0 | 1.0 | 1.0 | 1.0 |
| Pervious Urban | 0.8 | 1.0 | 1.0 | 1.0 | 1.0 | 1.0 |

Table 2-7. Monthly Hydrology Parameters

| Month | Fraction Max Crop UZSN | Fraction Max Crop LZEPT | Grassland Base and Winter LZEPT | Forest Base and Winter LZEPT |
|--------------|-------------------------------|--------------------------------|--|-------------------------------------|
| Jan | 0.6 | 0.1 | 0.1 | 0.1 |
| Feb | 0.6 | 0.1 | 0.1 | 0.1 |
| Mar | 0.6 | 0.1 | 0.1 | 0.1 |
| Apr | 0.6 | 0.1 | Base | 0.1 |
| May | 0.6 | 0.1 | Base | Base |
| Jun | 0.7 | 0.5*Base | Base | Base |
| Jul | 0.95 | 0.67*Base | Base | Base |
| Aug | 1.0 | Base | Base | Base |
| Sep | 1.0 | Base | Base | Base |
| Oct | 0.8 | 0.67*Base | Base | Base |
| Nov | 0.7 | 0.5*Base | Base | 0.1 |
| Dec | 0.65 | 0.1 | 0.1 | 0.1 |

Table 2-8. Hydrology Calibration Parameter Values

| Parameter | Piedmont | Coastal Plain | Watts Branch |
|-----------|----------|---------------|--------------|
| LAND_EVAP | 0.6 | 0.5 | 0.6 |
| CCFACT | 0.289 | 0.230 | 0.418 |
| INFILT | 0.028 | 0.032 | 0.100 |
| LZSN | 7.39 | 3.66 | 4.44 |
| UZSN | 1.70 | 0.562 | 1.03 |
| AGWR | 0.989 | 0.993 | 0.997 |
| INTFW | 4.36 | 5.00 | 2.11 |
| IRC | 0.107 | 0.103 | 0.050 |
| LZETP | 0.325 | 0.490 | 0.434 |
| RETSC | 0.109 | 0.005 | 0.115 |

Table 2-9. Hydrology Calibration Results

| Statistic | 10 (NW Branch at Colesville) | 40 (NW Branch Near Hyattsville) | 110 (NE Branch at Riverdale) | 150 (Watts Branch) |
|-------------------------------------|------------------------------------|---------------------------------------|------------------------------------|-----------------------|
| Water Balance | 91% | 95% | 99% | 99% |
| Flows < 50 th Percentile | 128% | 104% | 108% | 102% |
| Flows > 90 th Percentile | 84% | 99% | 104% | 103% |
| Daily R ² | 0.66 | 0.78 | 0.79 | 0.82 |
| Monthly R ² | 0.76 | 0.86 | 0.86 | 0.87 |

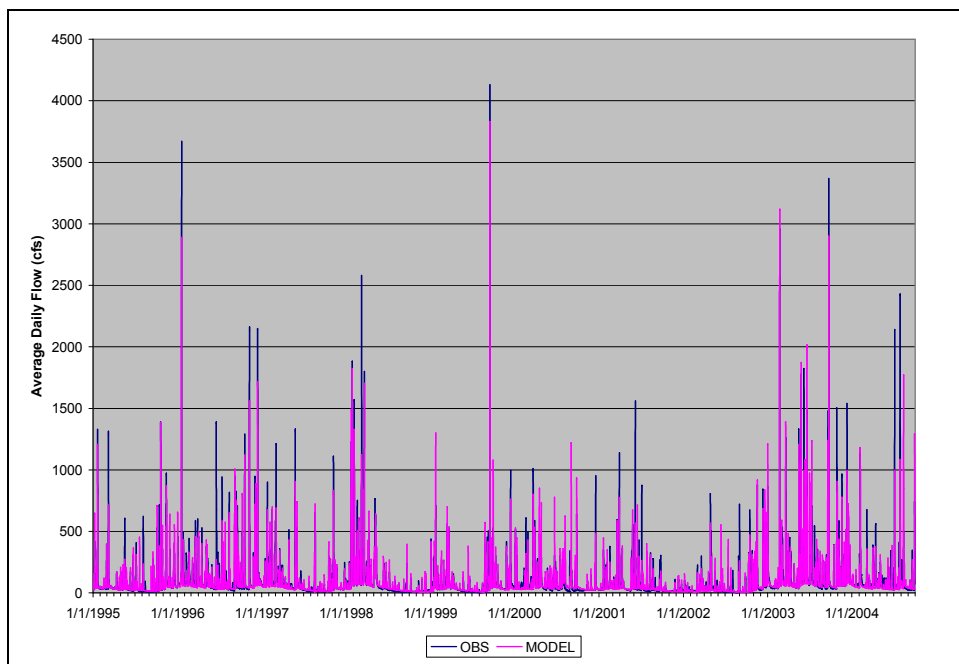


Figure 2-3. Time Series. Simulated and Observed Daily Average Flow. Northeast Branch.

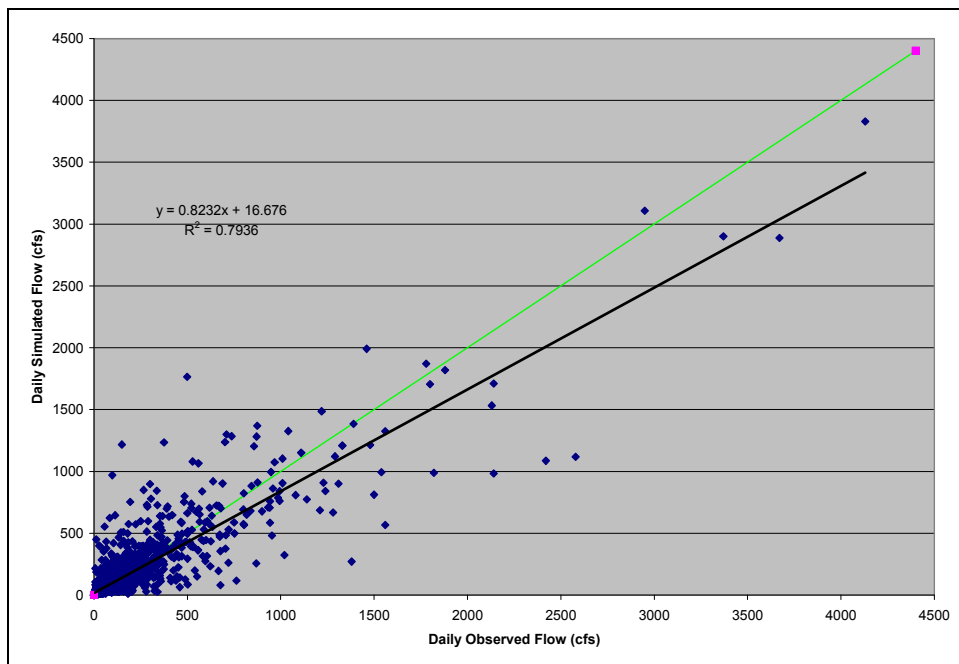


Figure 2-4. Scatter Plot. Simulated and Observed Daily Average Flow. Northeast Branch

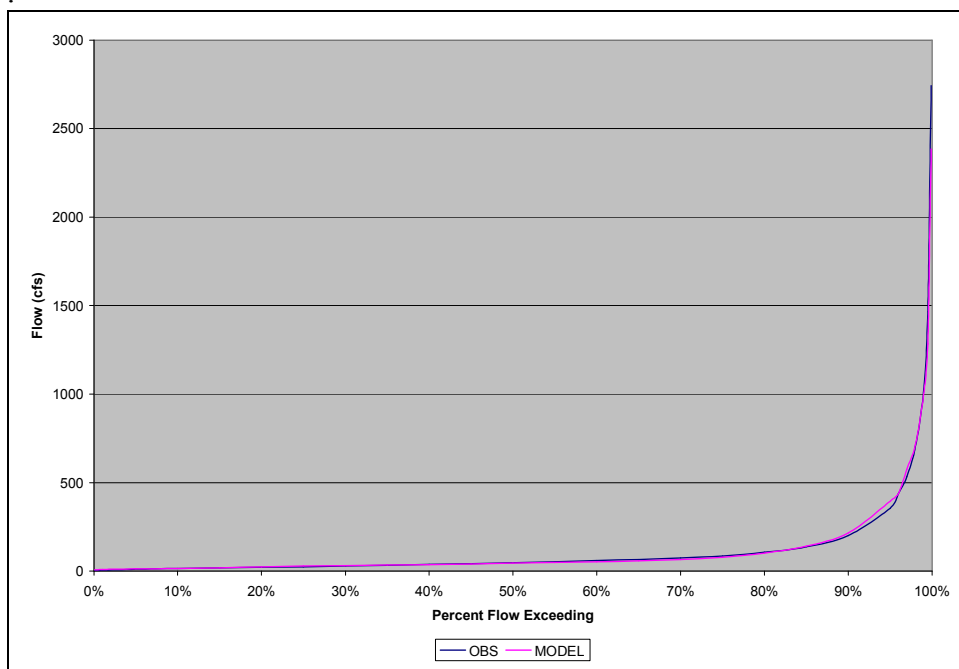


Figure 2-5. Cumulative Distribution Function. Simulated and Observed Daily Average Flow, Northeast Branch

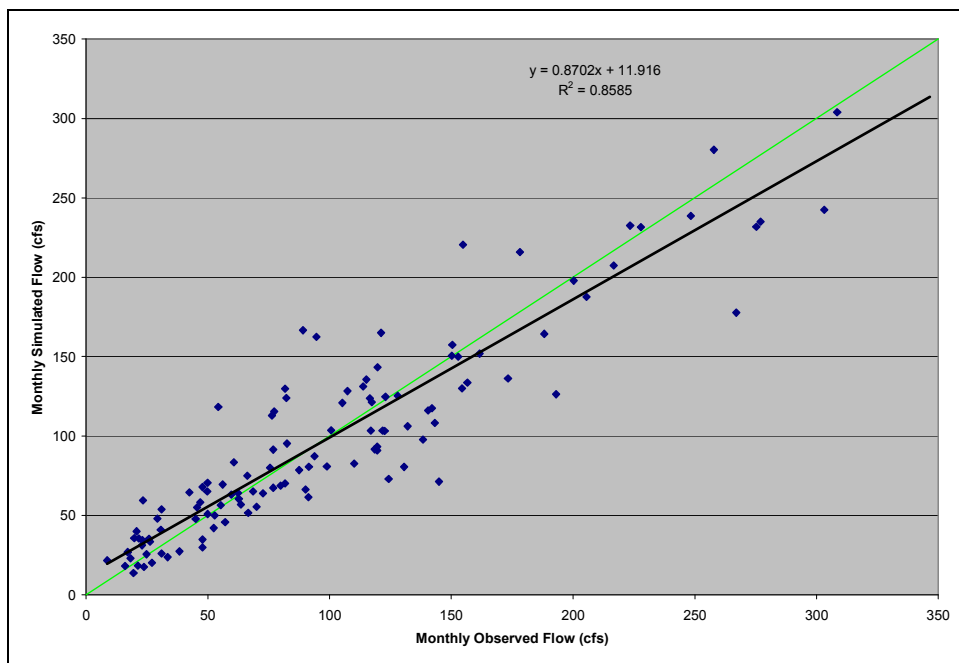


Figure 2-6. Scatter Plot. Simulated and Observed Monthly Average Flow, Northeast Branch.

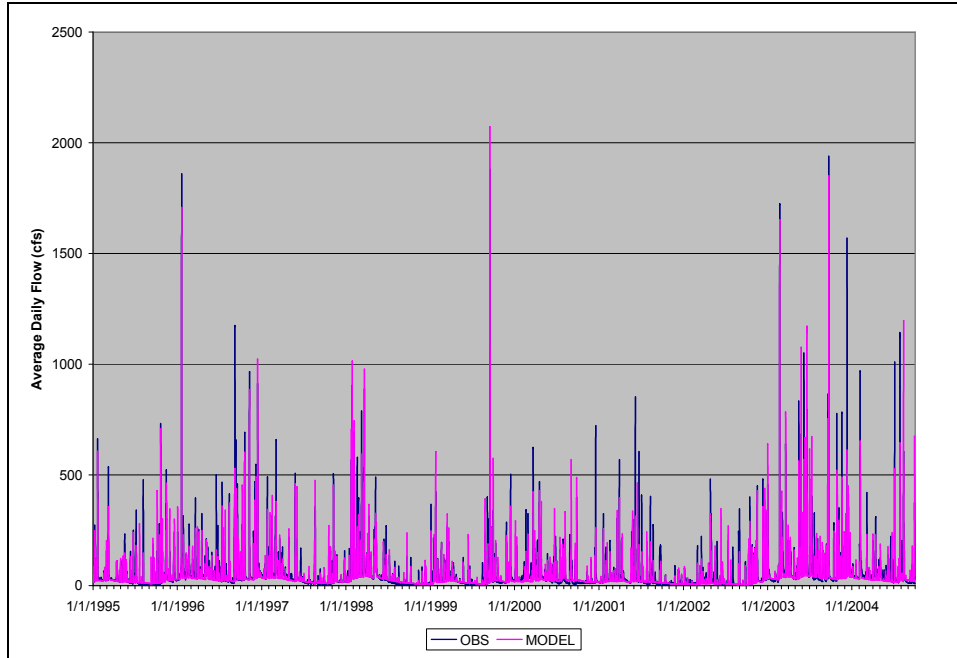


Figure 2-7. Time Series. Simulated and Observed Daily Average Flow. Northwest Branch at Riverdale.

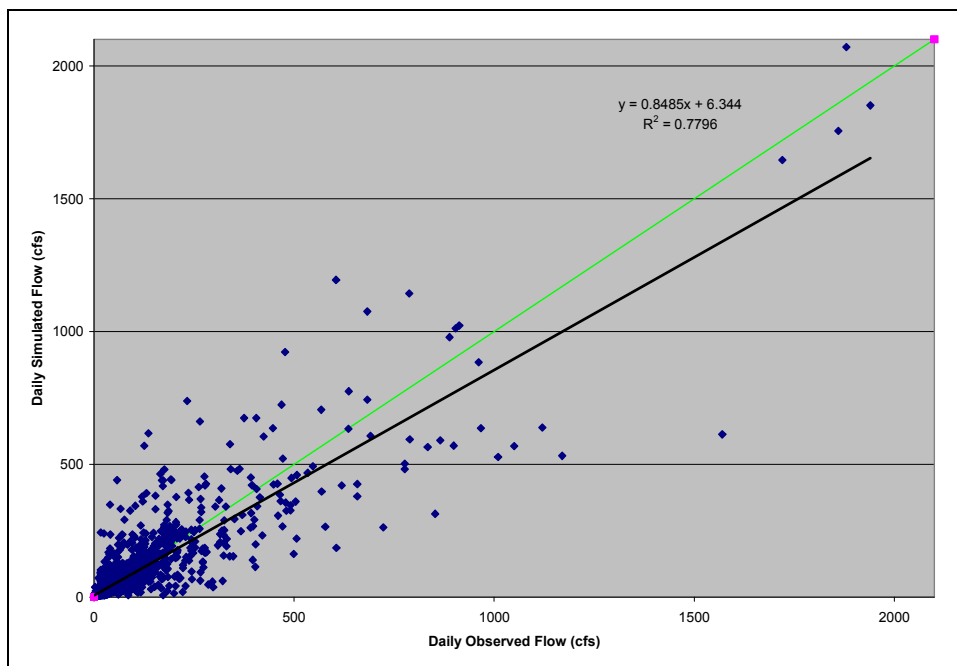


Figure 2-8. Scatter Plot. Simulated and Observed Daily Average Flow. Northwest Branch at Riverdale

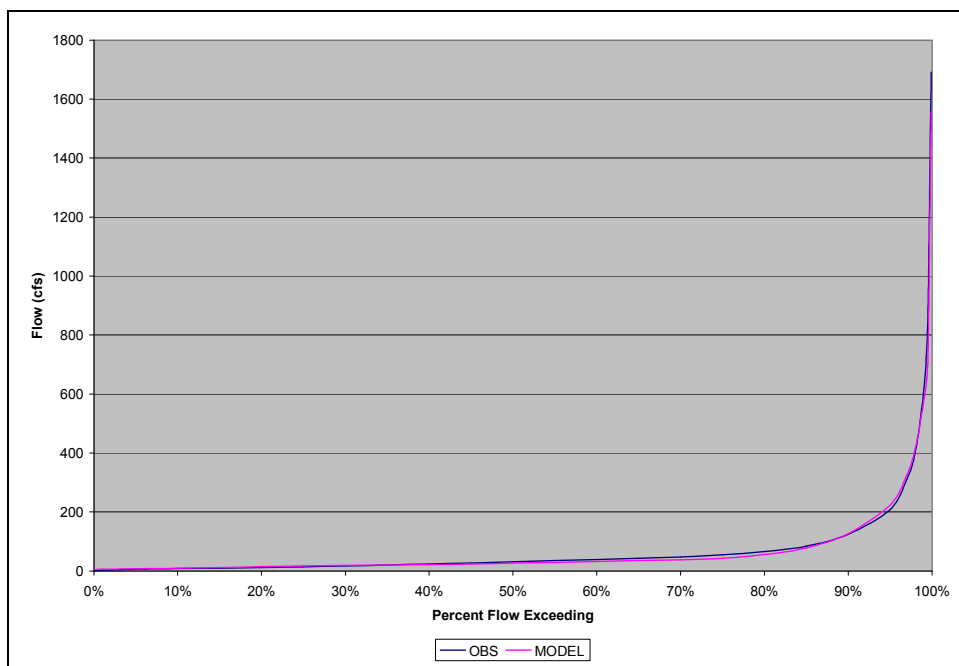


Figure 2-9. Cumulative Distribution Function. Simulated and Observed Daily Average Flow. Northwest Branch at Riverdale.

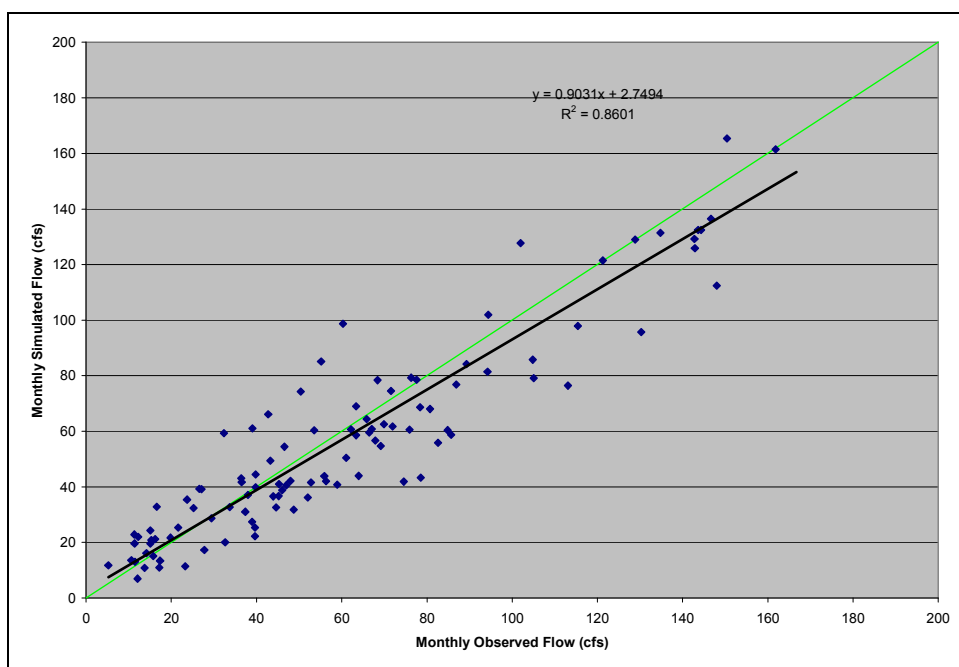


Figure 2-10. Scatter Plot. Simulated and Observed Monthly Average Flow. Northwest Branch at Riverdale.

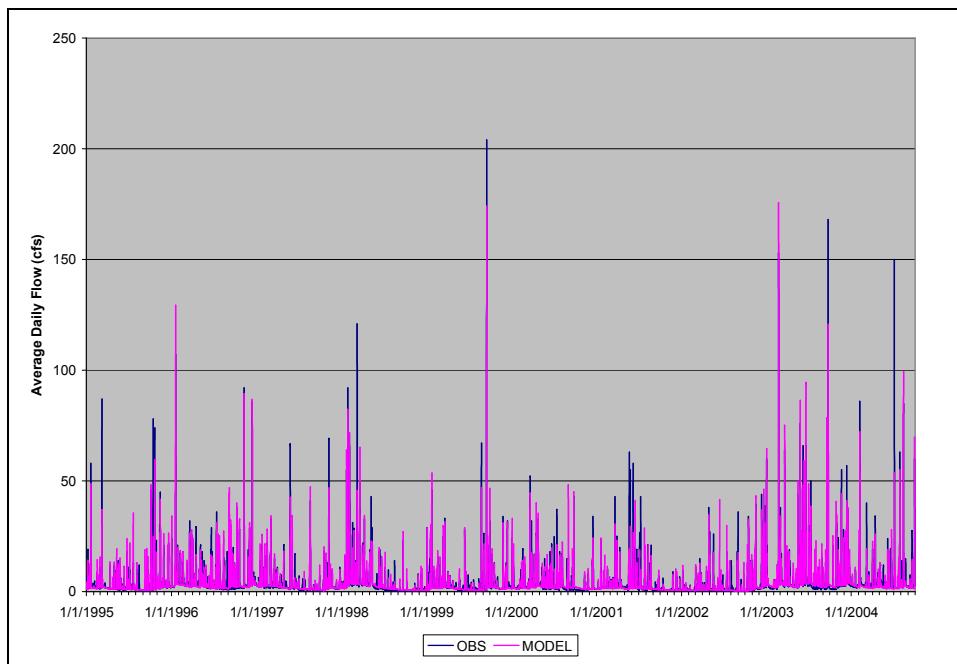


Figure 2-11. Time Series. Simulated and Observed Daily Average Flow. Watts Branch.

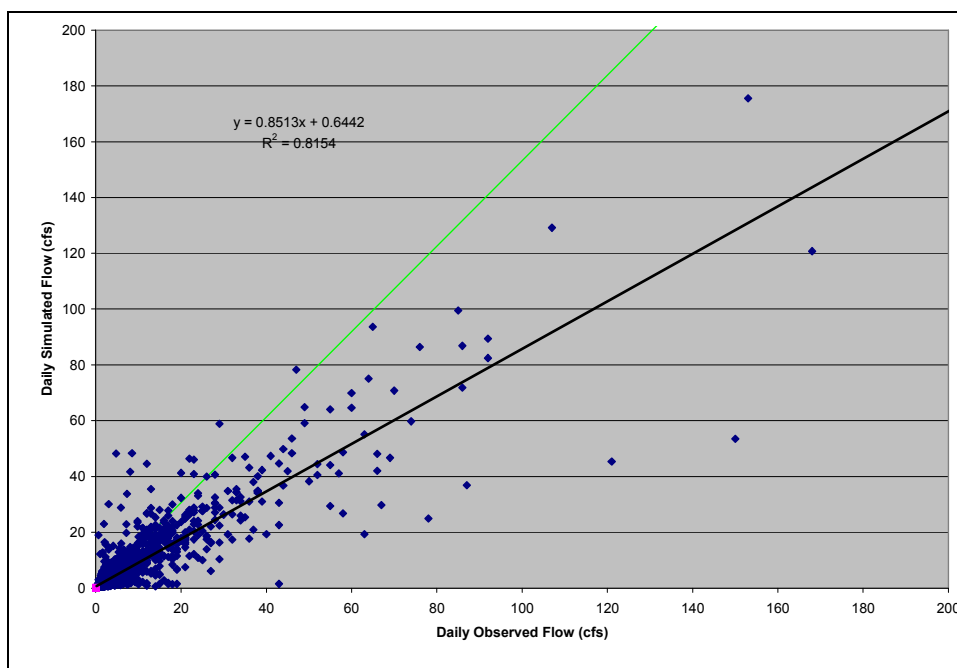


Figure 2-12. Scatter Plot. Simulated and Observed Daily Average Flow. Watts Branch

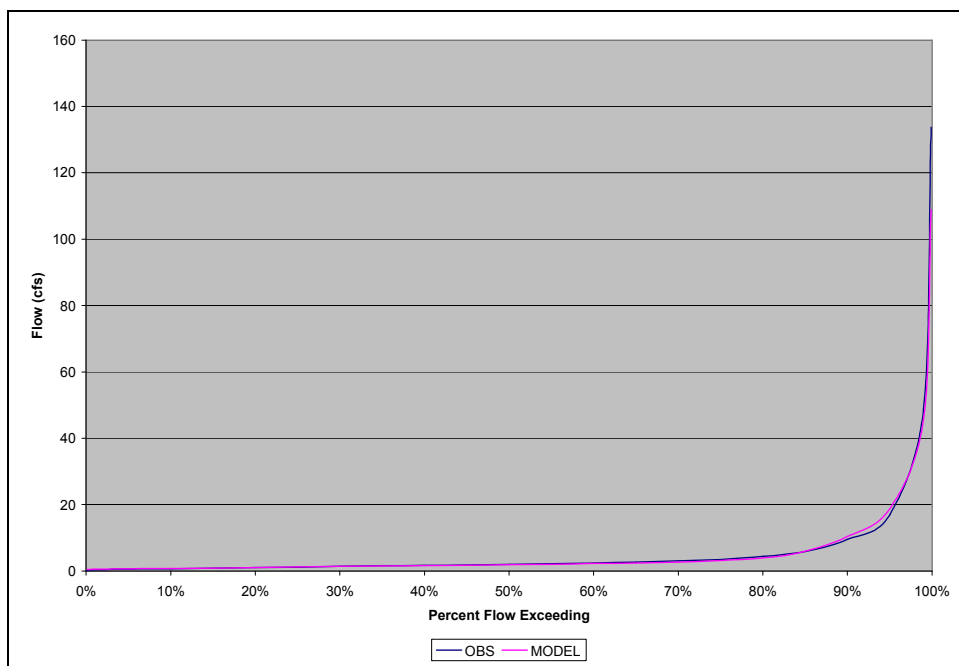


Figure 2-13. Cumulative Distribution Function. Simulated and Observed Daily Average Flow. Watts Branch.

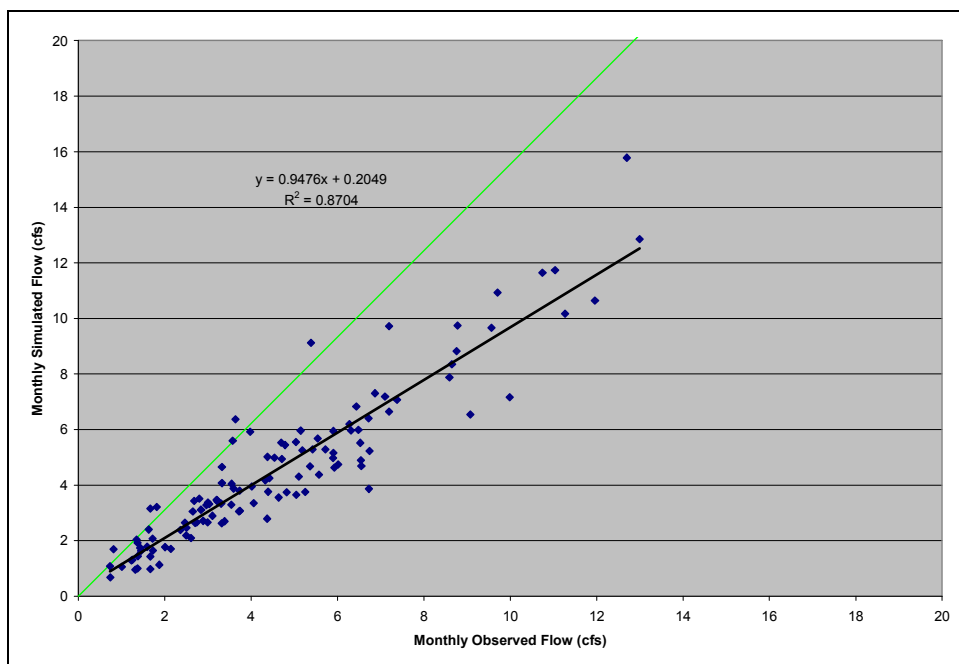


Figure 2-14. Scatter Plot. Simulated and Observed Monthly Average Flow. Watts Branch.

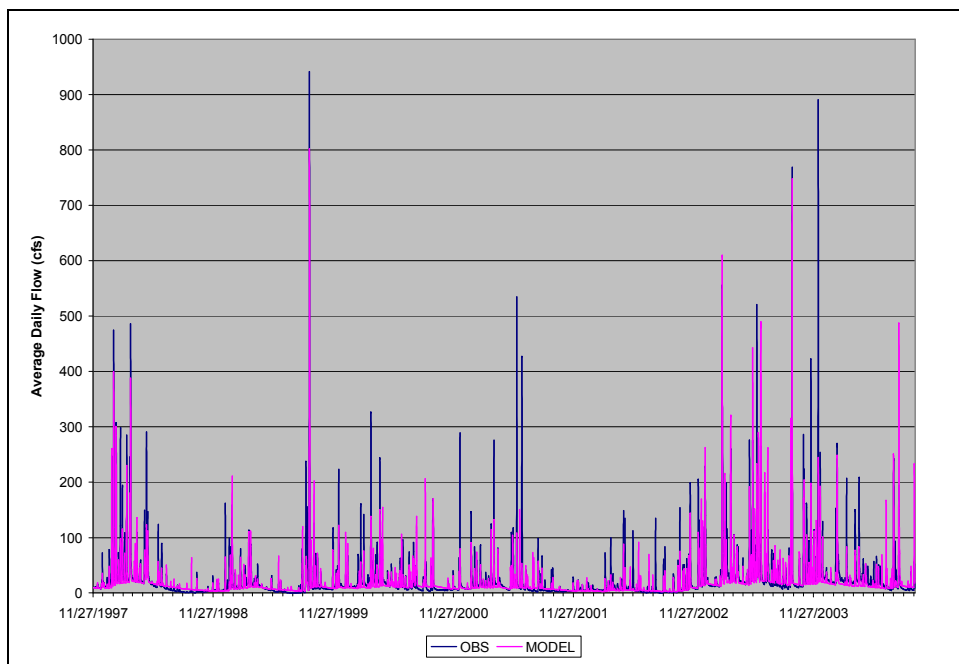


Figure 2-15. Time Series. Simulated and Observed Daily Average Flow. Northwest Branch at Colesville

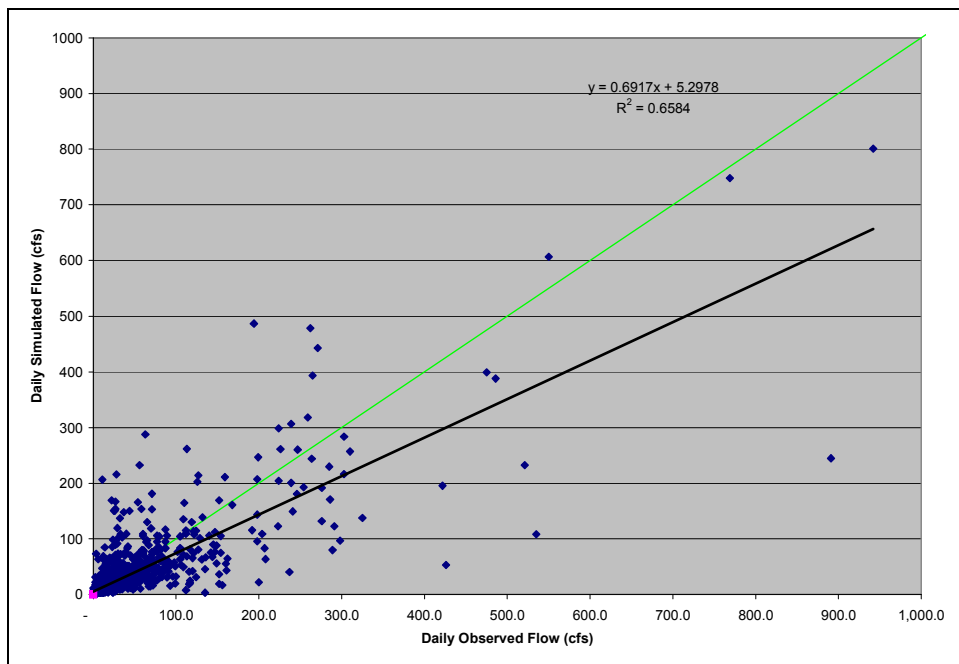


Figure 2-16. Scatter Plot. Simulated and Observed Daily Average Flow. Northwest Branch at Colesville

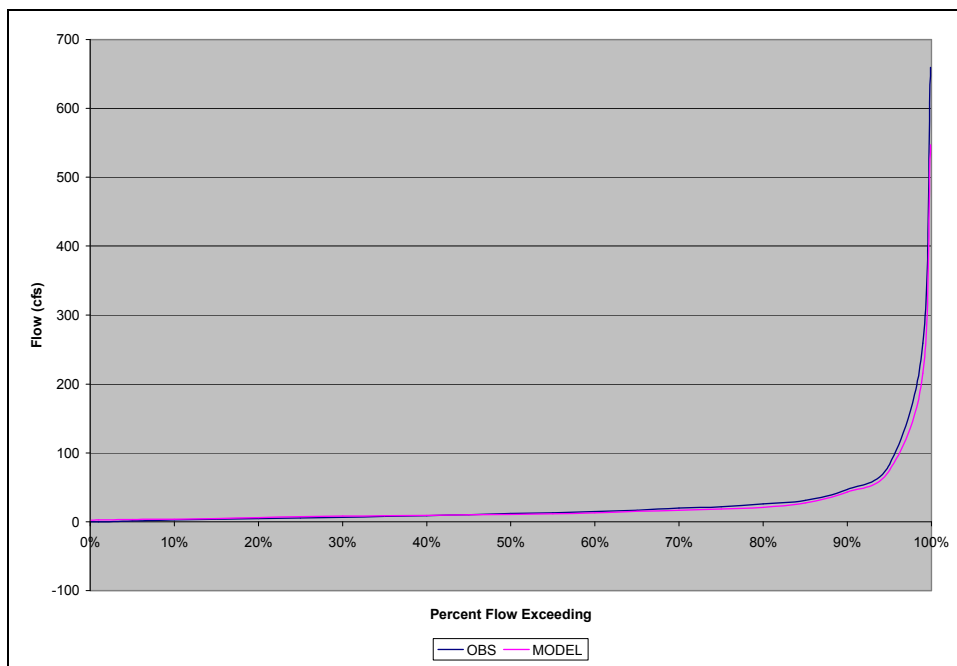


Figure 2-17. Cumulative Distribution Function. Simulated and Observed Daily Average Flow. Northwest Branch at Colesville

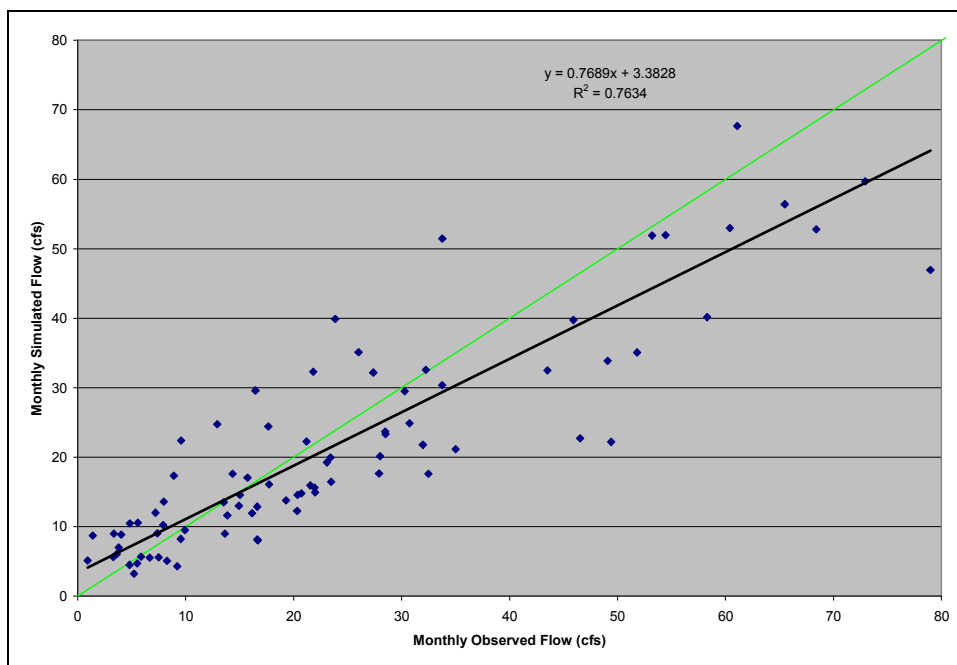


Figure 2-18. Scatter Plot. Simulated and Observed Monthly Average Flow. Northwest Branch at Colesville.

2.5 Sediment Calibration

HSPF is capable of simulating the erosion of sediment from the land surface in PERLND and IMPLND modules and the deposition and scour of sediment in river reaches. Both types of processes were represented in the Phase III Model.

The overall sediment calibration target was the average annual total suspended solids load at the Northeast and Northwest Branch gaging stations as calculated by ESTIMATOR for the Tidal Anacostia Model's simulation period 1995-1997 (see Appendix A for ESTIMATOR results). Calibration targets were determined for each source of sediment in the Anacostia River Watershed. Target loads for land uses were determined independently of the ESTIMATOR loads. Target loads for streambank erosion were determined based on the difference between overall TSS loads and the contribution to total loads from individual land uses. Target loads for streambank erosion for Lower Beaverdam Creek, Watts Branch, and individual subwatersheds within the Northeast and Northwest Branches were determined based on the ratio of ESTIMATOR loads to an independent estimate of streambank erosion. This erosion estimate was based on a regression equation from Evans *et al.*(2003). The determination of these targets is explained below.

2.5.1 Edge-of-Field and Edge-of-Stream Calibration Targets and Calibration Results

ESTIMATOR loads can provide calibration targets for river reaches and therefore for the watersheds as a whole. Edge-of-field (EOF) and Edge-of-stream (EOS) concentration or load targets help determine the contribution of individual land uses to the watershed load. The EOS load is the load delivered to the represented river or stream from the land segments. EOF loads represent the load leaving a field. It is primarily used to characterize sediment loads, since sediment losses can be measured from a field and losses from a field can be estimated using accepted techniques like the Universal Soil Loss Equation (USLE) or its descendent, the revised Universal Soil Loss Equation (RUSLE). Not all of the EOF sediment load is delivered to the stream or river. Some of it is stored on fields down slope, at the foot of hillsides, or in smaller rivers or streams that are not represented in the model. The ratio of the sediment load at a watershed outlet to the EOF load generated in the watershed is the sediment delivery ratio. The EOS sediment load can therefore be represented as the product of the EOF load and the sediment delivery ratio.

Crops and Pasture: Agricultural EOF load targets were based on National Resource Inventory's (NRI) estimated average annual erosion rates for cropland and pasture for Montgomery and Prince George's Counties. These same erosion rates were used as the target erosion rates for the CBP Phase 5 Watershed Model. Table 2-10 shows the target average annual erosion rates for these land uses. CBPO estimates that conservation tillage would reduce the erosion rate by about 25%. As shown in Table 2-3 crops grown at BARC include corn, soybean, small grains, and hay. No-till is applied on all crops. Therefore, given the level of conservation practice and crop composition, the average annual erosion rate from cropland was set at 25% of the NRI average value for Prince George's County.

EOS loads for these land uses were determined by applying a sediment delivery ratio based on watershed size, using the following formula (SCS, 1983):

$$\text{Sediment Delivery Ratio} = 0.417762 * (\text{Watershed Area})^{-0.134958} - 0.127097 \quad \text{Equation 1}$$

Table 2-11 gives the sediment delivery ratio for each segment.

Forests: Target EOF annual average erosion rates for forest were derived from NRI estimates of watershed erosion rates used in the Phase 2 of the CBP Watershed Model which have continued to be used, at smaller scales, in the Phase 5 CBP Watershed Model. The sediment delivery ratios shown in Table 2-11 were applied to forest EOF loads.

Developed Land: Calibration targets for developed land were derived from average event mean concentrations reported for monitoring (performed as part of the Phase I MS4 permits for Montgomery and Prince George's Counties) at monitoring sites within the Anacostia Watershed. Table 2-12 gives the average event mean concentration (EMC) by site and land use. The EMCs were used to derive calibration target annual average loads by multiplying the EMC by the average annual runoff, as simulated in the model. Pervious and impervious land had the same calibration targets. These loads from developed land represent EOS loads: following the Phase I and Phase II Anacostia Models, it was assumed that the runoff from developed land represented storm water delivered to streams and therefore no sediment delivery ratio was applied to these loads.

Simulation of Urban BMPs: The approach used in the Phase II Anacostia Model was used to represent the impact of urban best management practices (BMPs). Table 2-13 shows the estimated BMP reduction efficiency for the major types of BMPs. No BMPs were represented in the Prince George's County portion of the watershed, but Montgomery County provided an updated GIS layer with the location and classification of installed urban best management practices. Using this layer, the number of acres of each modeled land use type under each type of BMP was estimated. Table 2-14 shows the results. The reduction in load for each land use type was calculated using the information in Table 2-13 and Table 2-14. Since most of the urban load comes from impervious land, BMPs were applied to impervious land only. Table 2-15 shows the net reduction in load by segment and by land use type used in the model.

EOF and EOS Sediment Calibration Results: EOF and EOS sediment loads were calibrated by land use and segment against the appropriate target annual average loads. The ten-year simulation period, 1995-2004, was used to calculate simulated average annual loads. The calibration was performed by adjusting the washoff rate of sediment with runoff. Table 2-16 gives the calibrated washoff parameters for each segment and land use. Generally, simulated average annual sediment loads are within 2% of their target values.

Table 2-10. Edge-of-Field Erosion Yield Targets (tons/acre/year)

| Land Use | Montgomery | Prince George's |
|----------|----------------|-----------------|
| Forest | 0.36 | 0.34 |
| Crop | Not Applicable | 5.35 |
| Pasture | 1.23 | 2.99 |

Table 2-11. Sediment Delivery Ratios (SDR) and Segment Physiographic Provinces

| Segment | SDR | Province |
|---------|------|---------------|
| 10 | 0.16 | Piedmont |
| 20 | 0.18 | Piedmont |
| 30 | 0.19 | Piedmont |
| 40 | 0.17 | Piedmont |
| 50 | 0.19 | Piedmont |
| 60 | 0.19 | Piedmont |
| 70 | 0.17 | Coastal Plain |
| 80 | 0.17 | Coastal Plain |
| 90 | 0.18 | Coastal Plain |
| 100 | 0.15 | Coastal Plain |
| 120 | 0.19 | Coastal Plain |
| 130 | 0.21 | Coastal Plain |
| 140 | 0.26 | Coastal Plain |
| 150 | 0.23 | Coastal Plain |
| 210 | 0.21 | Piedmont |
| 270 | 0.24 | Coastal Plain |

Table 2-12. Calibration Target EOS TSS Concentrations for Developed Land Uses

| Land Use | Residential | Commercial | Industrial |
|--------------------------|-------------|------------|------------|
| TSS Concentration (mg/l) | 120 | 132 | 205 |

Table 2-13. Urban BMP Types and Efficiencies

| Structure_Type | Abbreviation | Efficiency |
|-----------------------------------|--------------|------------|
| Detention Structure, Dry Pond | DP | 0.1 |
| Extended Detention Structure, Dry | EDSD | 0.6 |
| Extended Detention Structure, Wet | EDSW | 0.6 |
| Infiltration Basin | IB | 0.9 |
| Oil/Grit Separator | OGS | 0.84 |
| Retention Structure, Wet Pond | WP | 0.8 |
| Sand Filter | SF | 0.85 |
| Shallow Marsh | SM | 0.8 |
| Underground Storage | UG | 0.8 |

Table 2-14. BMP Acres By Segment and Land Use

| Segment | Land Use | DP | EDSD | EDSW | IB | OGS | WP | SF | SM | UG |
|---------|------------|----|------|------|----|-----|----|----|-----|----|
| 10 | Commercial | 14 | 5 | | 2 | 8 | 10 | 5 | 2 | 0 |
| | HDR | 56 | 0 | 4 | | 21 | 31 | 0 | 1 | 0 |
| | LDR | 6 | | | | 0 | 18 | 0 | 7 | |
| | MDR | 68 | 0 | | 5 | 10 | 49 | 1 | 33 | |
| 20 | Commercial | 3 | 0 | 1 | | 26 | 12 | 3 | | 9 |
| | HDR | | 0 | | 2 | 1 | 0 | 0 | | |
| | LDR | 0 | | 1 | | 3 | 7 | 0 | | 0 |
| | MDR | 27 | | 3 | | 2 | 3 | 0 | | 2 |
| 30 | Commercial | 4 | | 26 | | 16 | 6 | 1 | 119 | 1 |
| | HDR | 1 | | 11 | | 1 | | | 33 | 0 |
| | Industrial | | | | | 0 | | 3 | | |
| | LDR | 2 | | 67 | | 3 | 0 | | 138 | |
| | MDR | | | 6 | | 1 | | | | |
| 40 | Commercial | 0 | | | | 11 | | 1 | | |
| | HDR | | | | | 1 | | | | |
| | LDR | 3 | | | | 0 | | 1 | | |
| | MDR | | | | | 0 | | | | |
| 50 | Commercial | 10 | | 0 | | 5 | 5 | 0 | 4 | 1 |
| | HDR | 3 | | | | | | | | |
| | LDR | 3 | | 1 | | 0 | 9 | | 0 | 0 |
| | MDR | 51 | 9 | 5 | | 1 | 10 | 1 | 3 | 0 |
| 60 | Commercial | 3 | 10 | 3 | 1 | 11 | 18 | 7 | | 2 |
| | HDR | 21 | 0 | | | 1 | 9 | | | |
| | Industrial | 20 | | 60 | | 29 | 15 | 4 | 1 | 4 |
| | LDR | | | 1 | | | | 0 | | 0 |
| | MDR | 13 | 29 | | 3 | 3 | 15 | 24 | | 0 |
| 70 | Commercial | 58 | 8 | 27 | 0 | 3 | 8 | 2 | 0 | 1 |
| | HDR | 56 | 9 | 9 | | 1 | 28 | | | |
| | Industrial | | | 5 | 0 | 4 | 2 | | | |
| | LDR | 1 | | 4 | | | 4 | | | |
| | MDR | 9 | 40 | 14 | | 1 | 53 | | | |
| 210 | Commercial | 4 | | | | 7 | 0 | | 4 | 0 |
| | HDR | | | | | | | | | 0 |
| | LDR | 0 | | | | | 8 | 1 | 2 | 1 |
| | MDR | | | | | | | 0 | 1 | |
| 270 | Commercial | 2 | 2 | 0 | 2 | 1 | | | | |
| | HDR | 12 | | | | | | | | |
| | Industrial | 0 | | | 0 | | | | 2 | |
| | LDR | | | 0 | | | 0 | | | |
| | MDR | 4 | | 37 | | | 6 | 2 | 0 | |

Table 2-15. Sediment BMP Reduction By Segment and Land Use

| Segment | Commercial | Industrial | LDR | MDR | HDR |
|---------|------------|------------|-----|-----|-----|
| 10 | 18% | | 15% | 16% | 21% |
| 20 | 19% | | 5% | 2% | 3% |
| 30 | 33% | 32% | 34% | 59% | 23% |
| 40 | 2% | | 1% | | |
| 50 | 29% | | 16% | 11% | 8% |
| 60 | 13% | 36% | 5% | 15% | 8% |
| 70 | 11% | 14% | 37% | 15% | 20% |
| 210 | 19% | | 21% | 2% | 39% |
| 270 | 13% | 2% | 2% | 28% | 5% |

Table 2-16. Calibrated Sediment Removal Rates (tons/inches/hour) By Segment and Land Use

| Segment | Pervious Residential | Impervious Residential | Pervious Commercial | Impervious Commercial | Pervious Industrial | Impervious Industrial | Forest | Pasture | Crop |
|---------|----------------------|------------------------|---------------------|-----------------------|---------------------|-----------------------|--------|---------|-------|
| 10 | 0.085 | 0.0521 | 0.094 | 0.0571 | 0.147 | 0.088 | 1.875 | 1.450 | |
| 20 | 0.085 | 0.0521 | 0.094 | 0.0571 | 0.147 | 0.088 | 2.125 | 1.650 | |
| 30 | 0.085 | 0.0521 | 0.094 | 0.0571 | 0.147 | 0.088 | 2.275 | 1.700 | |
| 40 | 0.085 | 0.0521 | 0.094 | 0.0571 | 0.147 | 0.088 | 2.100 | 1.600 | |
| 50 | 0.084 | 0.0521 | 0.092 | 0.0571 | 0.144 | 0.089 | 2.200 | 1.700 | |
| 60 | 0.084 | 0.0521 | 0.092 | 0.0571 | 0.144 | 0.089 | 2.200 | 1.700 | |
| 70 | 0.0645 | 0.0543 | 0.071 | 0.0595 | 0.110 | 0.0926 | 1.400 | 2.550 | 4.850 |
| 80 | 0.0645 | 0.0543 | 0.071 | 0.0595 | 0.110 | 0.0926 | 1.350 | 2.350 | 4.500 |
| 90 | 0.0645 | 0.0543 | 0.071 | 0.0595 | 0.110 | 0.0926 | 1.500 | 2.700 | 5.200 |
| 100 | 0.0645 | 0.0543 | 0.071 | 0.0595 | 0.110 | 0.0926 | 1.250 | 2.125 | |
| 120 | 0.075 | 0.0527 | 0.082 | 0.0578 | 0.128 | 0.0899 | 0.975 | 0.080 | |
| 130 | 0.075 | 0.0527 | 0.082 | 0.0578 | 0.128 | 0.0899 | 1.085 | 0.080 | |
| 140 | 0.075 | 0.0527 | 0.082 | 0.0578 | 0.128 | 0.0899 | 1.370 | 0.080 | |
| 150 | 0.075 | 0.0527 | 0.082 | 0.0578 | 0.128 | 0.0899 | 1.190 | 0.080 | |
| 210 | 0.085 | 0.0521 | 0.094 | 0.0571 | 0.147 | 0.088 | 2.400 | 1.87 | |
| 270 | 0.0645 | 0.0543 | 0.071 | 0.0595 | 0.110 | 0.0926 | 2.050 | 1.350 | |

2.5.2 Streambank Erosion Targets and Calibration Results

HSPF can simulate the fate and transport in river reaches of three sediment classes, which, generally speaking, represent sand, silt, and clay.

Sand: Sand transport is simulated as a fixed carrying capacity of the river as a power function of the velocity.

$$PSAND = KSAND * AVVELE ** EXPSND$$

Equation 2

where

PSAND = potential sandload (mg/l)

KSAND = coefficient in sandload suspension equation

EXPSND = exponent in sandload suspension equation

VVELE = average velocity (ft/sec)

If the amount of sand transported is less than the carrying capacity, sand erodes; if the amount transported is greater than the capacity, it deposits. EXPSND was set to 0 in the Piedmont and 2 in the Coastal Plain. The sand transport simulation is then calibrated by adjusting the linear coefficient, KSAND.

Silts and clays: Silts and clays are eroded if the shear stress, as internally calculated by HSPF, is above a threshold. For clay, the threshold was set at the 95th percentile hourly shear stress, calculated over the ten-year simulation period; for silt, the threshold was set at the 99th percentile hourly shear stress. The amount of erosion can then be calibrated by adjusting the mass erosion rate, M.

$$S = M * (TAUC / TAUCS - 1.0)$$

Equation 3

where

S = scour rate (tons/ft²/hr)

M = erodibility coefficient (kg/m²/hr)

TAU = shear stress (lbs/ft²)

TAUCS = critical shear stress (lbs/ft²)

Conversely, there is a deposition threshold for silt and clay. The amount of deposition is a function of the sediment class's fall velocity. The depositional threshold was set at low values, compared to the scour threshold, since the Anacostia River is an eroding system.

Overall streambank erosion target: The constituent monitored at the USGS gages is total suspended solids (TSS), which include volatile solids in addition to the fixed or inorganic solids represented by the sediment classes, sand, silt and clay. Because sand transport occurs at all velocities, as shown by the transport equation, the sand state variable was used to represent volatile solids that constitute a large share of TSS at low velocities, and KSAND was adjusted to provide TSS concentrations in the range 1 – 10 mg/l under low flow conditions.

The calibration target for the total suspended solids load for the Northeast and Northwest Branches was the average annual load for the period 1995-1997, as calculated using ESTIMATOR (see Appendix A). Since the EOS load from the land is fixed in the EOS calibration, the simulation of streambank erosion was adjusted until there was agreement between the simulated average TSS loads for the period 1995-1997 and the ESTIMATOR values. The streambank erosion targets for the Northeast and Northwest Branches are therefore the difference between the ESTIMATOR average annual loads for 1995-1997 and the average annual EOS loads for the same period.

Subwatershed streambank erosion targets: The overall streambank erosion target for the Northwest and Branches does not identify which subwatersheds the erosion comes from. It also does not provide streambank erosion targets for either Lower Beaverdam Creek or the Watts Branch, where there were not enough monitoring data to use ESTIMATOR to calculate sediment loads. Streambank erosion targets for these tributaries, as well as the subwatersheds of the Northeast and Northwest Branches, were set with the help of Evans *et al.*'s (2003) statistically-based streambank erosion algorithm.

Evans *et al.* developed a three-step algorithm for predicting streambank erosion based on variables that can be determined through GIS analysis. The streambank erosion algorithm is part of Pennsylvania State University's extension of the GWLF model, AVGWLF, which is used extensively in Pennsylvania to develop TMDLs for sediment and nutrients in watersheds primarily impaired by nonpoint sources (Evans *et al.*, 2002). The streambank erosion algorithm has also been adapted for use in Virginia's sediment and nutrient TMDLs (BSE, 2005).

Streambank erosion is calculated on the basis of a lateral erosion rate (LER)

$$\text{LER} = a * Q^{0.6} \quad \text{Equation 4}$$

Where Q is monthly average streamflow (m³/s) and "a" is coefficient determined by the following equation

$$a = (0.00147 * \text{PD}) + (0.000143 * \text{AD}) + (0.000001 * \text{CN}) + (0.000425 * \text{KF}) + (0.000001 * \text{MS}) - 0.00016 \quad \text{Equation 5}$$

where

- PD = percent developed land in the model segment
- AD = animal density (in animal equivalent units (AEU²s)/acre)
- CN = area-weighted curve number value of the model segment
- KF = area-weighted k factor of the model segment
- MS = mean topographic slope (in percent) of the model segment

Streambank erosion is then the product of the lateral erosion rate, streambank length (m), bank height (m), and soil bulk density (kg/m³).

² 1 AEU = 1000 lbs animal weight.

For the calculation of the “a” factor, percent developed land was derived from the MDP and MWCOG land use layers and included the residential, institutional, industrial, and commercial land use categories. BARC personnel (D. Shirley, personal communication) provided livestock populations for BARC, which has the only significant concentration of pastured animals in the Anacostia watershed. Percent mean topographic slope per model segment was estimated from the U.S. Geological Survey’s 1-arc second (*i.e.*, 30 meter resolution) National Elevation Data (NED). Area-weighted curve numbers and “k” factors were derived from the Natural Soil Groups of Maryland (NSG-MD) digital data layer (Maryland Department of State Planning, 1973), which includes “k” factors and hydrologic soil group (HSG) values among its soil attributes. Using the HSG values and assuming good hydrologic conditions, CN values were obtained from the USDA’s TR-55 manual (USDA, 1986). The USGS’s 1997 National Hydrography Dataset (NHD) was used to determine total stream length by modeling segment.

Table 2-17 shows the stream length by segment and the values of PD, AD, CN, KF, and MS used to calculate the “a” factor, which is also given in the table. The default bank height (1.5 m) and default bulk density (1500 kg/m^3) were used in the calculations. Monthly average flows were taken from the HSPF model.

Table 2-17 is somewhat misleading, in that streambank erosion was calculated for all the subwatersheds in a drainage area using a composite “a”-factor weighted by the stream length in each segment. When a drainage area consists of more than one segment, the streambank erosion for an individual segment is calculated by subtracting the contribution of upstream segments from the total for the drainage area. Table 2-18 gives the streambank erosion by segment.

It is unrealistic to expect the scour predicted by the calibrated HSPF model to agree with the streambank erosion calculated with the AVGWLF algorithm, since the regression equation for the a-factor, which is the heart of the algorithm, was determined with respect to the estimated sediment loads from GWLF. Average annual scour, as predicted by the HSPF model, is only somewhat larger than the estimate of average annual streambank erosion from the AVGLWF algorithm; average annual scour in the NW Branch is larger by a factor of 1.9, while average annual scour in the NE Branch is larger by a factor of 1.6. However, it is reasonable to suppose that the same factors that determine streambank erosion in the AVGWLF algorithm should determine the relative magnitude of scour in the HSPF Model. Therefore, the estimate of streambank erosion from the AVGWLF algorithm was used to determine the proportion of streambank erosion predicted by the HSPF model that originates in a segment. That proportion is also given in Table 2-18, and is relative to the Northwest Branch, Northeast Branch, or Lower Beaverdam Creek. The targets for Lower Beaverdam Creek and Watts Branch were determined by multiplying the streambank erosion, calculated according to the erosion algorithm for those streams, by the ratio of HSPF streambank erosion to the erosion from the streambank algorithm for the NE Branch.

Streambank erosion calibration results: Streambank erosion calibration targets, and therefore the overall calibration targets for the Northeast and Northwest Branches, were met successfully. Table 2-19 gives by segment the parameters for scour in river reaches that were used in the calibration.

The HSPF model was calibrated to the three-year window, 1995-1997. The average annual loads for the Northeast Branch, calculated over the ten-year simulation period, 1995-2004, matched those calculated for the same period using ESTIMATOR (Appendix A), but the HSPF model under-predicted Northwest Branch loads for the ten-year simulation period by about 15%.

Taking into account the under-prediction of loads on the Northwest Branch, the HSPF model reasonably captured monthly sediment loads on the Northwest and Northeast Branches, as calculated by ESTIMATOR over the ten-year simulation period, 1995-2004. Figure 2-19 and Figure 2-20 compare time series of monthly loads from the HSPF model and ESTIMATOR for the Northwest and Northeast Branches, respectively. Figure 2-21 and Figure 2-22 show scatter plots comparing monthly loads from HSPF and ESTIMATOR, and Figure 2-23 and Figure 2-24 show cumulative distribution plots comparing HSPF and ESTIMATOR results. The HSPF model captures the variability in ESTIMATOR monthly loads reasonably well. The coefficient of determination (R^2) is 0.60 for the Northwest Branch and 0.51 for the Northeast Branch. As the scatter plots show, HSPF tends to under-predict the largest ESTIMATOR loads and over-predict some of the smaller monthly loads. The cumulative distribution plots also show the under-prediction of the largest monthly loads calculated by ESTIMATOR. The HSPF estimate of the larger monthly loads, however, is generally within the 95% confidence interval for ESTIMATOR's predictions of the monthly loads.

Comparison With Previous Sediment Load Estimates: Table 2-20 compares the average annual sediment loads from the Phase III HSPF Model of the Non-tidal Anacostia River Watershed with the estimates from (1) the first two phases of model development, (2) the average annual sediment loads that were used in the TAM/WASP Sediment Model, and (3) the sediment loads from the Anacostia Watershed segment (540) of CBP Phase 4.3 Watershed Model.

As described in the introduction to this chapter, the phases of the Non-tidal Anacostia Model differ in their simulation period and the monitoring data that were used to calibrate the models. The Phase I Anacostia Model's load estimates stand out as larger than other estimates, and in retrospect were probably based on a mistaken calibration strategy, as was subsequently demonstrated by Mandel *et al.* (2003). The Phase I Model tried to match observed storm grab sample measurements to daily average simulated concentrations. Since instantaneous storm concentrations can be a good deal larger than daily averages, the model overestimated sediment loads during storm events. The Phase II Anacostia Model, in contrast, was calibrated against the observed storm loads.

The Phase I calibration strategy was devised to overcome the perceived inadequacy of the sediment load estimates used in the TAM/WASP model. For the TAM/WASP model, sediment loads for the NE and NW Branches were determined by first determining the median stormflow and baseflow concentrations for the NW Branch, as well as the baseflow concentration for the NE Branch—no stormflow data were available for the NE Branch until the completion of monitoring for the WASA LTCP. A baseflow separation was then performed on daily flow records at the NE and NW Branch gages using HYSEP. The daily load at each gage was then estimated as the sum of the product of the median concentration with its respective flow component. If there is a positive correlation of concentration with flow, as there is for TSS, this

procedure will underestimate storm loads. The Phase I Anacostia Model represents an overcorrection to the defects of the estimation of loads for the TAM/WASP Model.

As was explained above, the Phase II Anacostia Model was calibrated to specific storm loads. This is a methodologically sound procedure, but the simulation period of the Phase II Model was restricted to a period of sustained low-flow conditions punctuated by an extreme event. In contrast, by calibrating against monthly ESTIMATOR loads, the Phase III Anacostia Model was able to make efficient use of all of the data collected in the Anacostia, yet provide a flexible simulation period that would enable it to be used with the successor to the TAM/WASP model of the tidal river. Given the methodological defects of the first load estimates for the original TAM/WASP Sediment Model, it is not unreasonable to expect, as Table 2-20 shows, that the estimated average annual loads from the Phase III Anacostia Model would lie somewhere between the overestimated loads of the Phase I Anacostia Model and the sediment loads for the original TAM/WASP Model.

Comparing the estimates of average annual sediment loads from Lower Beaverdam Creek and Watts Branch is more difficult. As has been pointed out more than once before, there is no USGS gage on Lower Beaverdam Creek. Prince George's County does perform storm monitoring for its MS4 permit on Lower Beaverdam Creek, at the outlet of Segment 120. While there is a gage on Watts Branch, no storm monitoring is performed there. The TAM/WASP Sediment Model loads for these two streams are derived from HSPF Models. The Lower Beaverdam Creek model was developed by Tetra Tech (2000) on behalf of Prince George's County. The Watts Branch HSPF Model was developed from the TAM/WASP Eutrophication Model (Mandel and Schultz, 2000). The Tetra Tech model simulated sediment but the model was not calibrated against observed data. The HSPF model of the Watts Branch was calibrated to the extent possible without storm samples, which, in the case of simulating sediment, leaves room for considerable uncertainty.

The Phase I and II Anacostia Models did not simulate Watts Branch, but did try to calibrate sediment in Lower Beaverdam Creek using the Prince George's MS4 storm data. In both phases, as Table 2-20 shows, the average annual sediment load from Lower Beaverdam Creek was estimated to be about the same order of magnitude as the load from the NW Branch, despite the fact that Lower Beaverdam Creek is about one-third the size of the NW Branch. In other words, the sediment yield (load/acre) from Lower Beaverdam Creek would have to be about three times that of NW Branch. While Lower Beaverdam Creek is more heavily urbanized than the NW Branch as a whole, the difference in yield seemed greater than can be justified. TAM/WASP model tends to overestimate TSS concentrations in the vicinity of Lower Beaverdam Creek, which suggests that baseline loads from the Phase III Anacostia Model may already be too high. TAM/WASP simulations with sediment loads from Lower Beaverdam Creek larger than baseline loads would produce simulated TSS concentrations in the tidal Anacostia at variance with observed concentrations.

For these reasons, a consistent framework for setting sediment calibration targets was adopted for the Anacostia watershed as a whole, in which the scour target for both Lower Beaverdam Creek and Watts Branch was set on the basis of the observed sediment load at the Northeast Branch gage and a weighing factor derived from the AVGWLF streambank erosion algorithm, as

described in the previous section. Nevertheless, it should be noted that the Phase III Anacostia Model under-predicts peak sediment concentrations in Segment 120. Figure 2-25 compares the observed daily maximum TSS concentration with the maximum simulated concentration on the same day. The model consistently under-predicts the observed maximum, especially for observed concentrations over 1000 mg/l. It is unlikely, however, for the reasons given above, that average annual sediment loads from Lower Beaverdam Creek in the Phase III Anacostia Model, which are already four times the loads used in the original TAM/WASP sediment model, are in fact larger still again by the factor of two to five that would be necessary if HSPF simulated storm concentrations were to match the observed storm concentrations.

For the Watts Branch, average annual sediment loads simulated in the Phase III Anacostia Model are 38% less than the load estimates for the original TAM/WASP model but comparable to EPA Region III's estimate of an annual TSS load of 318 tons/year for the Watts Branch (USEPA, 2003). A more accurate accounting of loads from Lower Beaverdam Creek and Watts Branch is probably the most pressing need for improving the non-tidal HSPF Anacostia Model. Collecting storm samples on the Watts Branch at the gaging station is probably the best way to get more accurate load estimates for the lower Anacostia watershed, especially if they could be collected in such a manner that ESTIMATOR could be used to calculate monthly and annual loading rates.

The CBP Phase 4.3 Model is, like the Phase III Anacostia Model, an HSPF model. The 2000 Progress Scenario, which was used to compare to the Phase III Anacostia Model results, simulates 10 years of hydrology, 1985-2004, but represents 2000 land use and level of BMP implementation. No reaches are represented in the Anacostia segment of the model and the segment was not calibrated against any observed data in the Anacostia watershed. The Phase 5 Watershed Model is remedying these defects. It will have two reaches, one representing the NE Branch and one representing the NW Branch, and the model will be calibrated on each branch. It will be interesting to see, when Phase 5 is completed, if the Phase 5 sediment loads are larger than the Phase 4.3 loads because of the representation of scour in river reaches, and if the load estimates from the Phase 5 Model agree with the Phase III HSPF Model of the Non-tidal Anacostia Watershed.

Table 2-17. Watershed Factors Used in the AVGWLF Streambank Erosion Algorithm

| Segment | Percent Developed | Animal Density (AU/ha) | Average Curve Number | Average Soil K | Mean slope | a | Stream length (m) |
|---------|-------------------|------------------------|----------------------|----------------|------------|----------|-------------------|
| 10 | 73.200 | | 68.4 | 0.32 | 6.441 | 0.001127 | 81,311 |
| 20 | 84.501 | | 69.1 | 0.32 | 8.773 | 0.001296 | 108,831 |
| 30 | 91.059 | | 70.9 | 0.32 | 6.274 | 0.001392 | 13,848 |
| 40 | 86.993 | | 77.2 | 0.34 | 5.853 | 0.001347 | 169,230 |
| 50 | 63.195 | | 67.5 | 0.32 | 5.815 | 0.000980 | 27,518 |
| 60 | 87.562 | | 77.2 | 0.33 | 7.558 | 0.001351 | 56,843 |
| 70 | 61.278 | | 74.7 | 0.36 | 5.976 | 0.000972 | 101,678 |
| 80 | 21.004 | | 68.0 | 0.32 | 3.640 | 0.000354 | 58,711 |
| 90 | 59.182 | 0.074 | 79.6 | 0.36 | 4.680 | 0.000957 | 28,978 |
| 100 | 75.084 | | 79.7 | 0.34 | 5.372 | 0.001175 | 225,261 |
| 110 | 94.219 | | 81.9 | 0.35 | 4.572 | 0.001460 | 18,241 |
| 120 | 82.309 | | 82.6 | 0.36 | 6.232 | 0.001291 | 22,647 |
| 130 | 73.484 | | 77.5 | 0.34 | 6.965 | 0.001150 | 15,480 |
| 140 | 71.135 | | 83.4 | 0.37 | 6.198 | 0.001133 | 47,633 |
| 150 | 75.715 | | 78.5 | 0.35 | 7.683 | 0.001188 | 11,701 |
| 160 | 75.435 | | 81.4 | 0.36 | 5.201 | 0.001189 | 20,102 |
| 170 | 97.914 | | 86.3 | 0.36 | 7.156 | 0.001526 | 24,617 |
| 210 | 53.402 | | 66.6 | 0.32 | 5.171 | 0.000834 | 20,646 |
| 270 | 78.128 | | 77.6 | 0.41 | 7.712 | 0.001248 | 8,941 |

Table 2-18. AVGWLF Streambank Erosion Rates and HSPF Subwatershed Erosion Targets

| Segment | Average Annual Monthly Flow ^{0.6} (cfs) | Average Annual AVGWLF Streambank Erosion (tons/yr) | Fraction of Total Watershed Load | Average Annual HSPF Scour Target 1995-2004 (tons/yr) |
|---------|--|---|--|--|
| 10 | 73.8 | 1,686 | 0.18 | 2,953 |
| 20 | 93.2 | 1,648 | 0.17 | 2,887 |
| 30 | 43.1 | 242 | 0.03 | 424 |
| 40 | 129.2 | 5,871 | 0.61 | 10,285 |
| 50 | 38.9 | 306 | 0.02 | 492 |
| 60 | 63.9 | 934 | 0.07 | 1,504 |
| 70 | 99.5 | 2,240 | 0.16 | 3,608 |
| 80 | 62.2 | 377 | 0.03 | 608 |
| 90 | 60.6 | 490 | 0.04 | 789 |
| 100 | 181.2 | 9,337 | 0.68 | 15,038 |
| 120 | 50.3 | 429 | 0.36 | 691 |
| 130 | 35.0 | 182 | 0.15 | 293 |
| 140 | 70.7 | 587 | 0.49 | 946 |
| 150 | 28.6 | 116 | 1.00 | 187 |
| 210 | 30.8 | 155 | 0.02 | 3,406 |
| 270 | 24.0 | 78 | 0.01 | 1,559 |

Table 2-19. Scour Calibration Parameters

| Segment | KSAND | TAUCS-Silt | M-Silt | TAUCS-Clay | M-Clay |
|---------|-------|------------|--------|------------|--------|
| 10 | 5.0 | 0.235 | 6.8 | 0.137 | 0.058 |
| 20 | 5.0 | 0.756 | 2.5 | 0.434 | 0.020 |
| 30 | 2.5 | 0.558 | 0.24 | 0.269 | 0.003 |
| 40 | 2.5 | 0.311 | 8.4 | 0.176 | 0.007 |
| 50 | 0.01 | 0.597 | 1.6 | 0.333 | 0.027 |
| 60 | 0.01 | 0.455 | 2.9 | 0.226 | 0.022 |
| 70 | 0.01 | 1.048 | 16.8 | 0.670 | 0.025 |
| 80 | 0.01 | 0.252 | 3.3 | 0.147 | 0.023 |
| 90 | 0.01 | 0.739 | 2.4 | 0.364 | 0.024 |
| 100 | 0.10 | 0.251 | 37.0 | 0.154 | 0.024 |
| 120 | 0.2 | 0.178 | 1.75 | 0.091 | 0.160 |
| 130 | 0.2 | 0.451 | 0.99 | 0.234 | 0.090 |
| 140 | 0.2 | 0.097 | 4.0 | 0.052 | 0.500 |
| 150 | 0.067 | 0.212 | 0.10 | 0.016 | 0.007 |
| 210 | 3.75 | 0.316 | 1.25 | 0.130 | 0.008 |
| 270 | 0.01 | 0.35 | 1.75 | 0.230 | 0.0175 |

Table 2-20. Comparison of Average Annual TSS Load Estimates from Anacostia Models (tons/yr)

| Model | Reference | NW Branch | NE Branch | NW and NE Branches | Lower Beaverdam Creek | Watts Branch | Total Load to Tidal Anacostia River |
|---------------------------------------|------------------------------|-----------|-----------|--------------------|-----------------------|--------------|-------------------------------------|
| TAM/WASP | Schultz (2003) | | | 30,407 | 750 | 715 | 31,872 |
| Phase I | Manchester and Mandel (2001) | 26,109 | 23,637 | 49,746 | 21,422 | | 71,168* |
| Phase II | Mandel <i>et al.</i> (2003) | 4,960 | 15,817 | 20,777 | 6,334 | | 27,111* |
| Phase III | current report | 14,420 | 25,391 | 39,811 | 3,228 | 446 | 43,485 |
| CBP Watershed Model 4.3 2000 Progress | CBPO (2006) | | | | | | 27,621 |

* excludes Watts Branch

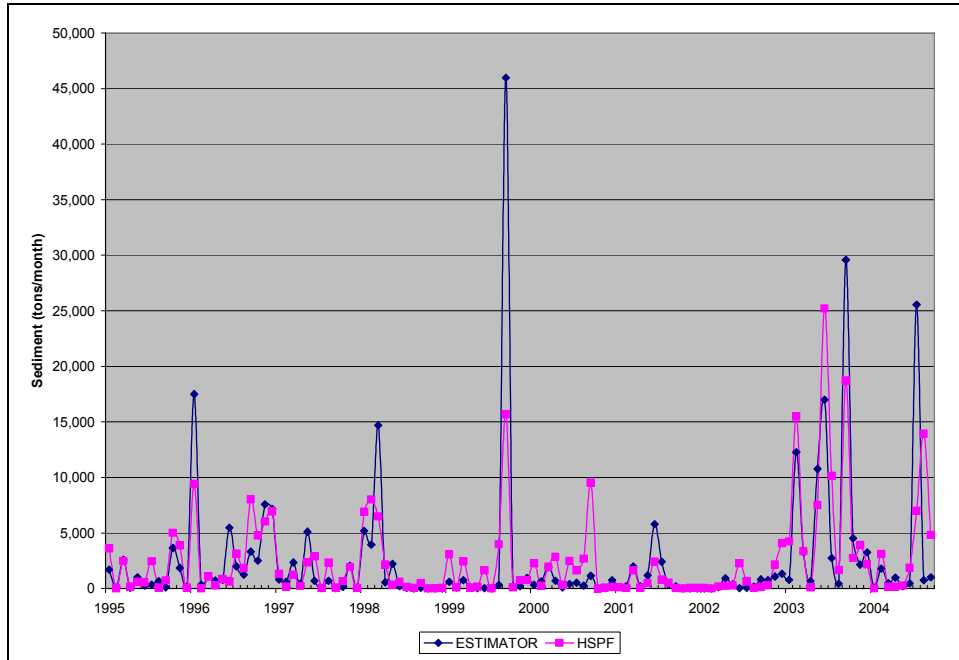


Figure 2-19. Time Series. ESTIMATOR and HSPF Monthly TSS Load. Northeast Branch.

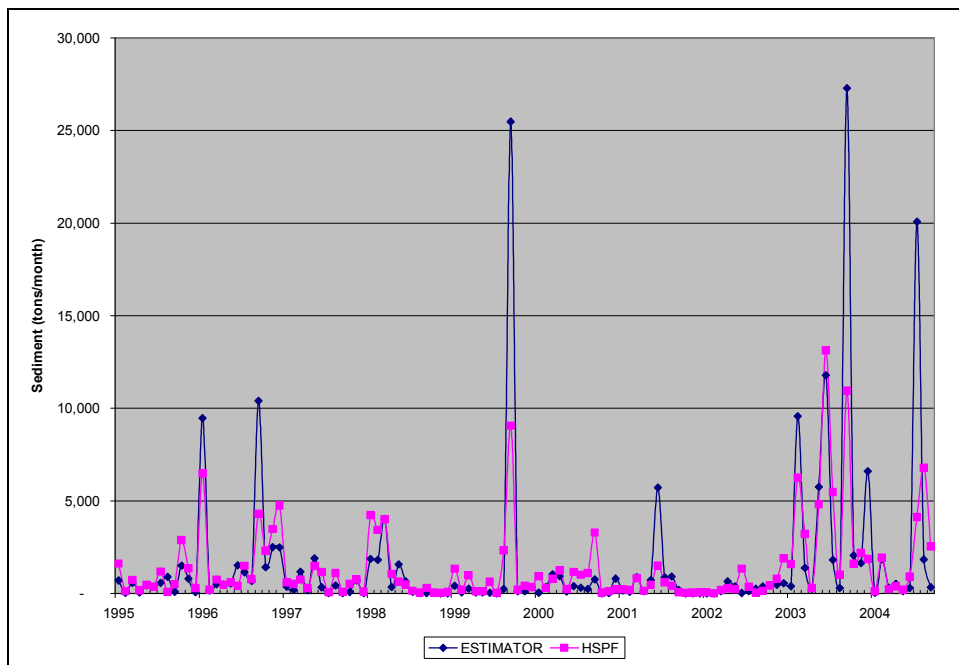


Figure 2-20. Time Series. ESTIMATOR and HSPF Monthly TSS Load. Northwest Branch

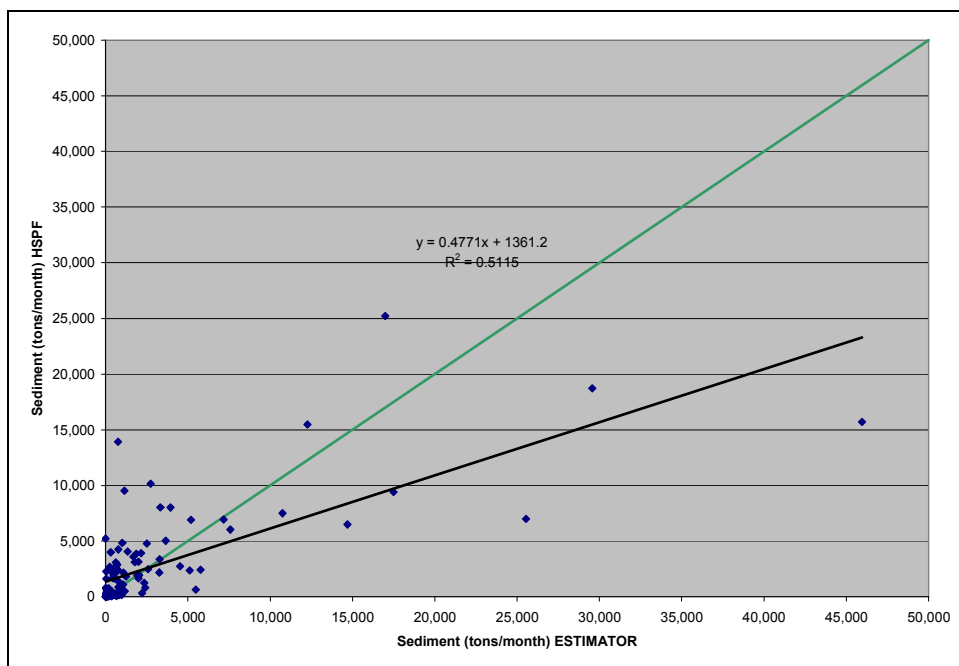


Figure 2-21. Scatter Plot. ESTIMATOR and HSPF Monthly TSS Load. Northeast Branch.

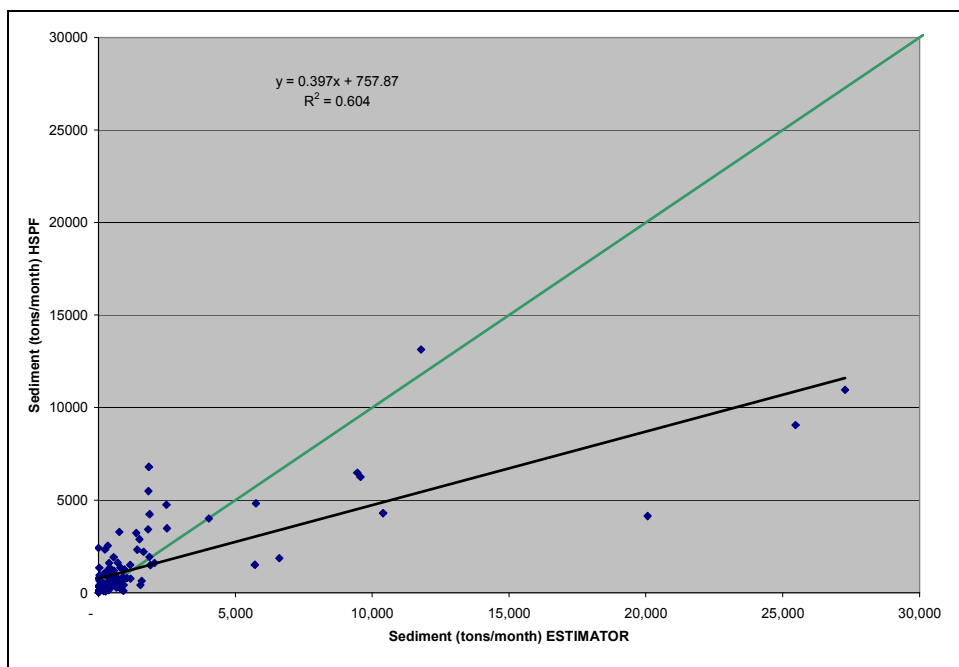


Figure 2-22. Scatter Plot. ESTIMATOR and HSPF Monthly TSS Load. Northwest Branch.

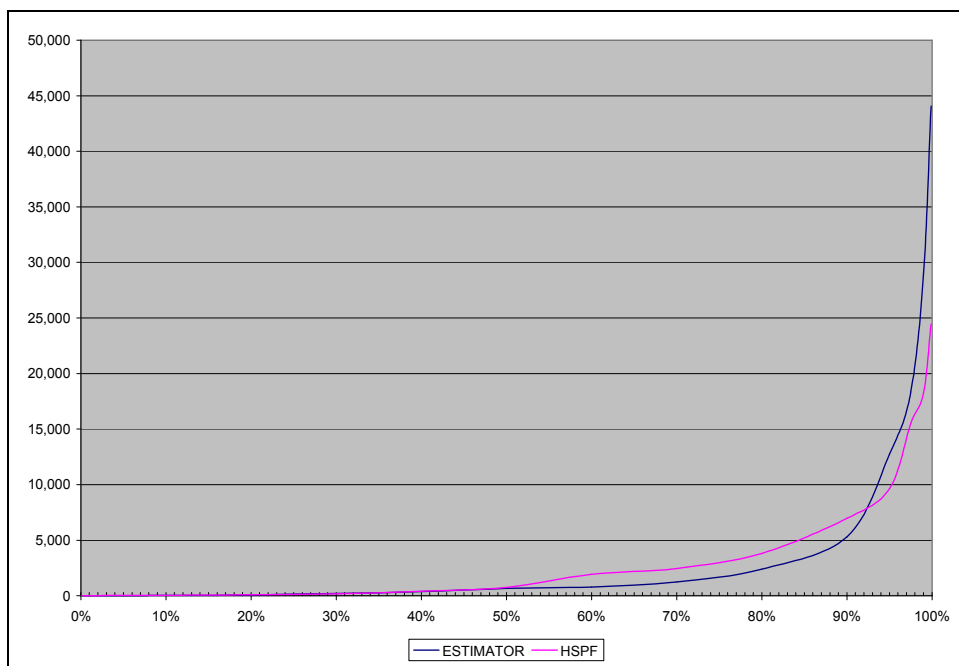


Figure 2-23. Cumulative Distribution Function. ESTIMATOR and HSPF Monthly TSS Load. Northeast Branch.

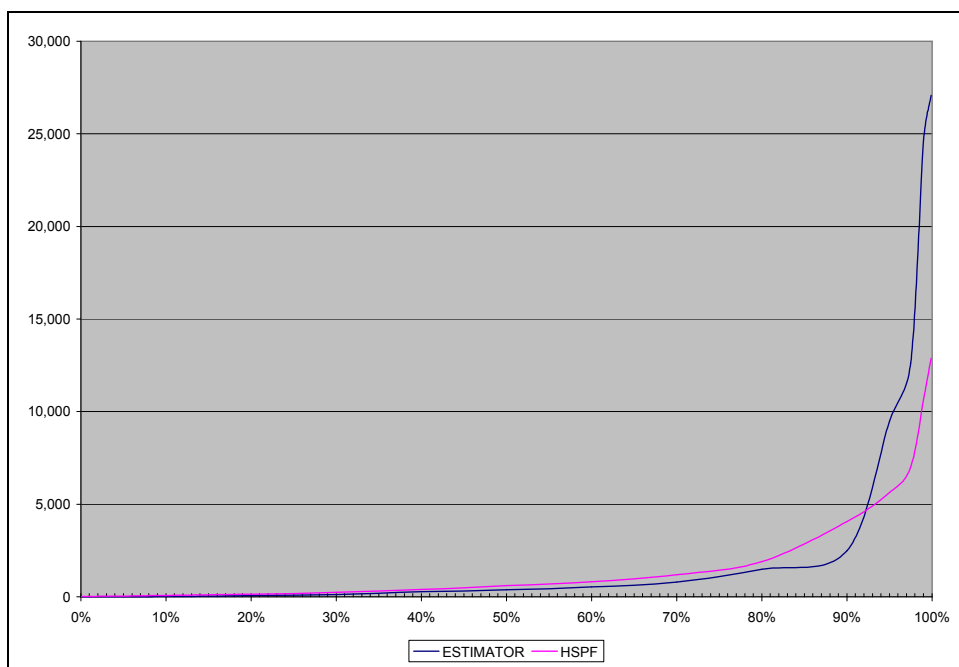


Figure 2-24. Cumulative Distribution Function. ESTIMATOR and HSPF Monthly TSS Load. Northwest Branch.

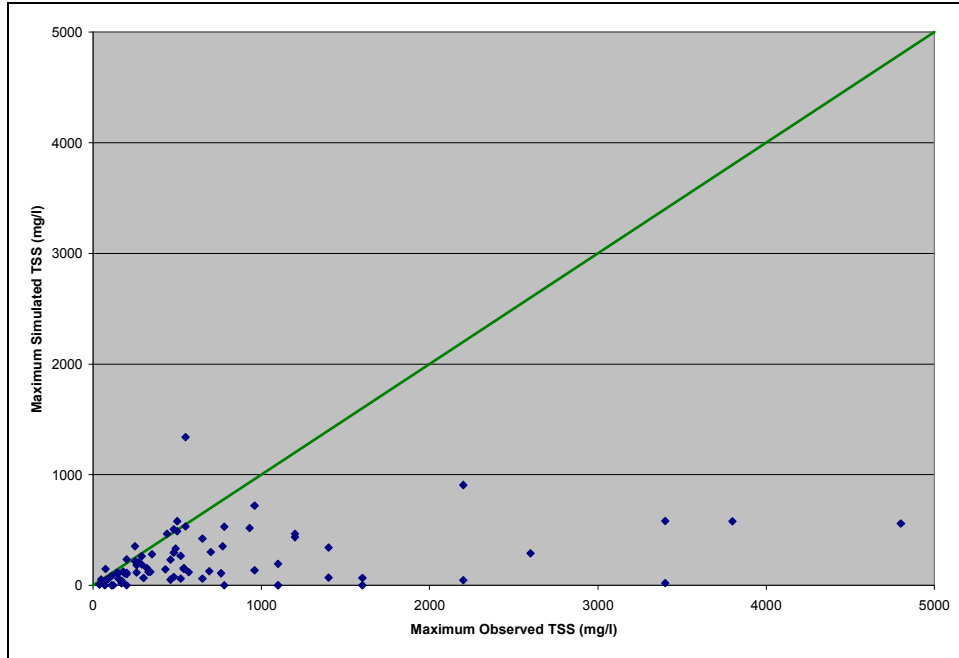


Figure 2-25. Observed and Simulated Daily Maximum TSS Concentrations, Lower Beaverdam Creek

3 VERSION 3 TAM/WASP TIDAL WATER CLARITY MODEL

3.1 Overview

This chapter describes Version 3 of the TAM/WASP water clarity model, a set of coupled computer programs which can simulate the loading, fate, and transport of pollutants in the tidal portion of the Anacostia River and predict daily concentrations of TSS, chlorophyll *a*, and Secchi depth. Earlier versions of TAM/WASP modeling components have been used in previous studies of the tidal Anacostia. The first version of TAM/WASP was used to simulate algal growth and sediment oxygen demand for the District of Columbia's Anacostia dissolved oxygen TMDL (Mandel and Schultz, 2000), and also to evaluate management options for the District of Columbia Water and Sewer Authority (DCWASA) Long Term Control Plan (LTCP) for combined sewer overflows (DCWASA, 2002). The model's sediment transport capabilities were further developed, in TAM/WASP Version 2 (Schultz, 2003), for use by the District of Columbia and by USEPA Region 3 for the tidal Anacostia sediment TMDL (DCDOH, 2002; USEPA, 2002a; 2002b). Version 3 of the model incorporates a number of upgrades, described below.

TAM/WASP is a one-dimensional (1-D) modeling framework, capable of simulating hydrodynamic and water quality variations along the length of the river, but making the assumption that conditions are uniform throughout any channel transect (*i.e.* from left bank to right bank and from the water's surface to the channel bottom). Approximating the river as a one-dimensional system is reasonable given the results of the summer 2000 SPAWAR study (Katz *et al.*, 2000), which concluded that throughout a channel transect the water in the river was generally well-mixed, and current velocities were relatively homogenous and primarily directed along the axis of the channel. It is also supported by model simulations carried out subsequent to a dye study conducted in 2000 by LimnoTech, Inc. (LTI) (LTI, 2000). These results showed that a 1-D model was capable of simulating the time evolution of dye concentrations in the tidal river fairly well (DC WASA, 2001; Schultz, 2003).

To support MDE's development of sediment TMDL load allocations for the tidal Anacostia River, the following four TAM/WASP components are used to predict water clarity conditions (as measured by Secchi disk depth). A schematic diagram depicting the linkage of these components is given in Figure 3-1.

- I. Hydrodynamic component, based on the Tidal Anacostia Model (TAM), originally developed at MWCOG in the 1980s (Sullivan and Brown, 1988). This component simulates the changes in water level and water flow velocities throughout the river due to the influence of tides and of flows from tributaries and sewer systems discharging into the tidal river. The TAM hydrodynamic model used in this study, described in detail in Schultz (2003), incorporates side embayments to model Kingman Lake, Kenilworth Marsh, and the tidal portions of tributaries.
- II. Load estimation component, constructed by ICPRB using Microsoft ACCESS. Water containing sediment and other pollutants flows into the river every day from a variety of sources, including the upstream tributaries (the NEB and NWB), the tidal basin tributaries (LBC, Watts Branch and others), the CSOs, the minor tributaries and separate storm (SS) sewer system, and ground water. The ICPRB load estimation component estimates daily water flows and pollutant loads into the river based on a variety of

methodologies, using USGS gage data, available monitoring data, USGS ESTIMATOR model results (see Appendix A), and Anacostia Phase 3 HSPF watershed model results, as described in Section 3.2.

- III. Sediment transport component, based on the USEPA's Water Quality Analysis Simulation Program, Version 5 (WASP-TOXI5) water quality model for solids and toxic contaminants (Ambrose *et al.*, 1993). This component simulates the physical processes that transport sediment that has entered the river, and estimates daily values of TSS in each model water column segment. The TAM/WASP sediment transport model includes ICPRB enhancements to WASP-TOXI5 which simulate sediment erosion and deposition processes more realistically, basing them on hydrodynamic conditions (see Mandel and Schultz, 2000; Schultz, 2003). The TAM/WASP sediment transport model used in this project, Version 3, has been upgraded to 38 segments (see Figure 3-2), and has undergone very minor adjustments to the calibration parameters used in Version 2 which govern erosion and settling.
- IV. Eutrophication component, based on the USEPA's Water Quality Analysis Simulation Program, Version 5 (WASP-EUTRO5) water quality model for dissolved oxygen, nutrients, and algae (Ambrose *et al.*, 1993). This component simulates the physical processes that affect dissolved oxygen levels in the river, and estimates daily concentrations of phytoplankton (algae), dissolved oxygen, and nutrients (Mandel and Schultz, 2000). The TAM/WASP eutrophication model used in this study, Version 3, has been upgraded to 36 segments, and incorporates new modifications by ICPRB which couple it to the sediment transport model and allow it to estimate daily water clarity conditions based on TSS and algae concentrations. This coupled model is capable of simulating the effect of potential solids load reductions on algal growth.

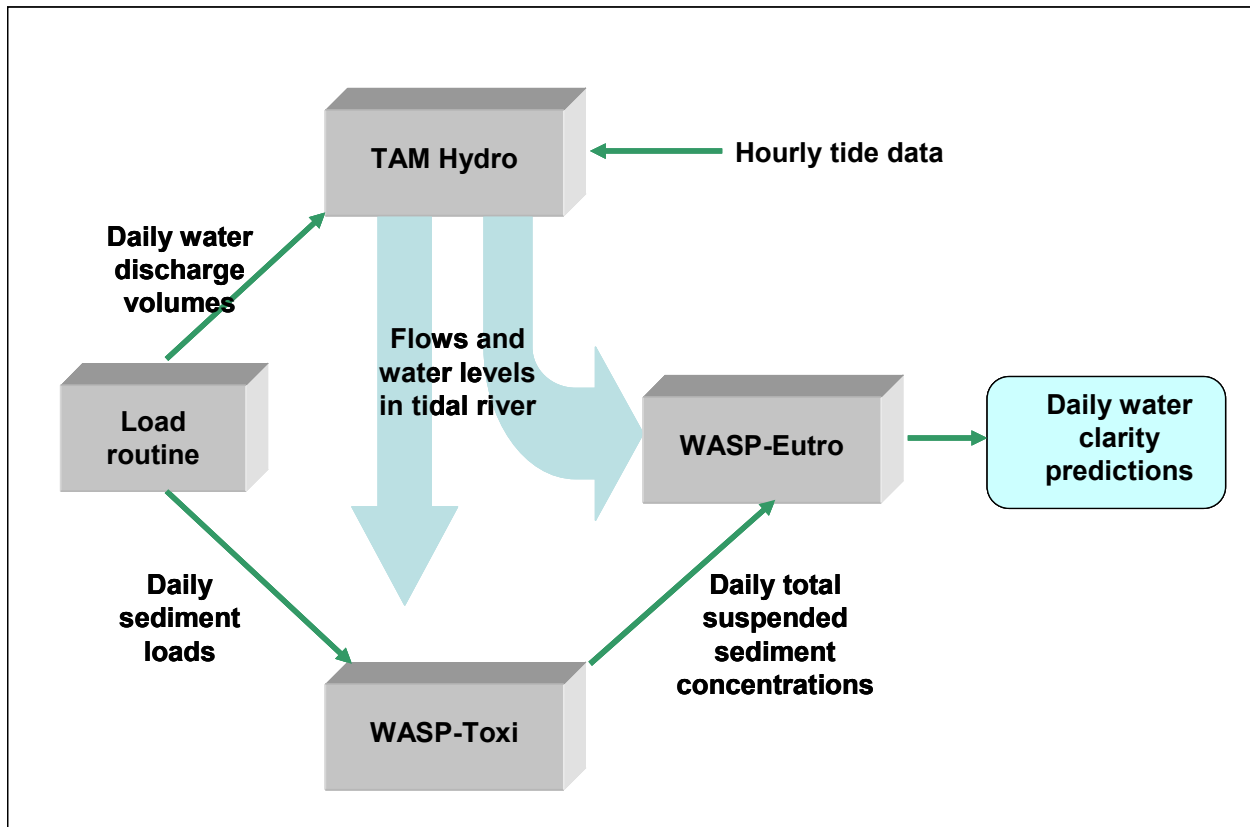


Figure 3-1. Schematic diagram of TAM/WASP water clarity model components

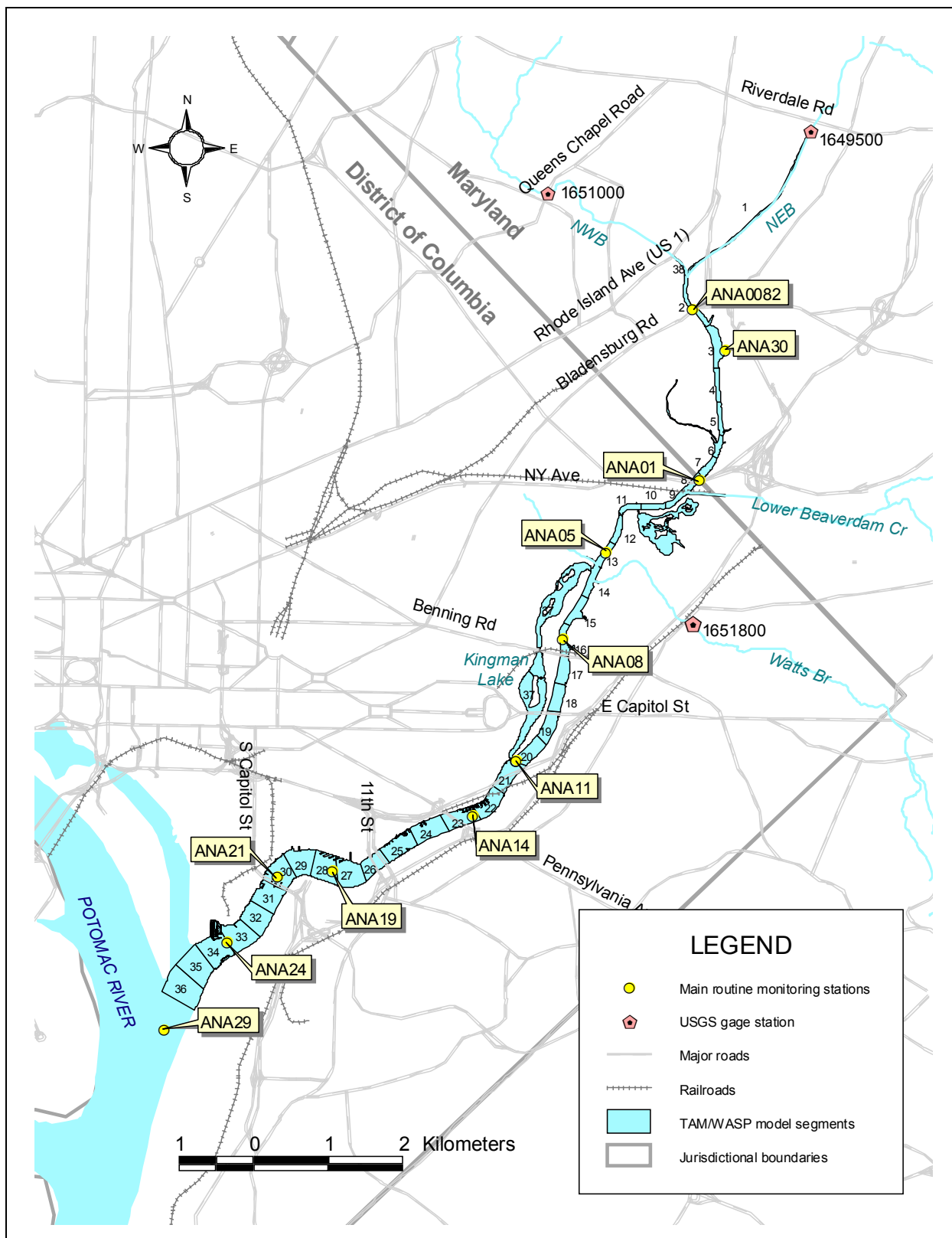


Figure 3-2. TAM/WASP V3 segmentation, with locations of main routine monitoring stations

3.2 Model inputs

3.2.1 Model geometry

Sediment transport component:

Version 3 of the TAM/WASP sediment transport model represents the main channel of the tidal Anacostia as a one-dimensional system of 36 segments, as pictured in Figure 3-2, where segment 1 represents the tidal portion of the NEB, from the USGS gage station at Riverdale Road to Bladensburg Road in Prince George's County, Maryland, and segments 2 through 36 represent portions of the tidal river's main channel from Bladensburg Road to the Anacostia's confluence with the Potomac in Washington, DC. Additionally, two model segments are represented as side embayments: segment 37, representing Kingman Lake, adjoins segment 20, and segment 38, representing the NWB, adjoins segment 2. In the Version 3 geometry, the demarcation of the head-of-tide of the Northwest Branch is the US 1 Bridge rather than upstream at the USGS gage station at Queens Chapel Road.

Segment geometry inputs, given in Table 3-1, are based on estimates of the average length, width, and depth of each of the reaches represented by the water column segments. Segment length and width estimates were obtained using the geographical information system (GIS) representation of the tidal river prepared by NOAA (George Graettinger, NOAA, private communication), based primarily on the National Capitol Parks - East GIS layer of the Anacostia River. Estimated segment widths range from approximately 21 meters for segment 1, the tidal NEB, to 508 meters for segment 36, just above the confluence with the Potomac. Average mean-tide segment depth estimates were also provided by NOAA based on 1999 depth sounding data provided by the U.S. Army Corps of Engineers (US ACE) (US ACE, 1999) and an additional data set collected in the summer of 2000 by the Navy's SPAWARs data collection team (see Katz *et al.*, 2000). NOAA used the ESRI Arcview Spatial Analyst software interpolation capabilities to estimate river depths at each point on a 10 ft by 10 ft grid. Average segment depths were then computed by averaging depths at all grid points within the segment. Estimated segment depths range from 1.0 meters for segments 1 and 2, to 5.6 meters for segment 31. The actual depth of segment 2, based on sounding data, is 0.54 m. However, because the TAM hydrodynamic model is not capable of simulating hydrodynamics of segments under nearly dewatered conditions, this depth was artificially increased to 1.0 m to allow the model to function throughout the model simulation period, including some very low tide days. For the same reason, model segments 1 and 38, representing the tidal portions of the Northwest and Northeast Branches, were artificially set at 1.0 m in depth, though no depth data was actually available in these locations.

The water column segments are underlain by two layers of sediment segments, as shown schematically in Figure 3-3. The uppermost layer of the sediment bed, represented by model segments 39 through 76, is 1 cm in depth. The next 5 cm of the sediment bed are represented by segments 77 through 114.

Eutrophication component:

Version 3 of the eutrophication component has been upgraded to the 36 segment geometry described by Schultz (2003). This geometry is essentially identical to that of the 38 segment

model, described above, except for the most upstream segment, which includes the tidal portion of the Northwest and Northeast Branch tributaries.

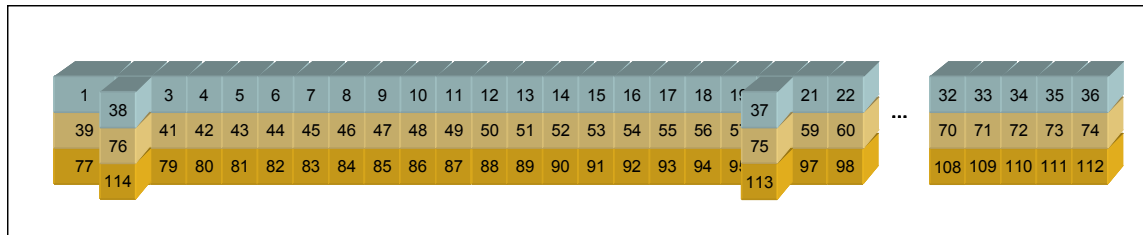


Figure 3-3. Schematic diagram of sediment transport model geometry

Table 3-1. Sediment transport model geometry

| Adjacent Embayment | WASP Segment Number | River Km (distance at midpoint from confluence) | Segment Length (m) | Segment Width (m) | Segment Depth (m from MSL) | Main Channel Area (m2) | Total Segment Area (m2) | Total Segment Volume (m3) | Transect Convey. Area (m2) | Transect Depth (m) | Mannings Roughness |
|--------------------|---------------------|---|--------------------|-------------------|----------------------------|------------------------|-------------------------|---------------------------|----------------------------|--------------------|--------------------|
| NWB | 1 | -1.30 | 2600 | 21.4 | 1.00 | 55,567 | 55,567 | 55,567 | 21 | 1.00 | 0.01 |
| | 2 | 0.48 | 959 | 71.3 | 1.00 | 68,413 | 68,413 | 68,413 | 46 | 1.00 | 0.01 |
| | 3 | 1.17 | 425 | 119.1 | 1.16 | 50,636 | 50,636 | 58,974 | 103 | 1.08 | 0.01 |
| | 4 | 1.61 | 450 | 58.0 | 2.21 | 26,090 | 26,090 | 57,634 | 149 | 1.69 | 0.01 |
| | 5 | 2.06 | 442 | 63.3 | 2.17 | 27,993 | 27,993 | 60,790 | 133 | 2.19 | 0.01 |
| Dueling Cr | 6 | 2.43 | 312 | 93.0 | 1.90 | 29,031 | 56,638 | 107,672 | 159 | 2.04 | 0.01 |
| | 7 | 2.74 | 305 | 92.6 | 1.86 | 28,246 | 28,246 | 52,621 | 175 | 1.88 | 0.01 |
| LBD Cr | 8 | 3.05 | 320 | 90.3 | 1.83 | 28,910 | 38,969 | 71,399 | 169 | 1.85 | 0.01 |
| | 9 | 3.37 | 315 | 74.4 | 2.06 | 23,424 | 23,424 | 48,159 | 160 | 1.94 | 0.01 |
| Kenilworth | 10 | 3.69 | 330 | 74.2 | 2.08 | 24,485 | 24,485 | 50,841 | 153 | 2.07 | 0.01 |
| | 11 | 4.01 | 312 | 77.4 | 2.02 | 24,163 | 212,343 | 429,707 | 155 | 2.05 | 0.01 |
| | 12 | 4.37 | 405 | 73.1 | 2.12 | 29,605 | 29,605 | 62,862 | 156 | 2.07 | 0.01 |
| Hickey Run | 13 | 4.76 | 370 | 86.0 | 1.78 | 31,814 | 33,630 | 59,946 | 155 | 1.95 | 0.01 |
| Watts Br | 14 | 5.17 | 445 | 96.7 | 1.50 | 43,021 | 44,126 | 66,311 | 150 | 1.64 | 0.01 |
| | 15 | 5.61 | 445 | 113.7 | 1.33 | 50,606 | 50,606 | 67,539 | 149 | 1.42 | 0.01 |
| Kingman | 16 | 6.06 | 453 | 105.3 | 1.92 | 47,681 | 47,681 | 91,427 | 178 | 1.63 | 0.01 |
| | 17 | 6.48 | 375 | 146.1 | 1.84 | 54,799 | 54,799 | 100,967 | 236 | 1.88 | 0.02 |
| | 18 | 6.85 | 375 | 157.5 | 1.50 | 59,057 | 59,057 | 88,644 | 254 | 1.67 | 0.02 |
| | 19 | 7.25 | 425 | 164.3 | 1.30 | 69,840 | 69,840 | 91,030 | 226 | 1.40 | 0.02 |
| | 20 | 7.68 | 435 | 185.0 | 1.33 | 80,459 | 80,459 | 107,235 | 230 | 1.32 | 0.02 |
| | 21 | 8.12 | 440 | 205.4 | 1.92 | 90,378 | 90,378 | 173,920 | 318 | 1.63 | 0.02 |
| | 22 | 8.56 | 440 | 199.4 | 1.97 | 87,758 | 87,758 | 173,103 | 394 | 1.95 | 0.03 |
| | 23 | 9.01 | 455 | 218.8 | 1.98 | 99,535 | 99,535 | 197,156 | 413 | 1.98 | 0.03 |
| | 24 | 9.46 | 460 | 242.5 | 2.05 | 111,543 | 111,543 | 228,666 | 465 | 2.02 | 0.03 |
| | 25 | 9.92 | 460 | 235.8 | 3.43 | 108,481 | 108,481 | 371,704 | 655 | 2.74 | 0.03 |
| | 26 | 10.34 | 365 | 218.3 | 4.31 | 79,676 | 79,676 | 343,557 | 879 | 3.87 | 0.03 |
| | 27 | 10.69 | 353 | 340.3 | 4.58 | 120,140 | 120,140 | 550,303 | 1242 | 4.45 | 0.06 |
| | 28 | 11.03 | 323 | 353.4 | 5.10 | 114,137 | 114,137 | 582,039 | 1679 | 4.84 | 0.06 |
| | 29 | 11.36 | 335 | 348.3 | 5.28 | 116,693 | 116,693 | 616,495 | 1821 | 5.19 | 0.06 |
| | 30 | 11.70 | 335 | 347.4 | 5.10 | 116,383 | 116,383 | 593,380 | 1806 | 5.19 | 0.06 |
| Kingman | 31 | 12.03 | 335 | 351.2 | 5.61 | 117,642 | 117,642 | 660,057 | 1870 | 5.35 | 0.06 |
| | 32 | 12.36 | 320 | 368.2 | 5.36 | 117,829 | 117,829 | 631,411 | 1973 | 5.48 | 0.06 |
| | 33 | 12.70 | 355 | 376.8 | 4.81 | 133,762 | 133,762 | 642,905 | 1893 | 5.08 | 0.06 |
| | 34 | 13.06 | 365 | 415.2 | 4.25 | 151,554 | 151,554 | 644,722 | 1794 | 4.53 | 0.06 |
| | 35 | 13.41 | 340 | 447.0 | 4.25 | 151,978 | 151,978 | 645,249 | 1832 | 4.25 | 0.06 |
| | 36 | 13.75 | 350 | 507.9 | 4.25 | 177,761 | 177,761 | 756,277 | 2029 | 4.25 | 0.06 |
| | 37 | | | | 1.33 | 250,000 | 250,000 | 333,197 | 2161 | 4.25 | 0.06 |
| | 38 | | | | 1.00 | 6,357 | 6,357 | 6,357 | 150 | 1.32 | 0.06 |
| NWB | | | | | | | | | 24 | 1.00 | |
| Totals: | | | | | | | 3,234,215 | 9,948,234 | | | |

3.2.2 Tide data

Tide data are used to determine the downstream water level boundary condition in the TAM hydrodynamic model. Hourly tidal heights were downloaded from the National Oceanic and Atmospheric Administration (NOAA) website, Tides Online (<http://tidesonline.nos.noaa.gov/>) for Station 8594900, which is located in the Washington Ship Channel in Washington, DC. Information on vertical datum for this station is given in Table 3-2. Tidal heights were downloaded in local standard time, in units of meters from the vertical datum, MLLW (mean low low water) for the National Tidal Datum Epoch (NTDE), 1983 to 2001³. For TAM/WASP Version 2, adjustments had been made to the tidal height data set to account for several periods of time for which no data were available and several days when extremely low tides caused dewatering of some model segments (see Schultz, 2003), a condition that cannot be handled in the current TAM/WASP framework. In Version 3, 0.1 to 0.4 meters were added to observed tidal heights from 10 pm, March 31 through 1 pm, April 1, 1997, to avoid dewatering when running the model for the 1995-97 time period. Additionally, 0.1 to 0.4 meters were added during certain hours of 11/21/1989 and 2/25/1990.

Table 3-2. Vertical datum for NOAA tide station, 8594900, located in the Washington Shipping Channel

| Tidal Datum | Height in Meters |
|---|------------------|
| Highest observed water level (10/17/1942) | 3.368 |
| Mean Higher High Water (MHHW) | 0.965 |
| Mean High Water (MHW) | 0.896 |
| Mean Sea Level (MSL) | 0.472 |
| North American Vertical Datum – 1988 (NAVD) | 0.425 |
| Mean Low Water (MLW) | 0.047 |
| Mean Lower Low Water (MLLW) | 0.000 |
| Station Datum | -1.387 |
| Lowest observed water level (2/26/1967) | -1.539 |

³ The National Tidal Datum Epoch (NTDE) is a 19-year period of tidal observations used to compute tidal datums such as MSL and MLLW. Earlier versions of the TAM/WASP model used tide data based on the old NTDE of 1960-1978. MSL (Mean Sea Level, as measured from the fixed Station Datum) for this earlier NTDE was 0.070 meters lower than for the current NTDE. MLLW for the earlier NTDE was 0.073 meters lower than for the current NTDE.

3.2.3 *Tributary, separate storm sewer system, and CSO flows*

Water flows into the tidal portion of Anacostia from many sources: from the Northeast Branch and Northwest Branch upstream tributaries, from combined sewer system and separate storm sewer system outfalls, from the Watts Branch, Lower Beaverdam Creek and other tidal tributaries, from direct drainage (*i.e.*, overland flow from areas adjacent to the river banks), and from ground water discharge. These flows are represented in TAM/WASP as daily flow inputs into each of the model segments.

Daily flows from the two major drainage areas upstream of the tidal river, the Northeast Branch and Northwest Branch tributary sub-sheds, are obtained directly from data for USGS gage station 01649500 on the Northeast Branch at Riverdale Road and station 01651000 on the Northwest Branch at Queens Chapel Road. Daily mean discharge data in cubic feet per second (cfs) from each of the stations were used to calculate flow from the non-tidal portion of the Northeast and Northwest Branch drainage areas. The Northwest Branch discharge was multiplied by 1.07653 to account for the contribution from the non-tidal drainage area between the USGS gage station and the US 1 (Baltimore Avenue) Bridge (see Figure 3-2).

Daily flow inputs from Watts Branch and Lower Beaverdam Creek sub-sheds were computed using output from the Phase 3 Anacostia HSPF watershed model, as described in Section 2 of this report. Flow inputs from minor tributaries and major separate storm sewer (SS) outfalls in the remaining portion of the “tidal drainage area” are based on a delineation of sub-sheds of the tidal drainage area by MWCOG (see Shepp *et al.*, 2000), and on a delineation of direct drainage sub-shed boundaries by ICPRB. Because no flow data exists for these minor tributary and SS sub-sheds, flows were computed using the sub-shed delineations and using HSPF model predictions of flow per acre for Watts Branch for three landuse categories, urban impervious, urban pervious, and forest. The locations of sub-shed outfalls relative to TAM/WASP segment boundaries, and the identification of sub-sheds associated with outfalls, given in Table 3-3, were determined by ICPRB using best engineering judgment based on partial information obtained from GIS layers prepared for the District Government by LTI in 1995 (LTI, 1995) and the DC Sewerage System map (DCWASA, 1986). Flows entering the tidal river from stream base flow and from ground water inflows are also estimated from HSPF model output.

A combined sanitary sewer and storm sewer system (CSS) drains over eight square miles of the Anacostia basin in the District of Columbia. During dry weather, effluent from this system flows to the District’s Blue Plains waste water treatment plant. However, during certain storm events, combined system overflows (CSOs) occur, and effluent from 17 CSO outfalls discharge directly into the tidal Anacostia River. The two largest are the Northeast Boundary CSO, which drains into the Anacostia near RFK Stadium, and the “O” Street Pump Station, just below the Navy Yard. Locations of the major CSO outfalls discharging into the tidal Anacostia are given in Table 3-3. The total daily flow for all model segments to the tidal Anacostia River from combined sewer overflows was originally estimated by ICPRB based on National Airport precipitation data using the regression equation developed by Whitney Brown of the COG (Sullivan and Brown, 1988; Mandel and Schultz, 2000).

Table 3-3. Sub-basins of the tidal drainage area of the Anacostia Watershed⁴

| Sub-Shed ID | Sub-shed Description | Model Segment⁵ | Bank | Type⁶ | Outfall Description⁷ |
|--------------------|-----------------------------|----------------------------------|-------------|-------------------------|---|
| 1 | Fort Lincoln | 11 | West | SSTrib | 66" diameter outfall located 200' east from eastern-most part of S Dakota Ave ramp to NY Ave |
| 2 | Hickey Run | 13 | West | SSTrib | open channel |
| 3 | Langston North | 37 | West | SSTrib | NA |
| 4 | Langston South | 37 | West | SSTrib | 48" corrugated metal pipe located southeast of M St and Maryland Ave |
| 5 | Spingam High School | 37 | West | SSTrib | 4' 6" diameter outfall located 150' north of Benning Rd Br |
| 6 | Oklahoma Ave | 37 | West | SSTrib | 54" diameter outfall located 700' north of E Capitol St Br |
| 7 | RFK Stadium | 37 | West | SSTrib | 6' x 5' outfall located 500' north of E Capitol St Br |
| 8 | NE Boundary Sewer | 21 | West | CSO | 15' 6" x 8' 6" outfall adjacent to service drive behind Swirl Facility and DC General |
| 9 | Barney Circle | 23 | West | CSO | 4' 6" x 9' outfall at Barney Circle and PA Ave |
| 10 | Area North of Navy Yard | 24 | West | CSO | 6' x 5' outfall at M and Water Streets |
| | | 26 | West | CSO | 5' diameter outfall at 12 th and O Streets, SE |
| | | 27 | West | CSO | 2' 6" x 3' 9", or 4' outfall on Navy Yard property, just upstream of the 5 piers, from narrow channel |

⁴ From Schultz (2003).

⁵ Using Version 3 segment numbers; based on ICPRB's best engineering judgement using partial information from GIS layers produced by LTI (see LTI, 1995) and the DC Sewerage System map (DCWASA, 1986).

⁶ SSTrib = separate storm sewer system and minor tributaries; CSO = combined sewer overflow; Watts = Watts Branch; LBD = Lower Beaverdam Creek.

⁷ Based on ICPRB's best engineering judgement using partial information from GIS layers produced by LTI (see LTI, 1995) and the DC Sewerage System map (DCWASA, 1986); NA = not available.

| Sub-Shed ID | Sub-shed Description | Model Segment ⁵ | Bank | Type ⁶ | Outfall Description ⁷ |
|-------------|---------------------------------|----------------------------|------|-------------------|---|
| | | 28 | West | CSO | 6' 3" diameter outfall on Navy Yard property, just downstream of the 5 piers |
| 11 | 6 th Street area | 28 | West | SSTrib | 13' x 18' outfall (Paul Miller, private communication) |
| 12 | B St/New Jersey Ave/Tiber Creek | 29 | West | CSO | 8' x 7' outfall (B St/NJ Ave) located at Main St. and O St. Pump Station |
| | | 29 | West | CSO | 4' 6" x 4' 3" outfall in SE Federal Center, aligned with 4th Street |
| | | 29 | West | CSO | 15' diameter outfall (B St/NJ Ave) located at Main St. and O St. Pump Station |
| | | 29 | West | CSO | 12' x 10' 6" outfall (relief sewer) located at Main St. and O St. Pump Station |
| | | 29 | West | CSO | 10' x 12' 6" outfall (Tiber Cr.) located at Main St. and O St. Pump Station |
| | | 29 | West | CSO | 54" diameter outfall (Canal St.) located at Main St. and O St. Pump Station |
| 13 | First Street | 30 | West | SSTrib | 60" diameter outfall located 1000' north of Douglass Bridge and 600' south of Main Sewerage Pumping Station |
| 14 | Buzzard Point | 33 | West | SSTrib | 7' 6" x 6' outfall located 1400' north of Greenleaf Point, 400' north of marina area |
| 15 | Nash Run via Kenilworth | 11 | East | SSTrib | NA |
| 16 | Watts Branch | 14 | East | Watts | open channel |
| 17 | Clay Street | 17 | East | SSTrib | 10' x 7' outfall 1400' north of E. Capital St. Bridge |
| 18 | Piney Run area | 19 | East | SSTrib | 21' x 7.5' outfall just south of East Capital St. Bridge |
| 19 | Ely's Run | 19 | East | SSTrib | 90" diameter outfall located 1200' south of E. Capital St. Bridge |
| 20 | Fort Dupont | 20 | East | SSTrib | 8' x 6' outfall located 1440' north of Conrail Bridge overpass |
| 21 | Pope Branch | 21 | East | SSTrib | concrete outfall located 2000' north of Sousa Bridge, and 400' south of RR Br |
| 22 | Texas Ave Tributary | 22 | East | SSTrib | 6' 9" x 6' outfall located 1200' north of Sousa Bridge, referred to as Naylor Run |
| | | 22 | East | SSTrib | 42" diameter outfall located 1100' north of Sousa Bridge |

| Sub-Shed ID | Sub-shed Description | Model Segment ⁵ | Bank | Type ⁶ | Outfall Description ⁷ |
|-------------|--|----------------------------|------|-------------------|---|
| 23 | Pennsylvania Ave | 23 | East | SSTrib | 72" diameter outfall located 600' north of Sousa Bridge |
| 24 | 22nd Street area | 23 | East | SSTrib | 42" diameter outfall located 150' south of Sousa Bridge, referred to as Young |
| 25 | Naylor Road area | 24 | East | SSTrib | 8' x 6' outfall located 1600' south of Sousa Bridge and 800' north of Anacostia Recreation Center |
| 26 | Fort Stanton | 25 | East | SSTrib | 6' x 6' outfall located 1100' north of 12 th St. Bridge and 300' south of Anacostia Pool and Recreation Center |
| 27 | Old Anacostia | 26 | East | CSO | 2' 6" x 8' / 5' x 12' outfall located between 11th St and Anacostia Bridges |
| | | 26 | East | CSO | 4' x 4' outfall located at Good Hope Rd and Welsh Memorial Bridge |
| | | 27 | East | CSO | 6' x 5' 3" outfall across from Navy Yard |
| 28 | Suitland/Stickfoot | 28 | East | SSTrib | 11' diameter outfall located 1000' upstream of Main Sewerage Pumping Station |
| 29 | Poplar Point/Howard | 31 | East | CSO | 5' x 5' 5" outfall (bypass sewer) located at Howard Rd and Robbins Rd |
| 30 | I-295/St. Elizabeth's Hospital (south) | 31 | East | SSTrib | 90" diameter outfall located 400' south of Douglas Bridge across river from Capital Ave |
| 33 | Lower Beaverdam | 8 | East | LBD | open channel |
| 35 | Dueling Creek | 6 | West | SSTrib | open channel |

Daily flows from CSOs were subsequently determined by simulating the WASA sewer system model (also called the “MOUSE” model) for the calibration period 1995-2002 (LTI, 2007).

3.2.4 Sediment load inputs

Sediment loads for Version 3 of the TAM/WASP sediment transport model are obtained from a combination of results from the Phase 3 HSPF model, described in Section 2 of this report, and ESTIMATOR model results, described in Appendix A. Baseline mean annual and mean growing season sediment loads by tributary and by land use type for the three-year period, 1995-1997, are given in Table 3-4. All Watts Branch and LBC baseline loads are obtained directly from HSPF model output. NEB and NWB baseline loads are computed using ESTIMATOR model daily output, with apportionment to land use categories made using HSPF model results. For the remaining portion of the tidal drainage area, the minor tributaries and SS sub-sheds, sediment loads were computed using the sub-shed delineations and using HSPF model predictions of sediment load per acre for Watts Branch for the following three land use categories: urban impervious, urban pervious, and forest.

Because the Phase 3 HSPF model was calibrated to monthly ESTIMATOR loads for the NEB and NWB, ESTIMATOR and HSPF predictions are consistent within the range of accuracy of the load estimates (see Appendix A). For the 1995-1997 time period used to compute baseline loads, the HSPF model prediction of the mean annual combined NEB/NWB sediment load is 40,010 tons, only 1.0% less than the ESTIMATOR prediction of 40,393 tons. The HSPF model prediction of mean growing season sediment load is 19,678 tons, 8.4% greater than the ESTIMATOR prediction of 18,026 tons. To apportion these loads to the land use categories appearing in Table 3-4, HSPF model predictions for the NWB and NEB were multiplied by the appropriate scale factor, 40,093/40,010 in the case of annual loads, and 18,026/19,678 in the case of growing season loads.

HSPF model estimates of NWB loads are computed for the 31,314 acre drainage area above the USGS gage station on Queens Chapel Road. The complete drainage area for the non-tidal portion of the NWB includes an additional 2,397 acres extending from the gage station to the US 1 bridge (Baltimore Avenue). Loads predictions by land use for the complete drainage area were extrapolated from predictions for the area above the gage station based on proportional areas, using scale factor of 1.06753.

Table 3-4. Mean annual and growing season sediment loads by tributary and land use (1995-1997)

| | | Baseline - Annual | | Baseline - 7 mo. GS | |
|--------------|--------------------------|----------------------|------------------|----------------------|------------------|
| | | TW Load (tons/yr) | Percent Total | TW Load (tons/yr) | Percent Total |
| NWB | Agricultural | 104 | 1% | 16 | 0% |
| | Forest | 49 | 0% | 4 | 0% |
| | Stream bank erosion - MD | 12,832 | 84% | 6,468 | 78% |
| | Urban - Mont. Co. | 1,521 | 10% | 1,125 | 14% |
| | Urban - PG Co. | 673 | 4% | 517 | 6% |
| | Urban - DC | 175 | 1% | 135 | 2% |
| | | 15,354 | 33% | 8,265 | 37% |
| NEB | Agricultural | 1,185 | 5% | 134 | 1% |
| | Forest | 271 | 1% | 12 | 0% |
| | Stream bank erosion - MD | 19,448 | 78% | 7,019 | 72% |
| | Urban - Mont. Co. | 839 | 3% | 508 | 5% |
| | Urban - PG Co. | 3,295 | 13% | 2,087 | 21% |
| | Municipal/Industrial | 2 | 0% | 1 | 0% |
| | | 25,040 | 53% | 9,761 | 44% |
| LBC | Agricultural | 1 | 0% | 0 | 0% |
| | Forest | 32 | 1% | 1 | 0% |
| | Stream bank erosion - MD | 1,784 | 55% | 988 | 49% |
| | Urban - PG Co. | 1,408 | 44% | 1,013 | 51% |
| | Urban - DC | 4 | 0% | 3 | 0% |
| | | 3,229 | 7% | 2,004 | 9% |
| Watts Br | Agricultural | 0 | 0% | 0 | 0% |
| | Forest | 5 | 1% | 0 | 0% |
| | Stream bank erosion - DC | 67 | 15% | 32 | 12% |
| | Stream bank erosion - MD | 119 | 27% | 58 | 21% |
| | Urban - PG Co. | 117 | 26% | 83 | 31% |
| | Urban - DC | 138 | 31% | 99 | 36% |
| | | 446 | 1% | 272 | 1% |
| Tidal | Agricultural | 0 | 0% | 0 | 0% |
| | Forest | 0 | 0% | 0 | 0% |
| | Stream bank erosion | 0.0 | 0% | 0 | 0% |
| | Urban - PG Co. | 576 | 20% | 413 | 21% |
| | Urban - DC | 1,210 | 43% | 864 | 43% |
| | Total SS & minor tribs | 1,786 | | 1,278 | |
| | CSO – DC | 1,052 | 37% | 733 | 36% |
| | | 2,838 | 6% | 2,010 | 9% |
| Total | | 46,906 | 100% | 22,312 | 100% |

Loads from streambank erosion were assumed to be negligible for the portion of the drainage area below the USGS gage.

The TAM/WASP model was calibrated using sediment loads from CSOs derived from earlier versions of the model (Schultz, 2003). As mentioned earlier, subsequent to the calibration of the model, LTI, on behalf of WASA, provided simulated CSO flows for the calibration period based on the model of the DC sewer system developed for the LTCP. Sediment loads from the CSOs were then calculated assuming a TSS concentration of 160.8 mg/l, the average of the event mean concentrations observed at the Anacostia outfalls in the monitoring performed for the LTCP. The calibrated TAM/WASP model was run with the revised CSO sediment loads, and the results of the simulation were indistinguishable from the original calibration. All reported sediment loads from CSOs are based on MOUSE model flows and the average even mean TSS concentration from the LTCP.

Baseline annual mean sediment loads for Version 3 of the TAM/WASP model, computed for the three-year time period, 1995-1997, appear in Table 3-5. For comparison, mean annual loads from Version 2 of the model, computed for the time period, 1988-1990, are also given. The total mean annual load estimate for 1995-1997 (Version 3), 42,311 kkg (1000 kilograms), is considerably larger than the total mean annual load for 1988-1990 (Version 2). This is primarily due to the fact that the Version 3 loads were computed for a three-year time interval that includes an exceptionally wet year, 1996. The annual combined upstream load estimates from the ESTIMATOR model are 16,886, 73,331, and 16,769 kkg for 1995, 1996, and 1997, respectively, demonstrating the significant impact of high flows on annual sediment loads.

Table 3-5. Mean annual sediment loads for TAM/WASP Version 3

| | TAM/WASP V3, 1995-97 loads | | | | | TAM/WASP V2, 1988-90 loads | |
|--|----------------------------|----------|-------------------------|----------------------|-------------------|----------------------------|-------------------|
| | Area (acres) | Area (%) | Sediment Load (1000 kg) | Sediment Load (tons) | Sediment Load (%) | Sediment Load (1000 kg) | Sediment Load (%) |
| NEB | 46,291 | 41.7% | 22,764 | 25,040 | 53.4% | | |
| NWB | 33,711 | 30.4% | 13,958 | 15,354 | 32.7% | | |
| Upstream Total | 80,002 | 72.0% | 36,722 | 40,394 | 86.1% | 27,642 | 87.7% |
| LBC | 9,631 | 8.7% | 2,935 | 3,229 | 6.9% | 682 | 2.2% |
| Watts Br | 2,119 | 1.9% | 405 | 446 | 1.0% | 655 | 2.1% |
| Tidal Drainage Area (SS and minor tribs) | 12,375 | 11.1% | 1,624 | 1,786 | 3.8% | 1,223 | 3.9% |
| CSOs | 6,946 | 6.3% | 956 | 1,052 | 1.5% | 1,316 | 4.2% |
| Total | 111,073 | 100.0% | 42,642 | 46,906 | 100.0% | 31,518 | 100.0% |

3.2.5 Load inputs to the TAM/WASP eutrophication model

The methods used to compute daily load inputs for the TAM/WASP eutrophication model are described in Mandel and Schultz (2000).

3.3 Data Support for model calibration

3.3.1 Sediment transport model

Water quality data related to suspended solids and water clarity in the tidal Anacostia are available from several monitoring programs and special studies, described below. Locations of monitoring stations are depicted in Figure 3-2. All of the data sets described below were used in this study for preliminary analyses of water clarity conditions in the tidal river. The first two of the data sets described below, the DC and MDDNR routine monitoring data, were used for final model calibration.

District of Columbia (DC) water quality monitoring program: The District of Columbia has been collecting water quality data on a routine basis since 1984. Data from 29 stations located in the tidal Anacostia main channel, two stations in Kenilworth Marsh, and two stations in Kingman Lake are included in the Chesapeake Bay Program's "CBP Water Quality Database (1984-present)", available at the Chesapeake Bay Program website's "Data Hub" (via <http://www.chesapeakebay.net/data/index.htm>).

MDDNR routine monitoring: The Maryland Department of Natural Resources (MDDNR) has collected water quality data in the tidal portion of the Anacostia on a routine basis since 1986. Data are available for a single station, located near the Maryland/DC line at the Bladensburg Road bridge. These data are included in the Chesapeake Bay Program's "CBP Water Quality

Database (1984-present)", available at the Chesapeake Bay Program website's "Data Hub" (via <http://www.chesapeakebay.net/data/index.htm>).

Academy of Natural Sciences – Patrick Center for Environmental Research (ANS-PCER) 1998 stormwater runoff study: The ANS-PCER conducted a study on the effects of stormwater runoff on the water quality of the tidal Anacostia River for the USEPA (Velinsky *et al.*, 1999). Water quality data on toxic chemicals, solids, organic carbon, and other parameters were collected on nine separate dates in 1998 at nine locations in the tidal Anacostia main channel, as well as at the USGS gage stations on the Northeast and Northwest Branches.

ICPRB/ANS-PCER 1999 suspended sediment study: ICPRB and ANS-PCER conducted a study of suspended sediment in the Anacostia main channel for DCDOH (Schultz and Velinsky, 2001). Data including values for total suspended solids, sediment particle size, and flow velocity were collected on four separate dates in July, September and November 1999, and April 2000, at ten locations in 1999 in the Anacostia main channel from Bladensburg Marina to the Potomac River. Time series data were also collected at two locations in July and November, 1999. Data in this study include depths profiles and measurements of current velocity.

Long-Term Control Plan (LTCP) 2000 wet weather study: A study of wet weather water quality in the Anacostia main channel was conducted by MWCOG and the US Naval Research Laboratory for DCWASA in support of the LTCP for CSOs (MWCOG, 2001a). Water quality data on solids and nutrients were collected during four separate multi-day sampling events in March, April, May, and August of 2002 at five locations in the Anacostia main channel from the New York Avenue bridge to the South Capitol Street bridge.

ANS-PCER 2002 toxic chemicals monitoring study: The ANS-PCER conducted a study of toxic chemicals in the Anacostia main channel for the DCDOH (private communication, David Velinsky). Water quality data, including total suspended solids and organic carbon, were collected on four separate dates in May, June, August, and October of 2002 at eight location in the Anacostia main channel from Bladensburg Marina to Haines Point. Post-storm time series data were also collected at one location, the CSX railroad bridge, in October, 2002.

Table 3-6. Main channel water quality data sets - solids and water clarity-related parameter values

| Study | Year | Secchi | Turbidity | TSS | VSS | POC | DOC | Chla |
|---|--------------------|--------|-----------|-----|-----|------------------|----------------|------|
| DC water quality monitoring | Routine since 1984 | x | x | x | | | x | x |
| MDDNR water quality monitoring | Routine since 1986 | | x | x | | | | x |
| ANS-PCER stormwater runoff study | 1998 | | x | x | | x | x | |
| ANS-PCER/ICPRB suspended sediment study | 1999 | x | x | x | | x | | x |
| LTCP wet weather study | 2000 | | | x | x | x ^{1,2} | x ² | |
| ANS-PCER toxics study | 2002 | | | x | | x | x | x |

1 Only available for one sampling event.

2 No electronic copy of data available.

3.3.2 Eutrophication model

Dissolved oxygen, nutrient, and chlorophyll *a* data for use in calibration/verification of the Version 3 TAM/WASP eutrophication model were obtained from the Chesapeake Bay Program (CBP) Water Quality Database (1984 – present), available at <http://www.chesapeakebay.net/data/index.htm>. The CBP database has data from the DC and the MDDNR routine water quality monitoring programs. During the study period, 1995 – 2004, data were collected on a regular basis (usually monthly or bi-monthly) at ten DC stations depicted in Figure 3-2, ANA01 through ANA30, and at the MDDNR station, ANA082. At the time this study was initiated, data for DC stations were only available through 2002.

3.3.3 Characterization of water clarity in the tidal Anacostia

Long-term growing season medians of 1995-2002 routine monitoring data are shown in Figure 3-4. Medians depicted in this graph were computed from data for the April 1- October 31 growing season specified in DC water quality standards. However, for the three upstream stations in or adjacent to MD waters (stations ANA0082, ANA30, and ANA01), all values plotted are identical to medians computed for the April 1- October 1 growing season specified in MD's water quality standards. This figure illustrates the spatial pattern of water clarity conditions in the tidal Anacostia, with poor light conditions typically occurring in the middle portion of the river. It is evident from Figure 3-4 that medians of TSS, turbidity, and inverse Secchi depth are all well-correlated along the length of the tidal river's main channel.

Long-term growing season medians of Secchi depth measurements in the tidal Anacostia are plotted in Figure 3-5. Long-term Secchi depth growing season medians for the most upstream segments, representing water clarity conditions from the confluence of the Northeast and Northwest Branches in MD to the New York Avenue bridge at approximately the MD-DC line, are at or above 0.4 meters, the criterion given in the Maryland WQSs (Code of Maryland Regulations, 26.08.02). Long-term Secchi depth medians depicted in Figure 3-5 for the two most downstream stations, from Buzzards Point to the confluence with the Potomac, are 0.8 meters, the DC water clarity criterion (DC Municipal Regulations, Title 21, Chapter 11). In the middle portion of the river, the Secchi depth medians are less than 0.8.

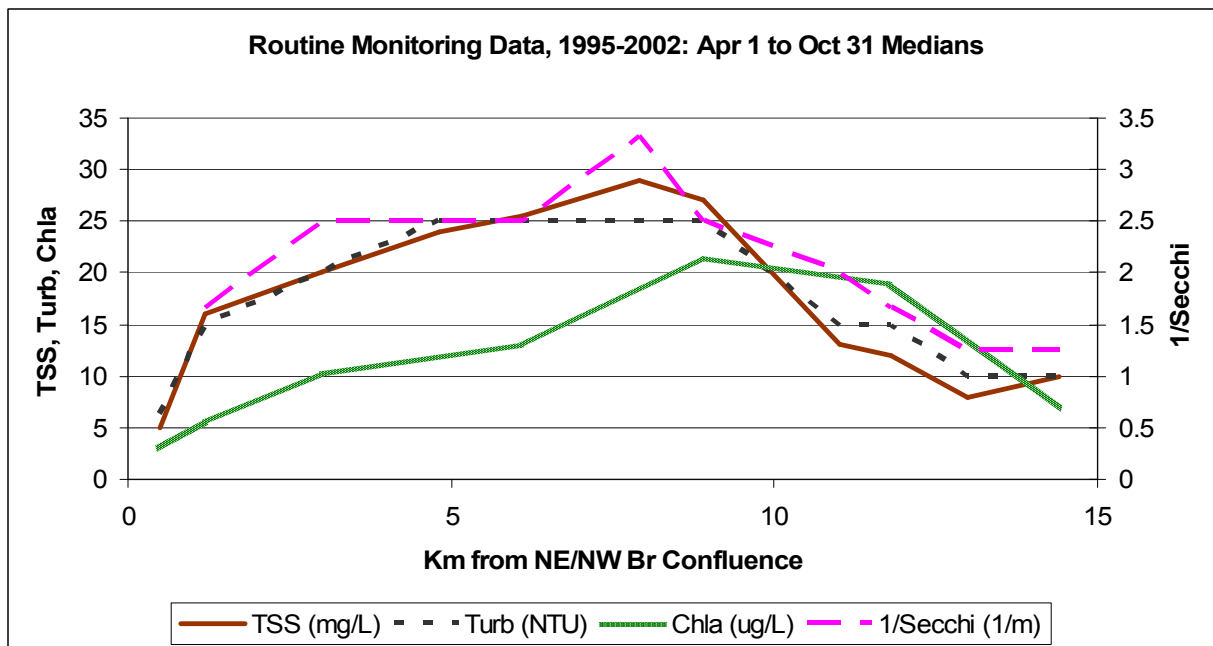


Figure 3-4. Long-term Growing Season Medians of Water Quality Parameters in the Tidal Anacostia River

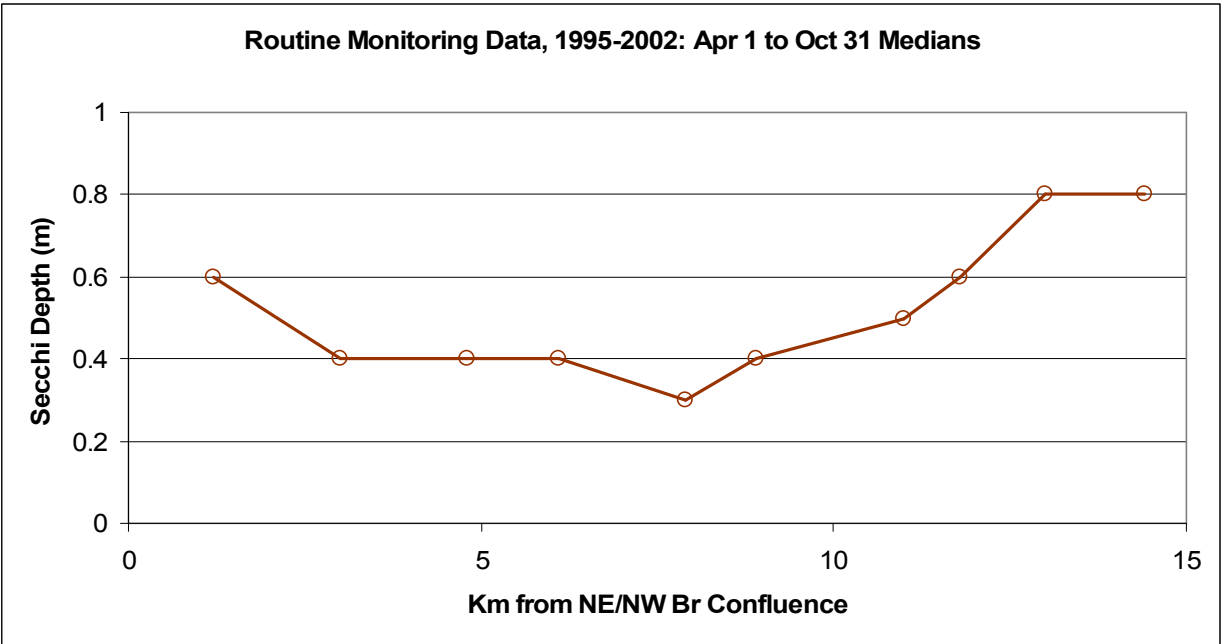


Figure 3-5. Long-term Growing Season Medians of Secchi Depth in the Tidal Anacostia River

3.4 Description of TAM/WASP water quality model components

The relationship between suspended sediment and water clarity is complicated by the interaction between water clarity and the growth of algae: good water clarity is one factor that promotes phytoplankton (algae) growth, but excessive phytoplankton growth tends to reduce water clarity, because algae itself is a form of suspended solid material. The TAM/WASP modeling framework, Version 3, has been designed to capture some of the complexity of this interaction, as depicted in Figure 3-6. WASP-Toxi is used to simulate the settling and re-suspension of total suspended solids as well as the mixing and longitudinal movement of suspended solids along the length of the tidal river. Predicted daily TSS concentrations from WASP-Toxi are read by the WASP-Eutro component of the model, which predicts daily concentrations of nutrients, phytoplankton, and dissolved oxygen. WASP-Eutro uses its prediction of phytoplankton concentration at a given point in the day, along with the daily TSS concentration obtained from WASP-Toxi, to compute a measure of water clarity referred to as the light attenuation coefficient. The light attenuation coefficient is used in turn to compute the model's estimate of phytoplankton growth and the resulting phytoplankton concentration at the subsequent model time step. WASP-Eutro has been re-configured to output daily estimates of Secchi depth, a measure of water clarity closely related to the light attenuation coefficient.

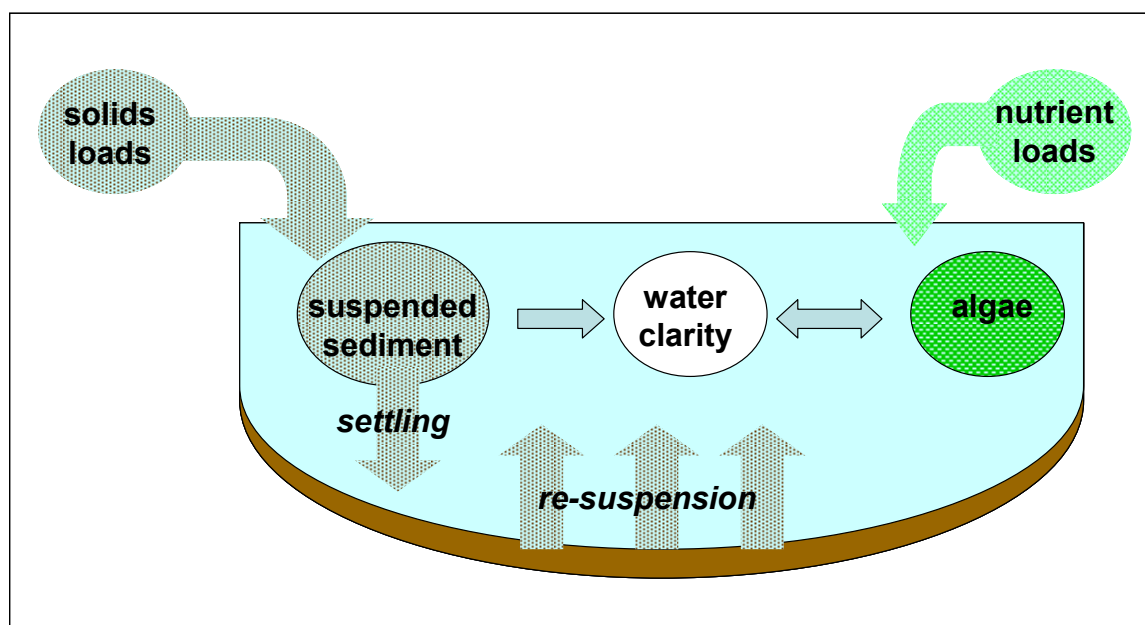


Figure 3-6. Conceptual model of impact of suspended sediment/algae interaction

The versions of WASP-Toxi and WASP-Eutro used in Version 3 of the TAM/WASP water clarity model both incorporate modifications made by ICPRB to improve their ability to simulate water clarity conditions. These modifications are described below.

3.4.1 Sediment transport model

The TAM/WASP sediment transport component simulates the loading, fate, and transport of solids in the tidal river, and predicts daily concentrations of total suspended solids (TSS). The effects of tidal currents and other hydrodynamic processes are simulated via linkage with the TAM hydrodynamic model. Estimated sediment loads are input on a daily basis for the four major tributaries (the Northwest Branch, the Northeast Branch, Lower Beaverdam Creek, and Watts Branch), the minor tributaries storm sewer system (primarily located within the District), and the DC CSOs. A complete description of Version 2 of the model (Schultz, 2003) is available at ICPRB's web-site, www.potomacriver.org. The sediment transport component is based on the USEPA's WASP-Toxi water quality model, and incorporates two modifications made by ICPRB: 1) Predicted daily TSS values are written to a file to be used as input by the TAM/WASP eutrophication model to help estimate daily light conditions, and 2) Algorithms have been added to simulate settling and re-suspension based on flow velocity. This leads to a more realistic simulation, with more erosion and less deposition occurring during high flow periods than in low flow periods. The TAM/WASP sediment transport component's main features and capabilities are summarized below:

- The model simulates the fate and transport of three classes of sediment based on particle grain size: fine-grained (clay and very fine silt, *i.e.* $< 30 \mu\text{m}$); medium-grained (silt and very fine sand, *i.e.* between 30 and 120 μm); and coarse-grained (sand and gravel, *i.e.* $> 120 \mu\text{m}$). These size fractions were determined based on the sediment grain size distribution found in the tidal Anacostia river bed in a study done by the GeoSea Consulting, Ltd. in 2000 (Hill and McLaren, 2000). The model also predicts the concentration of total suspended solids, computed as the sum of the concentrations of the three size fractions.
- Advective transport of suspended sediment is simulated based on flow velocities provided by the hydrodynamic component. Dispersive transport of suspended sediment (mixing) is simulated based on the value of the dispersion coefficient, a user-specified input parameter.
- The model simulates settling of suspended sediment and deposition to the river bed, and erosion and re-suspension of sediment from the river bed to the water column. Modifications have been made to the original WASP-Toxi code to compute erosion and deposition at each model time step based on flow velocity obtained from the hydrodynamic model. The fine-grained and medium-grained sediment fractions are treated as cohesive sediments, and the algorithms governing their transport follow the approach developed by Partheniades (1962) and Krone (1962), which has frequently been employed in other models, such as the HSPF model and the Army Corps of Engineers' HEC-6 model. In addition, the transport of coarse-grained sediment is modeled with a simple power law.
- The model predicts daily concentrations of each sediment grain size for both water column and bed sediment segments.

Version 2 of the TAM/WASP sediment transport model (Schultz, 2003) was used by the District of Columbia and by USEPA Region 3 to determine load allocations for the District's sediment TMDL for the tidal Anacostia (DCDOH, 2002; USEPA, 2002a; USEPA, 2002b). Version 3 of the model, developed for use in Maryland's Anacostia sediment TMDL analyses, incorporates the following minor changes:

- The model simulation period, originally 1/1/1985 to 7/30/2000, has been extended to 12/31/2002.
- Downstream boundary conditions for sand, silt, and clay were set at the constant values, 0.1 mg/L, 0.9 mg/L, and 8.0 mg/L, consistent with the median TSS value of 9.0 mg/L at monitoring station ANA24 for the time period, 1995 – 2002. Percentages of sand, silt, and clay at the downstream boundary were obtained via model calibration.
- Model geometry has been changed from 36 water column segments to 38 water column segments, to better represent the tidal portions of the Northeast Branch and Northwest Branch tributaries (see Figure 3-2).
- The sediment bed is represented by two layers: an upper layer, 1 cm in thickness, and a lower layer, 5 cm in thickness (see Figure 3-3).
- Minor adjustments have been made to model calibration parameters governing sediment settling and re-suspension rates and thresholds, based on model performance in the new calibration period, 1995 thru 2002.
- Predicted daily concentrations of TSS are written to text file, for input into the TAM/WASP eutrophication model, which uses the TSS concentrations to compute daily light conditions in the water column.

For the two cohesive sediment fractions, erosion and deposition are a function of bed shear stress. Erosion occurs when shear stress exceeds a critical shear stress and is proportional to the extent it exceeds the critical shear stress. Similarly, the deposition of cohesive sediment occurs when shear stress is less than a critical threshold--distinct from the critical shear stress for erosion--and occurs in proportion to the drop in shear stress below the threshold. Bed shear stress is calculated from the slope of the energy grade line, which is determined by solving Manning's equation, resulting in a relationship between bed shear stress and flow velocity. Distinct values of the zero-flow settling velocity, the erosion velocity multiplier, critical shear stress, and the critical deposition threshold are entered by the user for fine-grained and medium-grained sediment fractions.

The relationship between bed shear stress and flow velocity is

$$V = \frac{R^{1/6} \tau_b^{1/2}}{n \gamma^{1/2}}$$

Equation 6

where

| | | |
|----------|---|--|
| V | = | average flow velocity in the segment (m/s) |
| n | = | Manning's roughness factor. |
| τ_b | = | bed shear stress (Newton/m ²) |

$$\begin{aligned}\gamma &= \text{the weight of water (9806 Newton m/s)} \\ R &= \text{hydraulic radius (m)}\end{aligned}$$

For a cohesive sediment, deposition occurs if τ_b is less than τ_d , the threshold for deposition. For each of the two cohesive solids size fractions, the rate of deposition is given by the Krone equation:

$$\begin{aligned}M_d &= 0, & \tau_b > \tau_d \\ &= C_{WC} A V_s (1 - \tau_b/\tau_d), & \tau_b < \tau_d\end{aligned}\tag{Equation 7}$$

where

$$\begin{aligned}C_{WC} &= \text{concentration in water column segment (mg/l)} \\ M_d &= \text{mass deposited (g/d)} \\ A &= \text{area of the sediment bed in segment (m}^2\text{)} \\ V_s &= \text{settling velocity at zero flow (m/d)} \\ \tau_d &= \text{critical shear stress threshold for deposition.}\end{aligned}$$

Erosion occurs if τ_b is greater than τ_c , the critical shear stress. For each of the two cohesive sediment size fractions, the rate of erosion is given by the Parthenaides equation. In TAM/WASP, for each of the cohesive sediment size fractions modeled, the Parthenaides coefficient, is linearly dependent on the concentration of that size fraction in the sediment bed. Thus, the mass of eroded sediment is given by

$$\begin{aligned}M_e &= C_s V_e A (\tau_b/\tau_c - 1), & \tau_b > \tau_c \\ &= 0, & \tau_b < \tau_c\end{aligned}\tag{Equation 8}$$

where

$$\begin{aligned}M_e &= \text{mass eroded (g/d)} \\ C_s &= \text{concentration in bed sediment segment (g/m}^3\text{)} \\ V_e &= \text{erosion velocity constant (m/d)} \\ \tau_c &= \text{critical shear stress threshold for erosion.}\end{aligned}$$

Use of Equation 8 in the erosion algorithm provides some degree of simulation of “sediment armoring” in the model. That is, if the proportion of a cohesive size fraction is small, due, for example, to the presence of a significant amount of sand in the segment, then the erosion coefficient, M_p , for that size fraction is relatively small.

Sediment size fraction concentrations are computed at each model time step by WASP. Average segment depths, hydraulic radii, and segment velocities are taken from WASP and ultimately derived from the TAM hydrodynamic program. Distinct values of the settling velocity, erosion velocity constant, critical shear stress thresholds for deposition and erosion are entered by the user for fine-grained and medium-grained sediment fractions.

To model the transport of the coarse-grained sediment fraction, a simple power law method is used. The transport of the coarse-grained sediment fraction (*i.e.* sand and gravel) is modeled by determining the carrying capacity of the flow, which in turn is dependent on the flow's hydrodynamic properties. If flow conditions change so that the carrying capacity exceeds the concentration of sand currently being transported, additional sand will be eroded from the bed. If the concentration of sand exceeds its carrying capacity, sand will be deposited.

In the power function method, the transport capacity for coarse-grained sediments, C_p , (mg/l), is given as a simple power function of the velocity

$$C_p = q V^r \quad \text{Equation 9}$$

where

$$\begin{aligned} q, r &= \text{user-determined constants} \\ V &= \text{average segment flow velocity (m/s)} \end{aligned}$$

3.4.2 Eutrophication model

The TAM/WASP eutrophication component is used to simulate water clarity conditions and the growth of algae in the tidal Anacostia, and is based on a modified version of the WASP-Eutro water quality model. This model estimates concentrations of dissolved oxygen, phytoplankton, and other model constituents in the tidal river based on inputs including estimated daily nutrient loads from the four major tributaries and the SSTRIB and CSO systems. A complete description of the original version of this model, used to determine BOD load allocations for the District's dissolved oxygen TMDL for the tidal Anacostia (DCDOH, 2001), is available at ICPRB's website (see Mandel and Schultz, 2000). The main features and capabilities of the original TAM/WASP eutrophication model are described below:

- The model simulates the loading, fate and transport of dissolved oxygen (DO), biochemical oxygen demand (BOD), phytoplankton (PHYT), and the following nutrients: ammonia (NH₃), organic nitrogen (ORGN), nitrate + nitrite (NO₃), organic phosphorus (OP), and orthophosphate (PO₄). Model output for PHYT is converted to CHLA, by use of the carbon-chlorophyll ratio, Θ_c , to allow comparison of model predictions with available monitoring data (see below).
- Advective transport of dissolved oxygen, phytoplankton, and nutrients are based on flow velocities provided by the hydrodynamic model. Dispersion (mixing) is based on the value of the user-input dispersion coefficient.
- Phytoplankton growth is computed based on temperature, light availability, and nutrient concentrations. Light availability is measured by the "light extinction coefficient", K_e , defined below.

In order to better predict water clarity, ICPRB has partially coupled the eutrophication component to the TAM/WASP sediment transport component, as depicted in Figure 3-1. This modification was made to allow the model to simulate the response of algae growth to potential reductions of solids loads in the TMDL scenario runs. The first version of this coupled model

was used by the District in its draft TMDL for sediment in the tidal Anacostia (DCDOH, 2002). The following capabilities have been added to WASP-Eutro by ICPRB to couple it to the TAM/WASP sediment component:

- Daily TSS concentrations are read from the output file produced by the sediment transport component and used to estimate the concentration of non-algal solids.
- In Version 3 of the TAM/WASP water quality model, the effect of light availability on growth is simulated using the Smith light routine, one of the two user options available in WASP-Eutro. Daily light conditions are read by the model from a time series of solar radiation data from Reagan National Airport (with the exception of 1/1/1995 to 4/31/1995, for which data are from NOAA station in Sterling, VA). The Smith formulation is used because it has a variable carbon to chlorophyll *a* ratio, Θ_c . Θ_c is known to vary with ambient light conditions (Ambrose, 1993). In the alternative light formulation available in WASP, by diToro, used by Mandel and Schultz (2000), Θ_c was set to the constant value, 25 mg C/mg chlorophyll *a*, appropriate for the low light conditions typical of the Anacostia. However, use of the Smith light formulation in Version 3 allows the model to respond to the changes in light conditions which would occur when sediment loads are reduced.
- The growth rate of phytoplankton is a function of the light extinction coefficient, K_e , with lower values of K_e corresponding to higher growth rates. The value of K_e is computed from the concentration of non-algal solids and chlorophyll *a* using an algorithm incorporated by ICPRB into the Smith light sub-routine (see below).
- Daily values of Secchi depth are computed and added to model output, based on the simple relationship between Secchi depth and K_e described below.

The relationships between TSS, phytoplankton, and chlorophyll *a* concentrations, and K_e , and Secchi depth are described below.

The amount of light shining on the water's surface that reaches a given depth, *z*, diminishes approximately exponentially with depth, according to a relationship known as Beer's Law, which can be expressed as follows

$$I(z) = I_0 \exp(-K_e z) \quad \text{Equation 10}$$

where

| | | |
|----------|---|--|
| $I(z)$ | = | light intensity at depth, <i>z</i> ("photosynthetically active radiation", PAR, in units of) |
| <i>z</i> | = | depth from water's surface (m) |
| I_0 | = | light measured immediately below the water's surface ("photosynthetically active radiation", PAR, in units of) |
| K_e | = | light extinction coefficient (1/m) |

Secchi depth is inversely proportional to the light extinction coefficient (Walker, 1982), with a proportionality constant that can be determined from fitting Secchi disk measurements and measurements of irradiance to the exponential form given by Equation 10. In the development

of water quality standards based on the Chesapeake Bay waters, the proportionality constant, 1.45 has been used, that is,

$$K_e = 1.45/\text{Secchi depth} \quad \text{Equation 11}$$

The light extinction coefficient is assumed to be a linear function of non-algal solids concentration and chlorophyll *a*, corresponding to the Smith light option available in the WASP eutro model:

$$K_e = a + b * \text{naSS} + 0.017 * \text{CHLA} \quad \text{Equation 12}$$

where

$$\begin{aligned} \text{naSS} &= \text{non-algal suspended solids concentration (mg/L)} \\ \text{CHLA} &= \text{chlorophyll } a \text{ concentration (}\mu\text{g/L)} \end{aligned}$$

Phytoplankton concentration, PHYT, in units of mg C, is related to CHLA via the carbon-chlorophyll ratio, that is,

$$\text{PHYT} = \Theta_c \text{ CHLA}/1000 \quad \text{Equation 13}$$

where Θ_c , in units of mg C/mg chlorophyll *a*, is computed by WASP's Smith light sub-routine based on ambient light conditions. Θ_c is generally found to be in the range, 20 to 125, with lower values occurring for poorer water clarity conditions.

In ICPRB's modified version of the Smith light routine, non-algal solids in Equation 12 are computed from TSS and chlorophyll *a* concentrations using the relationship,

$$\begin{aligned} \text{naSS} &= (\text{TSS} - V_{\text{VSS:POC}} * \Theta_c * \text{CHLA}/1000), \text{ for } (\text{TSS} - V_{\text{VSS:POC}} * \Theta_c * \text{CHLA}/1000) > 5, \\ \text{naSS} &= 5, \quad \text{for } (\text{TSS} - V_{\text{VSS:POC}} * \Theta_c * \text{CHLA}/1000) \leq 5, \end{aligned} \quad \text{Equation 14}$$

where

$V_{\text{VSS:POC}}$ = ratio of volatile organic solids to particulate organic carbon, assumed to be 2.5 (Cerco *et al.*, 2004)

Θ_c = carbon/chla ratio (mg C/mg chla), computed by WASP eutro model based on light conditions

TSS = total suspended solids concentration (mg/L), obtained from daily predictions of the TAM/WASP sediment transport component

The first line of Equation 14 simply expresses the fact, in units of mg C/L, that total solids is the sum of algal solids and non-algal solids. The second line of Equation 14 is added to partially

account for the incomplete coupling of the sediment and eutrophication components in the TAM/WASP water clarity model. Though the eutrophication component has information about TSS concentration from the sediment component, the sediment component does not have information about algae growth. Therefore, the second line of Equation 14 assumes that non-algal solids concentrations are always at least 5 mg/L, near the model's estimate of minimum TSS concentrations due to tidal resuspension under no-load conditions (see Section 3.5.2).

The coefficients used in this study to compute the light extinction coefficient as a function of TSS and chl *a* are $a = 0.4$ and $b = 0.13$. These values were determined based on WASP-Eutro model calibration results (see Section 3.5).

3.5 Water clarity model calibration/verification

The TAM/WASP coupled sediment transport/water clarity model was calibrated for the time period, January 1, 1995 through December 31, 2002. Main channel chlorophyll *a* data are available for 1999 through 2002. The years, 1995 through 1997, which includes two relatively wet years, are used for the estimates of baseline loads and TMDL allocations.

3.5.1 Sediment transport component: configuration and input parameters

A time step of 1/400 days was used for model calibration runs. The relatively short time step was required for the calibration period in order to avoid instabilities caused by the large input loads on September 16, 1999 due to Hurricane Floyd. With the exception of sediment erosion and deposition velocities and shear stress thresholds, discussed below, all model inputs representing physical properties were set to the same values used in Version 2 of the sediment transport model (see Schultz, 2003). For daily sediment load inputs, the relative proportion of the three sediment grain size fractions was set at 17% coarse-grained, 15% medium-grained, and 68% fine-grained, based on bed sediment grain size data collected by GeoSea (Hill and McLaren, 2000), and on calibration results for Version 2 of the model. Anacostia River sediment density was assumed to be 2.5 gm/cm³, typical of Chesapeake Bay sediments (Velinsky *et al.*, 1997), and porosity was assumed to be 0.6 (David Velinsky, private communication). The longitudinal dispersion coefficient was set at 1.3 m²/sec, based on analysis of a dye study conducted by LTI, Inc. (MWCOG, 2001b).

3.5.2 Sediment transport component: calibration

In the calibration of Version 3 of the sediment transport model, minor changes were made to the parameters governing the erosion and deposition of cohesive sediments, $\tau_{c,2}$, $\tau_{d,2}$, $V_{e,2}$, and $V_{s,2}$, the critical shear stress for erosion and deposition and the erosion and deposition velocities for medium-grained sediment (silt), and $\tau_{c,3}$, $\tau_{d,3}$, $V_{e,3}$, and $V_{s,3}$, the critical shear stress for erosion and deposition and the erosion and deposition velocities for fine-grained sediment (clay). In the calibration of Version 2 of the model, values for these parameters were kept uniform along the length of the tidal river in order to better verify the usefulness of the erosion and deposition model described by equations 6 - 9. However, for the calibration of Version 3, parameter values for the lower portion of the tidal river were adjusted slightly to improve the model's ability to simulate the longitudinal profile of median Secchi depths. Calibration values for both Versions 2 and 3 are given in Table 3-7.

Calibration results: Parameter values in Table 3-7 were selected by comparing model predictions to observations depicted in Figures 3-7 through 3-9. In Figure 3-7 and Figure 3-8, calibrated model-predicted values of TSS are compared to available data from monitoring stations at segment 2 (ANA0082 – Bladensburg Rd), segment 3 (ANA30 – Bladensburg Marina), segment 8 (ANA01 – New York Ave), segment 16 (ANA08 – CSX Railroad), segment 23 (ANA14 – Pennsylvania Ave), and segment 30 (ANA21 – South Capitol St). Model results are only fair, though the graphs in Figure 3-8 indicate that the model is able to reproduce the effect of tidal re-suspension in the lower portion of the river. The graphs of the cumulative distribution function of predicted and observed results in Figure 3-9 (from all monitoring stations shown in Figure 3-1 at all dates on which data were collected) show that the model actually does a good job, on average, in predicting mid- and low values of TSS, but tends to over-predict TSS values on the high end of the CDF. This is consistent with the results shown in Figure 3-10, which compares plots of predicted and observed longitudinal profiles of TSS percentile values. The model does a good job of reproducing both medians and the 25th percentile values of TSS along the length of the tidal river, including the higher mid-river values. However, it over-predicts the 75th percentile values in the upper mid-river, and over-predicts the 90th percentile values everywhere along the length of the river.

Figure 3-11 shows model predictions of the bed sediment grain size distribution along the length of the tidal river, compared with segment averages derived from data. Predicted percentages were computed from model results for the upper layer bed sediment segments for the last day of the calibration run, December 31, 2002. Observed percentages were computed by taking segment averages of data from the GeoSea study of 2000 (see Schultz, 2003). The observed percentages were also used to set the bed sediment grain size distribution model initial conditions, for the first day of the calibration run, January 1, 1995. The first graph in Figure 3-11, the percentage of sand (grain size > 120 μm), shows that the sediment bed in the upstream portion of the river contains a large amount of sand, deposited by the NEB and NWB tributaries, whereas the downstream portion contains little sand. Mid-river sand peaks, near segments 8 and 14, are associated with the two other major tributaries, Lower Beaverdam Creek and Watts Branch. Conversely, the third graph shows that segments 27 through 36, in the slower moving downstream portion of the river, contain a high percentage of clay (grain size < 30 μm).

The ability of the TAM/WASP sediment transport model to reproduce the longitudinal profiles of the middle and low percentile values of TSS in the water column, as well as the general pattern of grain size distribution in the bed sediment, is an indication that the ICPRB-modified version of WASP-Toxi, incorporating the simple sediment deposition and erosion algorithms given by equations 6 - 9, has substantial predictive value in estuarine systems. The Version 3 calibration parameters, given in Table 3-7, were selected to provide a good match between predicted and observed median TSS values, as shown in Figure 3-10, and predicted and observed sand, silt and clay bed sediment percentages, as shown in Figure 3-11. The fact that the model does a good job reproducing median TSS values is important for this project because medians are used to evaluate water clarity conditions in the tidal river in Maryland's sediment TMDL. The fact that the bed sediment grain size distribution profiles remain fairly stable throughout model runs, as indicated by Figure 3-11, is important because the composition of the bed sediment is a significant factor governing tidal and other re-suspension processes.

Sensitivity runs: Two runs were done to investigate the effects of changes in model inputs and parameters. In the first of these sensitivity runs, erosion of the clay and silt fractions of the bed sediment was “turned off”, that is, the erosion velocity rates for silt and clay, $V_{e,2}$, and $V_{e,3}$ were set to zero for all model segments. Results for TSS percentile values, Figure 3-12, show that erosion accounts for a significant amount of TSS for the lower and mid percentile values. This is consistent with the observation that tidal re-suspension causes TSS values in the range of approximately 6 to 40 mg/L (5th to 95th percentiles) in dry weather conditions, with a median of approximately 12 mg/L (Schultz and Velinsky, 2001). It is evident from this sensitivity run that turning off erosion does not remedy the model’s over-prediction of high percentile TSS values.

In the second of the sensitivity runs, all sediment load inputs were set equal to zero. In this “no load” run, shown in Figure 3-13, the most significant reductions in TSS occur for the higher percentile values. The rise in the plots on the right-hand-side of Figure 3-13, representing the lower portion of the tidal river, is due to the effect of the Potomac boundary condition, which has TSS set at 8 mg/L based on monitoring data. It is also interesting to examine the effect of no sediment loads on the composition of the sediment bed. Figure 3-11 includes plots of bed sediment size fractions for the last day of the 1995-2002 “no load” run. In these plots, the percentage of sand in the sediment bed of the upper and middle reaches of the river has increased significantly, as the river’s flow has re-suspended and “washed” out a large portion of the clay. These plots demonstrate that a change in sediment loads changes the grain size composition of the sediment bed, with lower loads leading to a sandier bed.

These sensitivity tests indicate that model-simulated TSS concentrations are primarily controlled by sediment loads, especially on high flow days, when high tributary loads lead to high TSS concentrations in the tidal river. Bed sediment erosion apparently plays a more significant role on days when loads are low, due to re-suspension by tidal currents.

Table 3-7. Calibration values of parameters governing erosion and deposition of cohesive sediments

| Segment | TAM/WASP Version 3 | | | | | | | | TAM/WASP Version 2 | | | | | | | |
|---------|--------------------|--------------|-----------|-----------|--------------|--------------|-----------|-----------|--------------------|--------------|-----------|-----------|--------------|--------------|-----------|-----------|
| | Silt | | | | Clay | | | | Silt | | | | Clay | | | |
| | $\tau_{c,2}$ | $\tau_{d,2}$ | $V_{e,2}$ | $V_{s,2}$ | $\tau_{c,3}$ | $\tau_{d,3}$ | $V_{e,3}$ | $V_{s,3}$ | $\tau_{c,2}$ | $\tau_{d,2}$ | $V_{e,2}$ | $V_{s,2}$ | $\tau_{c,3}$ | $\tau_{d,3}$ | $V_{e,3}$ | $V_{s,3}$ |
| 1 | 0.04 | 0.02 | 0.00008 | 20.0 | 0.02 | 0.01 | 0.00002 | 1.0 | 0.04 | 0.02 | 0.00008 | 20.0 | 0.02 | 0.01 | 0.00002 | 1.0 |
| 2 | 0.20 | 0.02 | 0.00004 | 20.0 | 0.10 | 0.02 | 0.00001 | 2.0 | 0.20 | 0.02 | 0.00004 | 20.0 | 0.10 | 0.02 | 0.00001 | 2.0 |
| 3 | 0.20 | 0.02 | 0.00004 | 20.0 | 0.10 | 0.02 | 0.00001 | 2.0 | 0.20 | 0.02 | 0.00004 | 20.0 | 0.10 | 0.02 | 0.00001 | 2.0 |
| 4 | 0.20 | 0.02 | 0.00004 | 20.0 | 0.10 | 0.02 | 0.00001 | 2.0 | 0.20 | 0.02 | 0.00004 | 20.0 | 0.10 | 0.02 | 0.00001 | 2.0 |
| 5 | 0.20 | 0.02 | 0.00004 | 20.0 | 0.10 | 0.02 | 0.00001 | 2.0 | 0.20 | 0.02 | 0.00004 | 20.0 | 0.10 | 0.02 | 0.00001 | 2.0 |
| 6 | 0.20 | 0.02 | 0.00004 | 20.0 | 0.10 | 0.02 | 0.00001 | 2.0 | 0.20 | 0.02 | 0.00004 | 20.0 | 0.10 | 0.02 | 0.00001 | 2.0 |
| 7 | 0.20 | 0.02 | 0.00004 | 20.0 | 0.10 | 0.02 | 0.00001 | 2.0 | 0.20 | 0.02 | 0.00004 | 20.0 | 0.10 | 0.02 | 0.00001 | 2.0 |
| 8 | 0.20 | 0.02 | 0.00004 | 20.0 | 0.10 | 0.02 | 0.00001 | 2.0 | 0.20 | 0.02 | 0.00004 | 20.0 | 0.10 | 0.02 | 0.00001 | 2.0 |
| 9 | 0.20 | 0.02 | 0.00004 | 20.0 | 0.10 | 0.02 | 0.00001 | 2.0 | 0.20 | 0.02 | 0.00004 | 20.0 | 0.10 | 0.02 | 0.00001 | 2.0 |
| 10 | 0.20 | 0.02 | 0.00004 | 20.0 | 0.10 | 0.02 | 0.00001 | 2.0 | 0.20 | 0.02 | 0.00004 | 20.0 | 0.10 | 0.02 | 0.00001 | 2.0 |
| 11 | 0.20 | 0.02 | 0.00004 | 20.0 | 0.10 | 0.02 | 0.00001 | 2.0 | 0.20 | 0.02 | 0.00004 | 20.0 | 0.10 | 0.02 | 0.00001 | 2.0 |
| 12 | 0.20 | 0.02 | 0.00004 | 20.0 | 0.10 | 0.02 | 0.00001 | 2.0 | 0.20 | 0.02 | 0.00004 | 20.0 | 0.10 | 0.02 | 0.00001 | 2.0 |
| 13 | 0.20 | 0.02 | 0.00004 | 20.0 | 0.10 | 0.02 | 0.00001 | 2.0 | 0.20 | 0.02 | 0.00004 | 20.0 | 0.10 | 0.02 | 0.00001 | 2.0 |
| 14 | 0.20 | 0.02 | 0.00004 | 20.0 | 0.10 | 0.02 | 0.00001 | 2.0 | 0.20 | 0.02 | 0.00004 | 20.0 | 0.10 | 0.02 | 0.00001 | 2.0 |
| 15 | 0.20 | 0.02 | 0.00004 | 20.0 | 0.10 | 0.02 | 0.00001 | 2.0 | 0.20 | 0.02 | 0.00004 | 20.0 | 0.10 | 0.02 | 0.00001 | 2.0 |
| 16 | 0.20 | 0.02 | 0.00004 | 20.0 | 0.10 | 0.02 | 0.00001 | 2.0 | 0.20 | 0.02 | 0.00004 | 20.0 | 0.10 | 0.02 | 0.00001 | 2.0 |
| 17 | 0.20 | 0.02 | 0.00004 | 20.0 | 0.10 | 0.02 | 0.00001 | 2.0 | 0.20 | 0.02 | 0.00004 | 20.0 | 0.10 | 0.02 | 0.00001 | 2.0 |
| 18 | 0.20 | 0.02 | 0.00004 | 20.0 | 0.10 | 0.02 | 0.00001 | 2.0 | 0.20 | 0.02 | 0.00004 | 20.0 | 0.10 | 0.02 | 0.00001 | 2.0 |
| 19 | 0.20 | 0.02 | 0.00004 | 20.0 | 0.10 | 0.02 | 0.00001 | 2.0 | 0.20 | 0.02 | 0.00004 | 20.0 | 0.10 | 0.02 | 0.00001 | 2.0 |
| 20 | 0.20 | 0.02 | 0.00004 | 20.0 | 0.10 | 0.02 | 0.00001 | 2.0 | 0.20 | 0.02 | 0.00004 | 20.0 | 0.10 | 0.02 | 0.00001 | 2.0 |
| 21 | 0.20 | 0.02 | 0.00004 | 20.0 | 0.10 | 0.02 | 0.00001 | 2.0 | 0.20 | 0.02 | 0.00004 | 20.0 | 0.10 | 0.02 | 0.00001 | 2.0 |
| 22 | 0.20 | 0.02 | 0.00004 | 20.0 | 0.10 | 0.02 | 0.00001 | 2.0 | 0.20 | 0.02 | 0.00004 | 20.0 | 0.10 | 0.02 | 0.00001 | 2.0 |
| 23 | 0.20 | 0.02 | 0.00004 | 20.0 | 0.10 | 0.02 | 0.00001 | 2.0 | 0.20 | 0.02 | 0.00004 | 20.0 | 0.10 | 0.02 | 0.00001 | 2.0 |
| 24 | 0.15 | 0.02 | 0.00004 | 20.0 | 0.08 | 0.02 | 0.00004 | 2.0 | 0.20 | 0.02 | 0.00004 | 20.0 | 0.10 | 0.02 | 0.00001 | 2.0 |
| 25 | 0.15 | 0.02 | 0.00004 | 20.0 | 0.08 | 0.02 | 0.00004 | 2.0 | 0.20 | 0.02 | 0.00004 | 20.0 | 0.10 | 0.02 | 0.00001 | 2.0 |
| 26 | 0.15 | 0.02 | 0.00004 | 20.0 | 0.04 | 0.02 | 0.00004 | 2.0 | 0.20 | 0.02 | 0.00004 | 20.0 | 0.10 | 0.02 | 0.00001 | 2.0 |
| 27 | 0.15 | 0.02 | 0.00004 | 20.0 | 0.04 | 0.02 | 0.00004 | 2.0 | 0.20 | 0.02 | 0.00004 | 20.0 | 0.10 | 0.02 | 0.00001 | 2.0 |
| 28 | 0.15 | 0.02 | 0.00004 | 20.0 | 0.04 | 0.02 | 0.00004 | 2.0 | 0.20 | 0.02 | 0.00004 | 20.0 | 0.10 | 0.02 | 0.00001 | 2.0 |
| 29 | 0.15 | 0.02 | 0.00004 | 20.0 | 0.04 | 0.02 | 0.00004 | 2.0 | 0.20 | 0.02 | 0.00004 | 20.0 | 0.10 | 0.02 | 0.00001 | 2.0 |
| 30 | 0.15 | 0.02 | 0.00004 | 20.0 | 0.04 | 0.02 | 0.00004 | 2.0 | 0.20 | 0.02 | 0.00004 | 20.0 | 0.10 | 0.02 | 0.00001 | 2.0 |
| 31 | 0.15 | 0.02 | 0.00004 | 20.0 | 0.04 | 0.02 | 0.00004 | 2.0 | 0.20 | 0.02 | 0.00004 | 20.0 | 0.10 | 0.02 | 0.00001 | 2.0 |
| 32 | 0.15 | 0.02 | 0.00004 | 20.0 | 0.04 | 0.02 | 0.00004 | 2.0 | 0.20 | 0.02 | 0.00004 | 20.0 | 0.10 | 0.02 | 0.00001 | 2.0 |
| 33 | 0.15 | 0.02 | 0.00004 | 20.0 | 0.04 | 0.02 | 0.00004 | 2.0 | 0.20 | 0.02 | 0.00004 | 20.0 | 0.10 | 0.02 | 0.00001 | 2.0 |
| 34 | 0.15 | 0.02 | 0.00004 | 20.0 | 0.04 | 0.02 | 0.00004 | 2.0 | 0.20 | 0.02 | 0.00004 | 20.0 | 0.10 | 0.02 | 0.00001 | 2.0 |
| 35 | 0.15 | 0.02 | 0.00004 | 20.0 | 0.04 | 0.02 | 0.00004 | 2.0 | 0.20 | 0.02 | 0.00004 | 20.0 | 0.10 | 0.02 | 0.00001 | 2.0 |
| 36 | 0.15 | 0.02 | 0.00004 | 20.0 | 0.04 | 0.02 | 0.00004 | 2.0 | 0.20 | 0.02 | 0.00004 | 20.0 | 0.10 | 0.02 | 0.00001 | 2.0 |
| 37 | 0.15 | 0.02 | 0.00004 | 20.0 | 0.04 | 0.02 | 0.00004 | 2.0 | 0.20 | 0.02 | 0.00004 | 20.0 | 0.10 | 0.02 | 0.00001 | 2.0 |
| 38 | 0.15 | 0.02 | 0.00004 | 20.0 | 0.04 | 0.02 | 0.00004 | 2.0 | 0.20 | 0.02 | 0.00004 | 20.0 | 0.10 | 0.02 | 0.00001 | 2.0 |

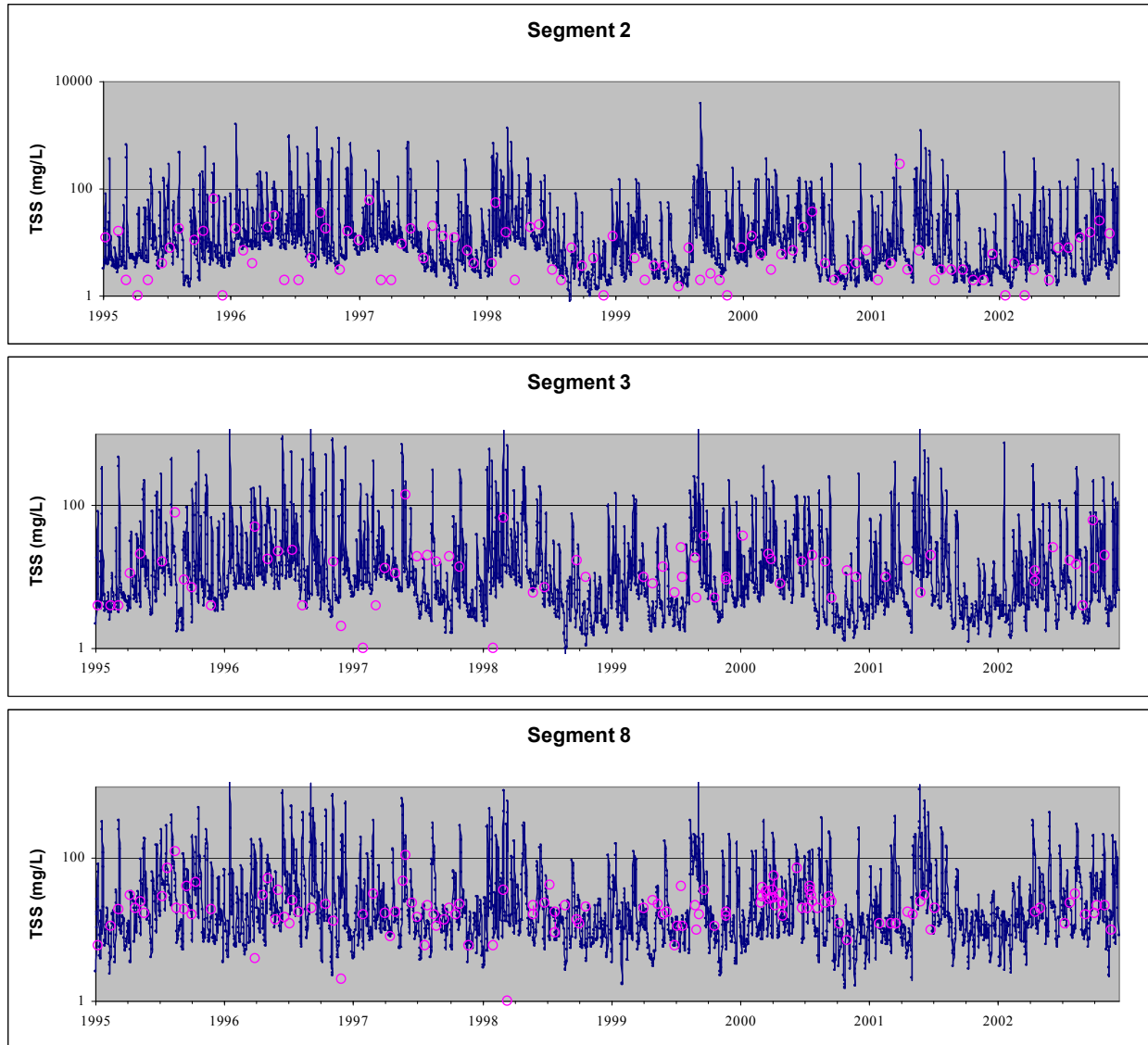


Figure 3-7. Daily TSS predictions versus observations at segments 1, 2, and 8

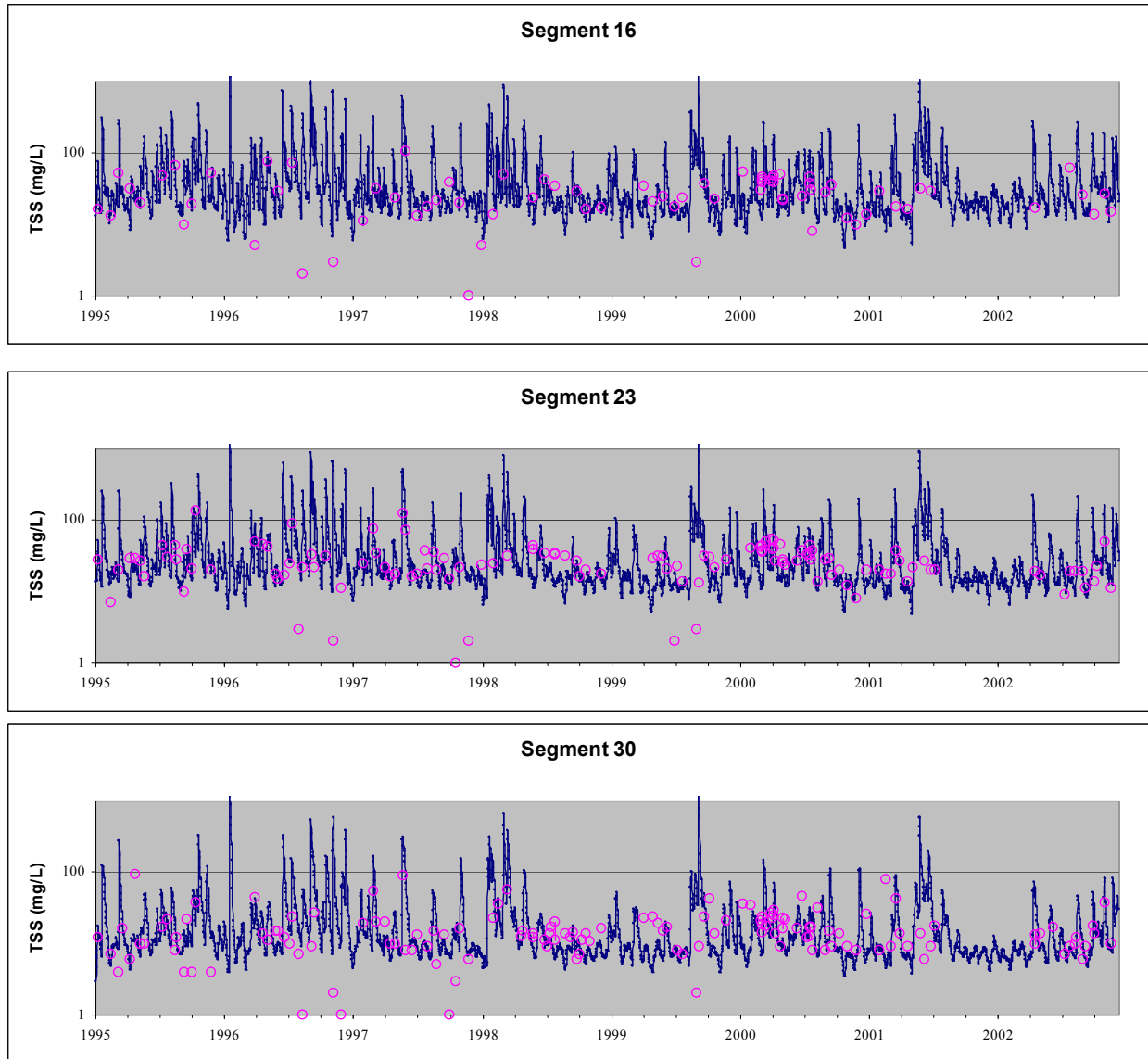


Figure 3-8. Daily TSS predictions versus observations at segments 16, 23, and 30

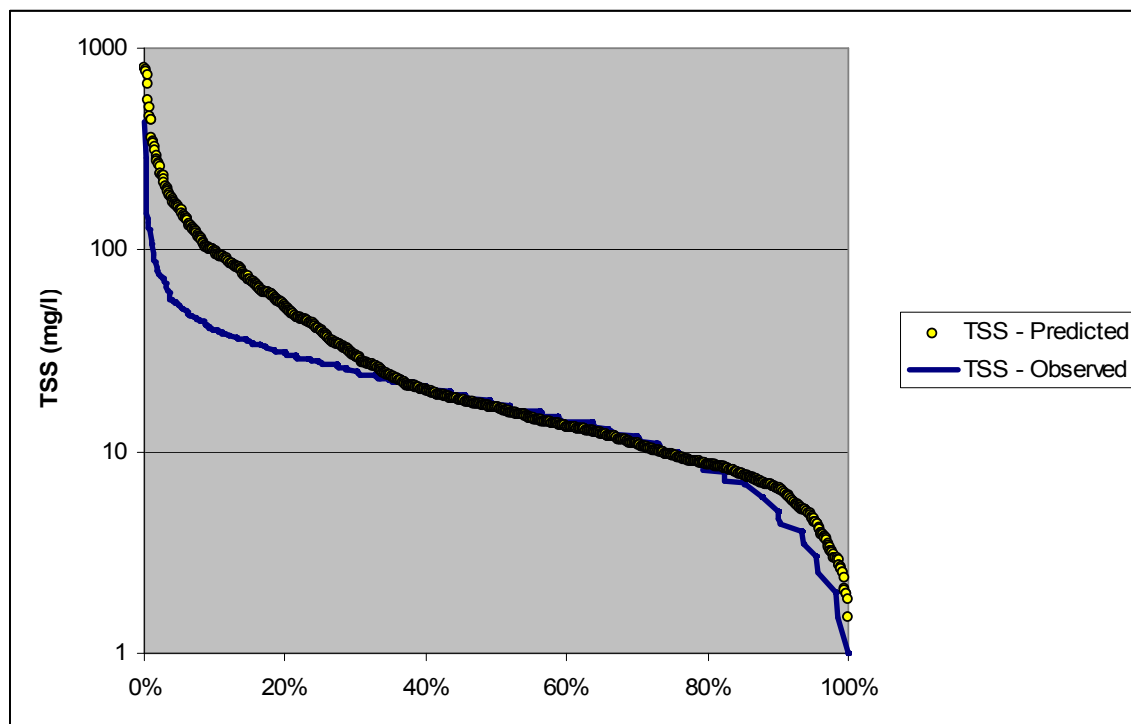


Figure 3-9. Cumulative distribution functions for predicted and observed TSS values

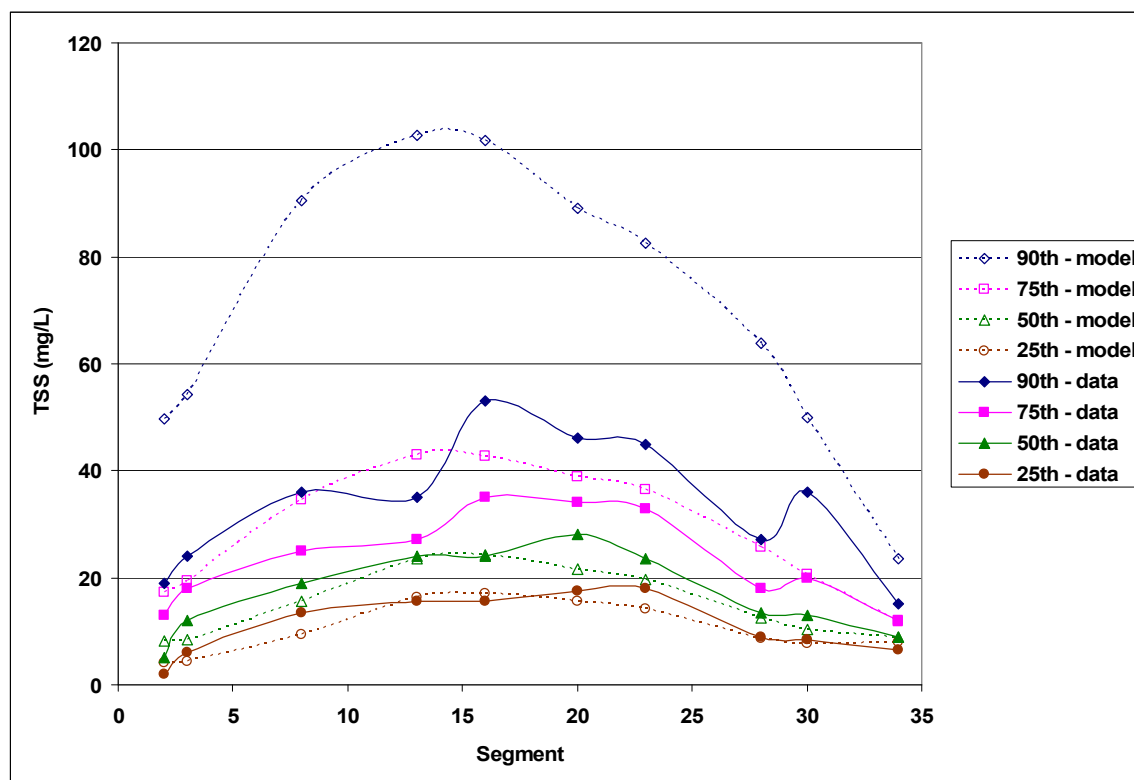


Figure 3-10. Longitudinal profiles of predicted (calibration run) and observed TSS values

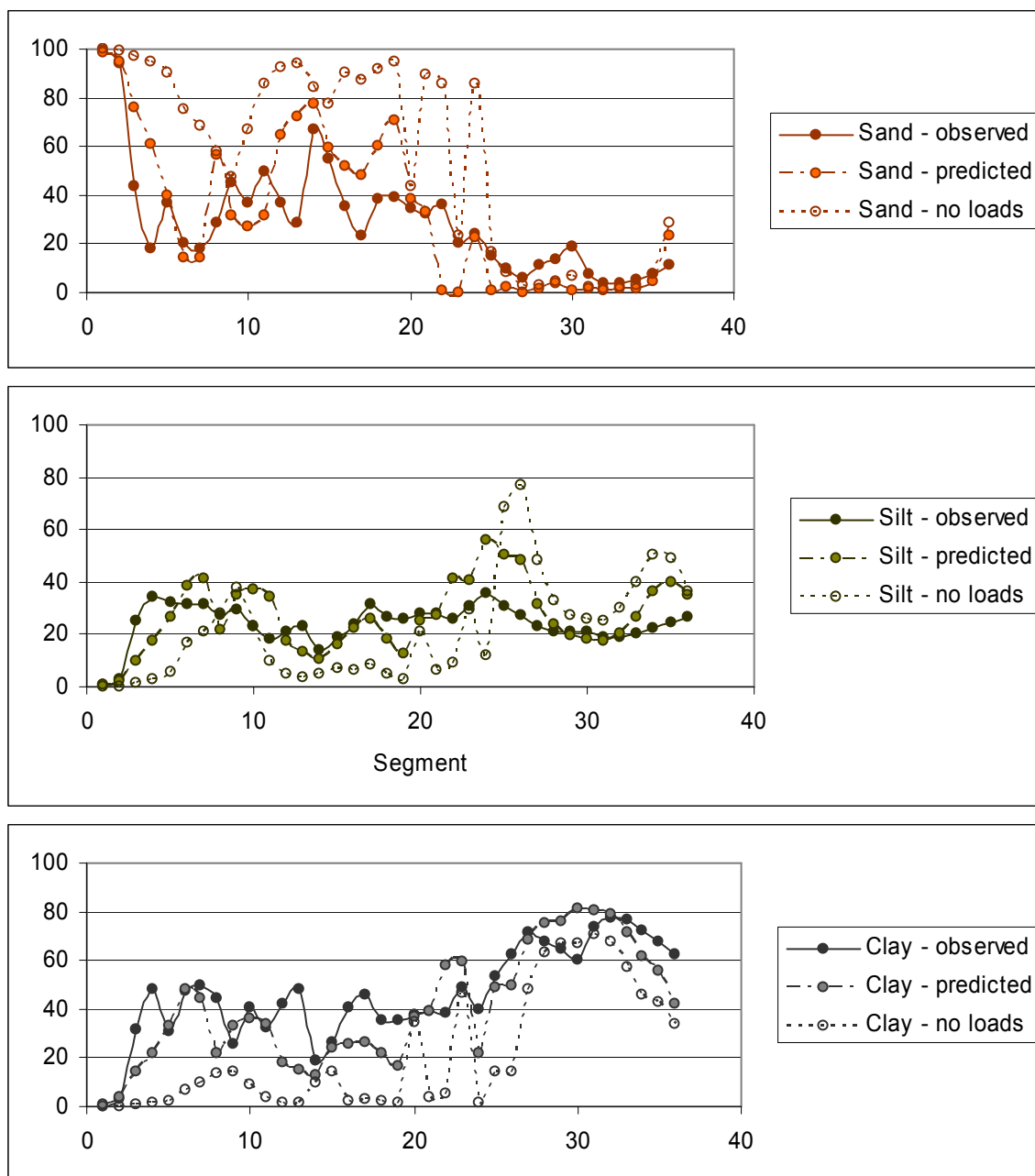


Figure 3-11. Longitudinal profiles of predicted TSS percentile values for calibration and "no erosion" run

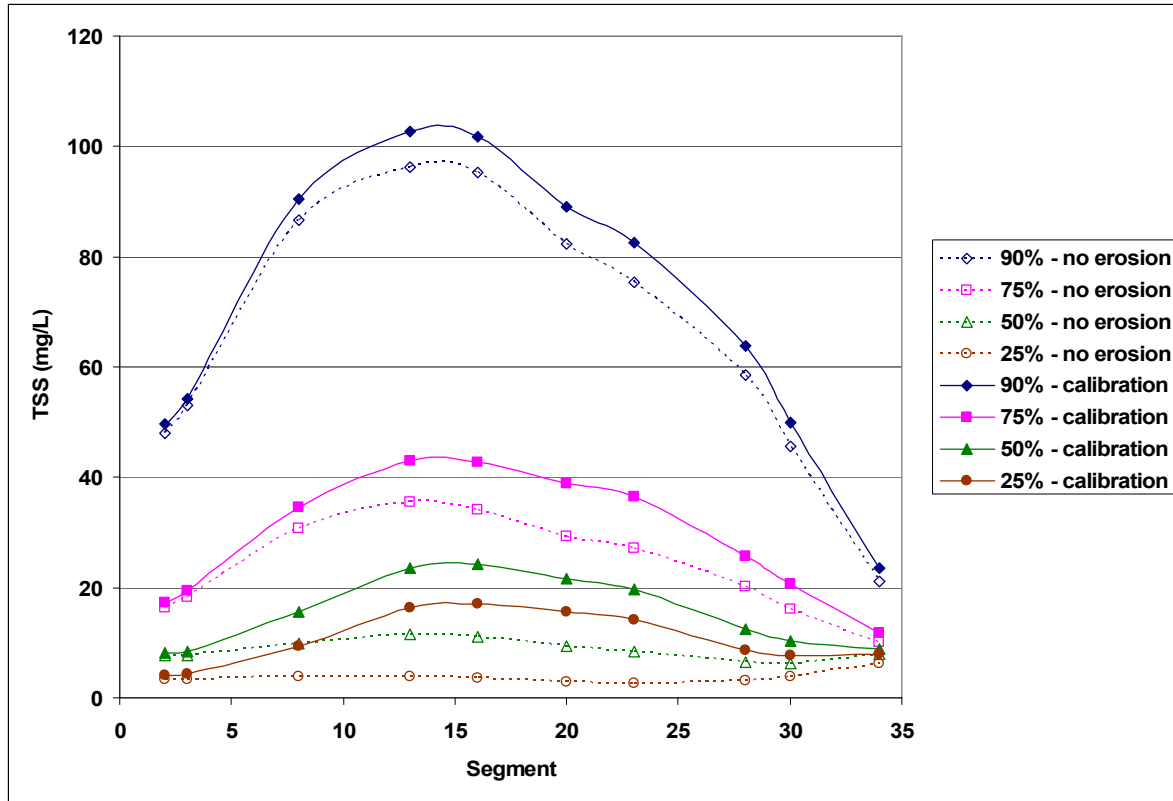


Figure 3-12. Longitudinal profiles of predicted TSS percentile values for calibration and "no erosion" run

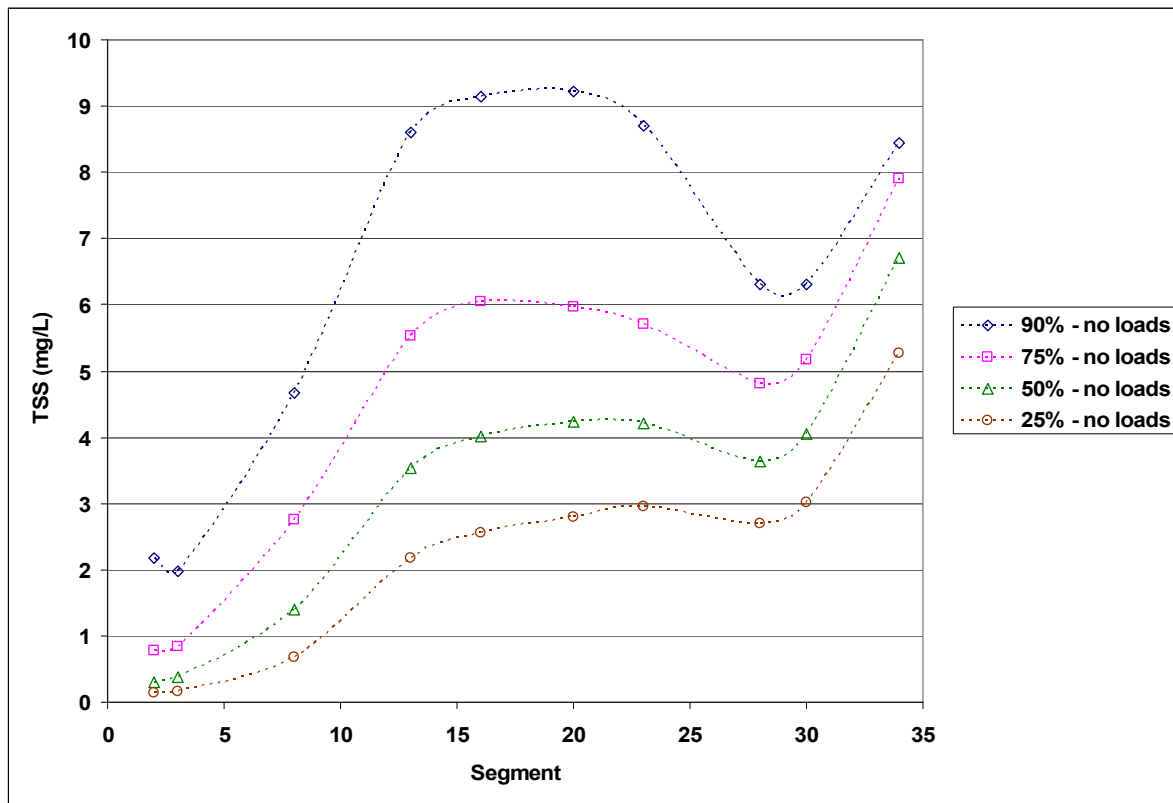


Figure 3-13. Longitudinal profiles of predicted TSS percentile values for calibration and "no loads" runs

3.5.3 Eutrophication component: configuration and input parameters

The eutrophication model was run with a time step of 1/200 day. Values for input parameters governing reaction kinetics were taken from Mandel and Schultz (2000), with the exception of the phytoplankton growth rate, K_c , and parameters related to light. Values for these parameters are discussed in Section 3.5.4, below. Input time series were prepared as described in Mandel and Schulz (2000), with the following exceptions:

- Time series representing downstream boundary conditions were constructed directly from available routine monitoring data at station ANA29, located near the Potomac confluence, for the calibration period, 1995 through 2002. Because no data were available for ON , PO_4 , or OP during the calibration time period, time series for these constituents were constructed using quarterly averages of ON and total phosphorus data from the period, 1984-1992. Similarly, for the years 1995 – 1998, in which no chlorophyll a data were available, quarterly averages of available data were used.
- Daily averages of hourly water temperature measured at the NOAA tide gage located in the Washington Shipping Channel (Station 8594900) were used to construct a time series of tidal Anacostia water temperature. For time periods in which the NOAA data was not available, water temperature measurements available from the DCDOH routine monitoring program were used. For each date with routine monitoring data, an average over all stations was used in the time series. NOAA water temperature daily averages were corrected based on results of a regression analysis of NOAA daily averages and DCDOH routine data station averages for same day, which yielded the following relationship (degrees C): (Anacostia daily water temp) = $-1.0 + 0.94 * (\text{NOAA daily mean water temp})$

3.5.4 Eutrophication component: calibration/verification

The TAM/WASP eutrophication component was calibrated to the longitudinal profile of median Secchi depths, and to available chlorophyll a data. Adjustments were made to the maximum phytoplankton growth rate constant, K_c , and to the two parameters, “a” and “b”, in the equation for the light extinction coefficient, Equation 12, to provide the best match to available data. A comprehensive recalibration of the original model (Mandel and Schultz, 2000) was not within the scope of this project, since the eutrophication component is only relied upon here to simulate chlorophyll a and Secchi depths, and a full upgrade of the eutrophication model is planned for the next phase of MDE’s Anacostia TMDLs.

The maximum phytoplankton growth rate constant, K_c , was reduced from 2.0 to 1.1 day^{-1} in order to reduce chlorophyll a predictions and provide a reasonable match to available data. The need for this fairly significant reduction was due to two changes made in this version of the model: the change from the diToro to the Smith light formulation, and the change in the assumed relationship between Secchi depth and the light extinction coefficient, given by Equation 11. In the original version of the TAM/WASP eutrophication model, this relationship was assumed to be $K_e = 1.9/\text{Secchi}$. The parameters, “a” and “b”, in Equation 12 were varied to provide a good fit of model predictions to Secchi depth growing season (April 1 to October 31) medians computed at the main DC routine monitoring stations over the calibration period, 1995 – 2002. The values, $a = 0.45$ and $b = 0.13$, produced the minimum mean square error for the values

tested. Eutrophication model predictions are compared with available data in Figure 3-14 through Figure 3-18. Predicted and observed median growing season Secchi depths are shown in Figure 3-18.

Table 3-8. TAM/WASP Version 3 eutrophication component parameter values

| Parameter | Units | WASP variable name | Value | Comment |
|--|---|-----------------------------------|--------------|---------------------------|
| Maximum phytoplankton growth rate constant | day ⁻¹ | K1C | 1.1 | 2.0 in TAM/WASP Version 1 |
| Maximum quantum yield | mg C/mole photons | PHIMX | 720 | WASP default value |
| Chlorophyll extinction coefficient | (mg chla/m ³) ⁻¹ m ⁻¹ | XKC | 0.017 | WASP default value |
| Parameter “a” in equation for light extinction coefficient (Equation 12) | m ⁻¹ | CLE1 | 0.45 | ICPRB-added parameter |
| Parameter “b” in equation for light extinction coefficient (Equation 12) | (m*mg/L) ⁻¹ | CLE2 | 0.13 | ICPRB-added parameter |

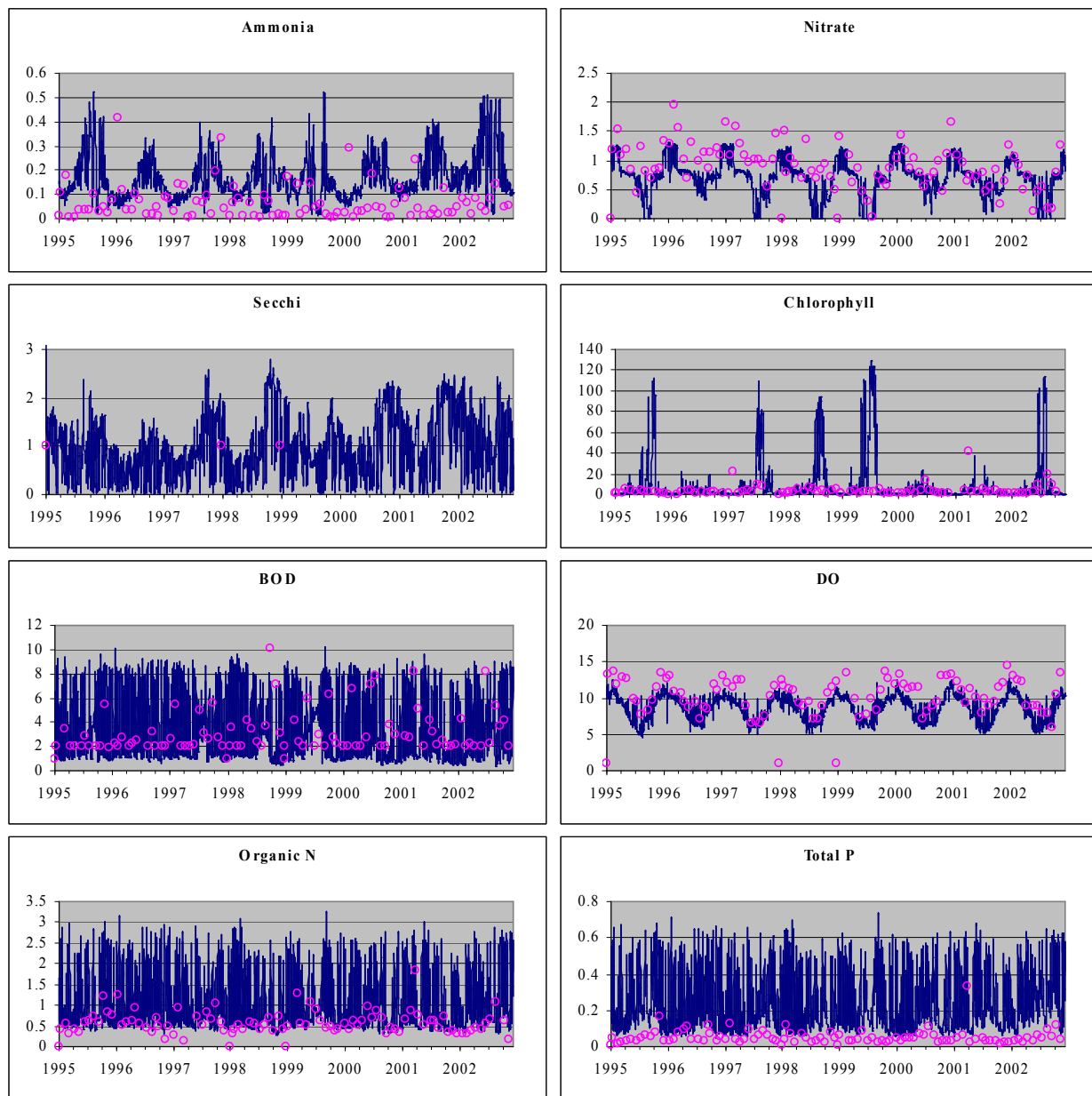


Figure 3-14. Predicted vs. observed concentrations at segment 2 (ANA0082 - Bladensburg Rd)

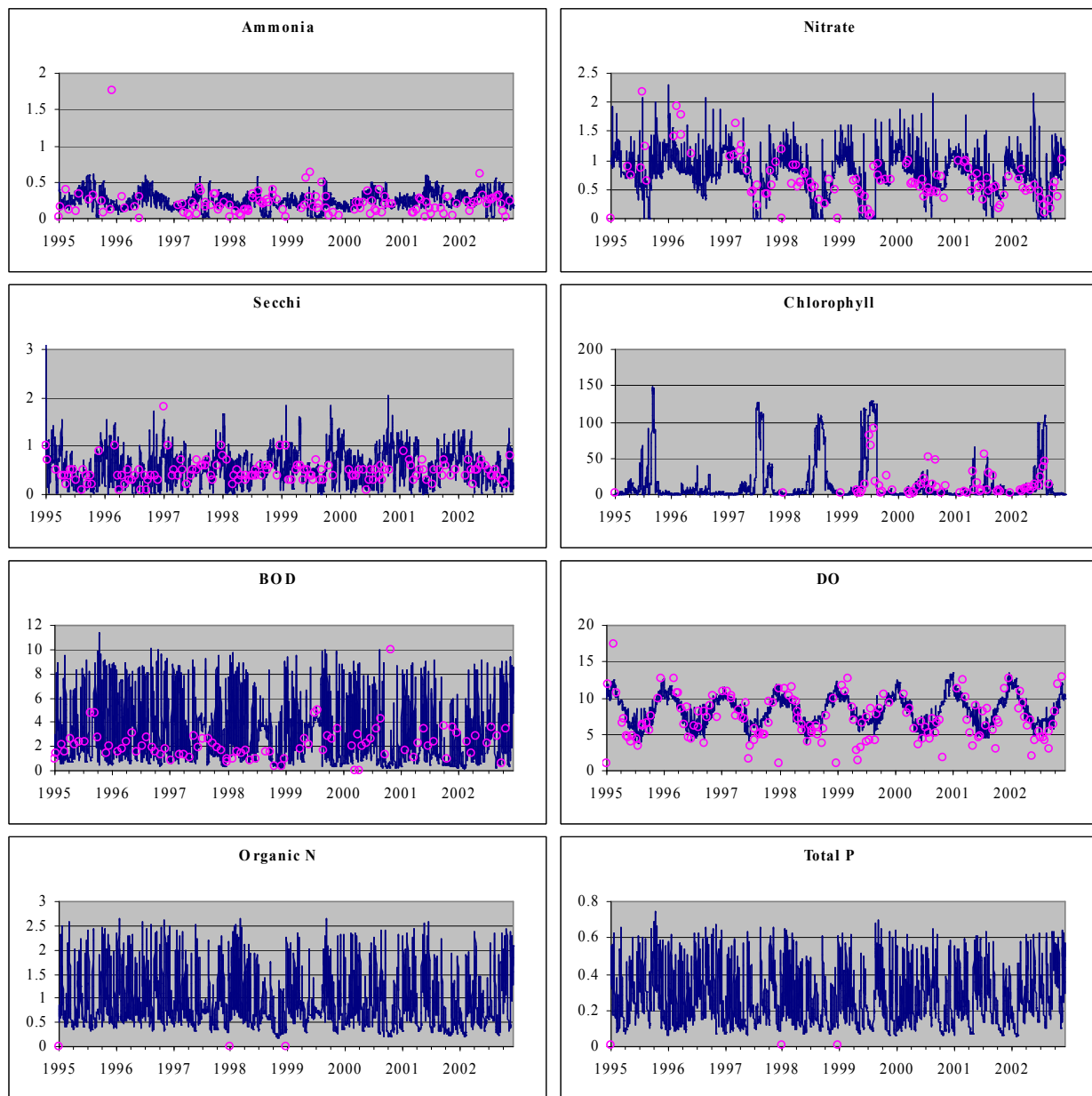


Figure 3-15. Predicted vs. observed concentrations at segment 8 (ANA01 - New York Ave)

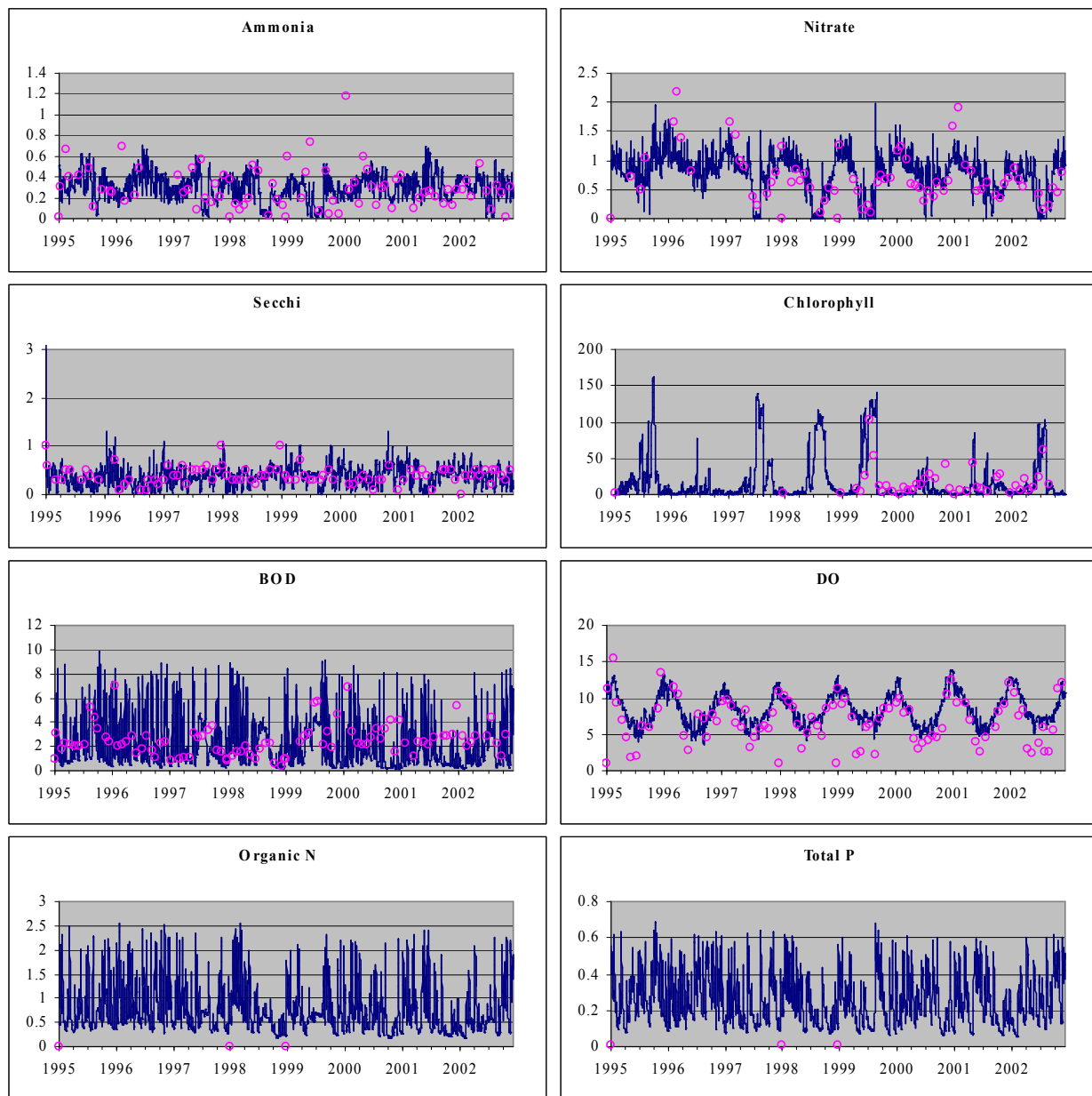


Figure 3-16. Predicted vs. observed concentrations at segment 16 (ANA08 - Benning Rd)

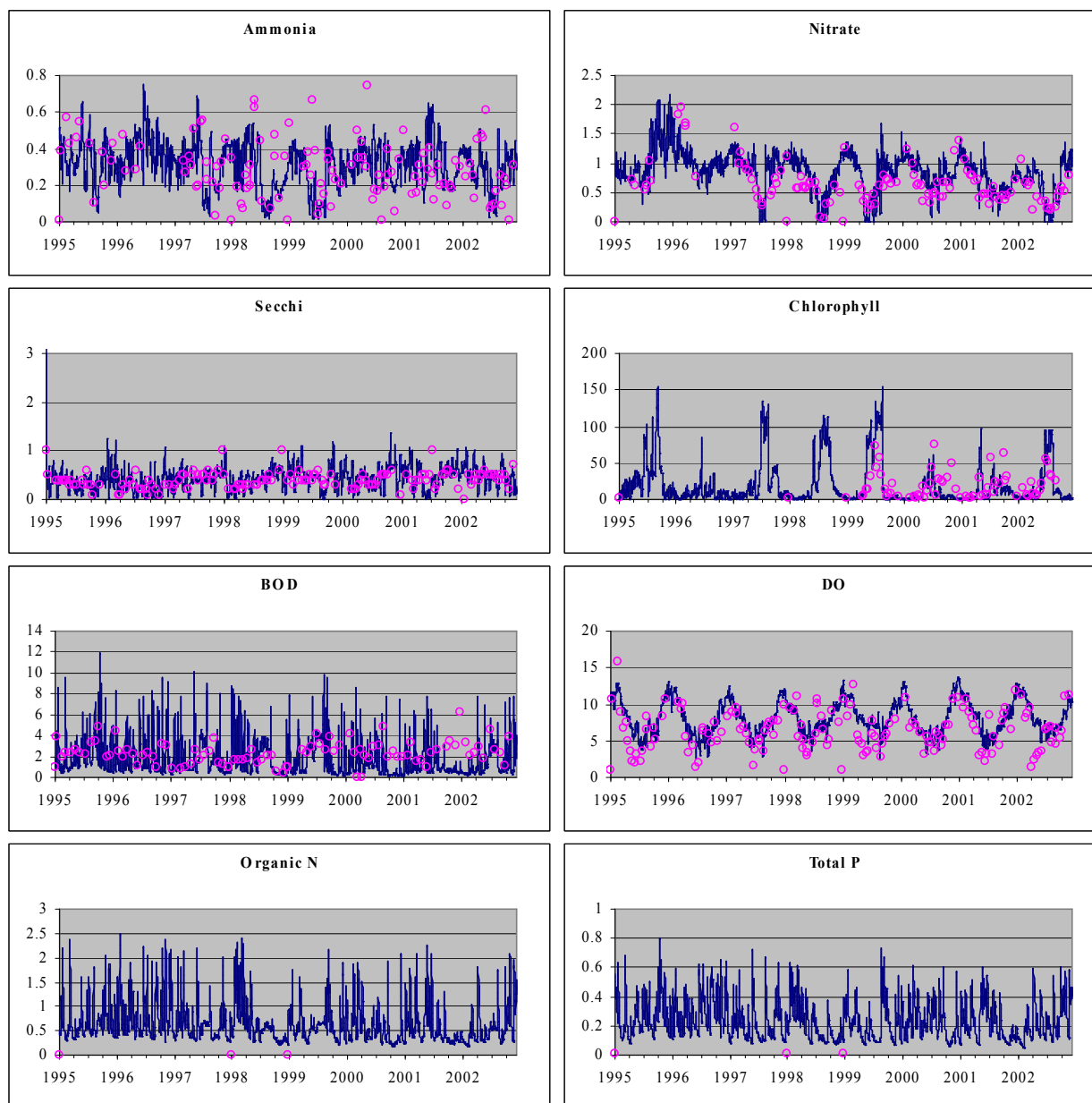


Figure 3-17. Predicted vs. observed concentrations at segment 23 (ANA14 - Pennsylvania Ave)

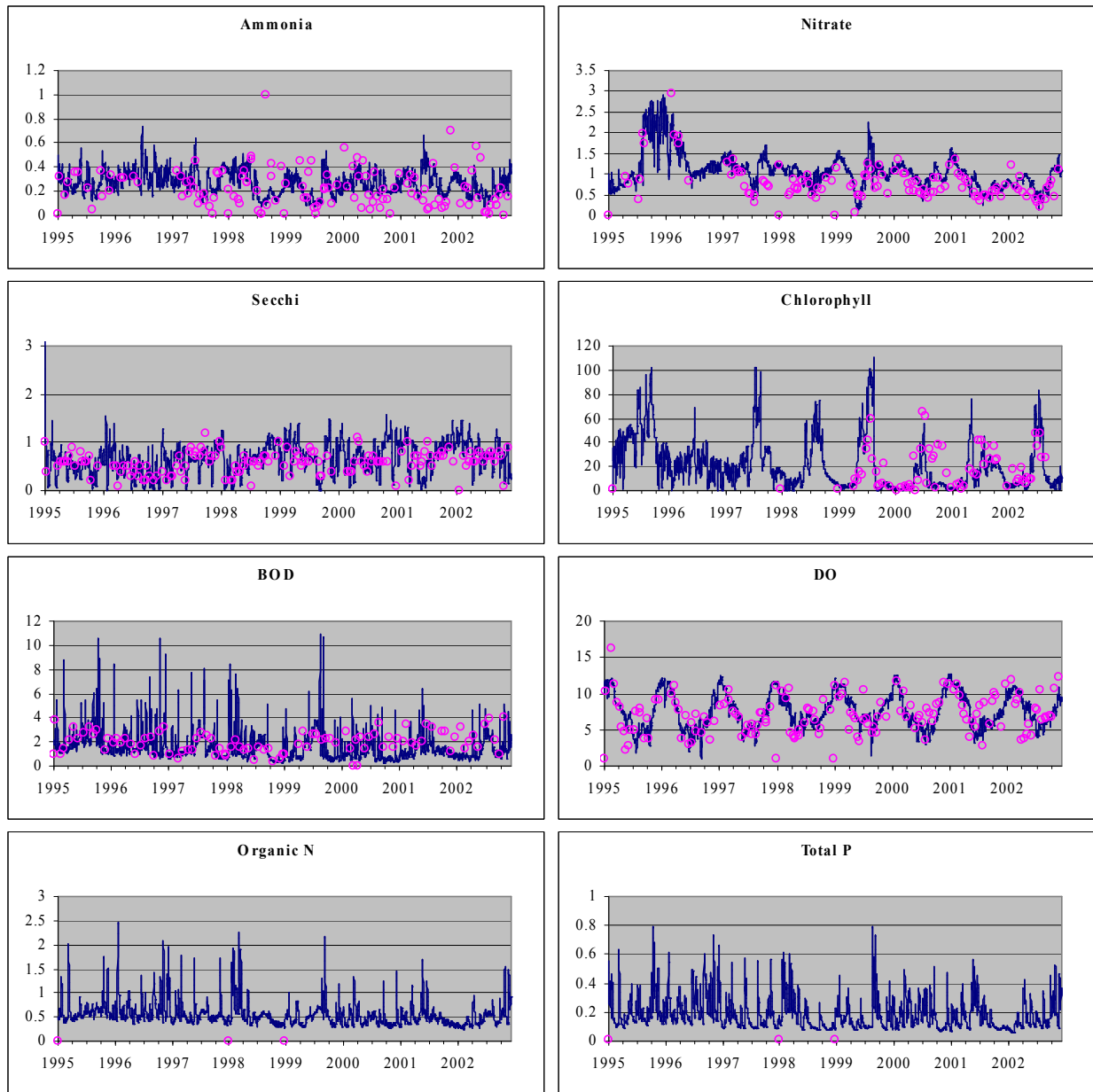


Figure 3-18. Predicted vs. observed concentrations at segment 30 (ANA24 - South Capitol St)

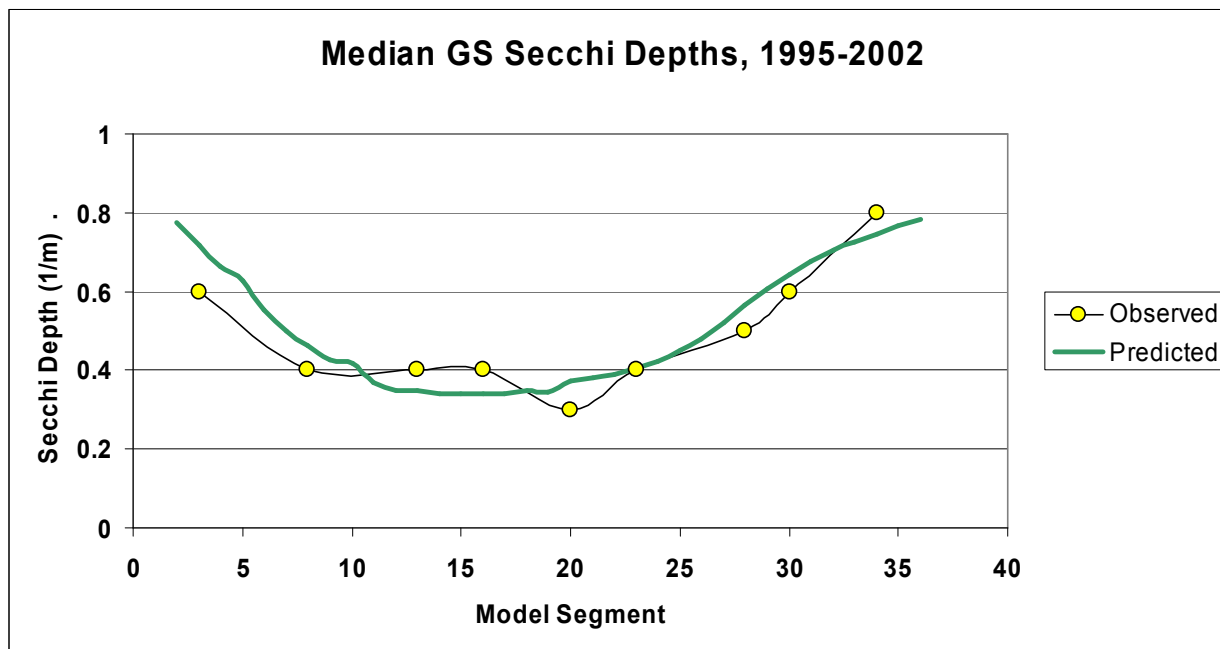


Figure 3-19. Longitudinal profiles of predicted and observed median Secchi depths

4 CONCLUSIONS

This report describes a set of modeling tools that simulate the loading, fate, and transport of sediment in both the non-tidal tributaries and the tidal portion of the Anacostia River. The Phase 3 Anacostia HSPF watershed model of the non-tidal tributaries simulates loads of sediment from land surface areas, erosion of sediment from stream channels, and transport of sediment by non-tidal streams. The TAM/WASP Version 3 water clarity model of the tidal river simulates the transport of suspended sediment by the river's current, sediment settling and re-suspension, light conditions, and the growth of algae. These models can be used together to simulate the existing daily sediment loads entering the tidal river and their impact on daily water clarity conditions. The TAM/WASP model can be also used to predict changes in water clarity due to hypothetical sediment load reduction scenarios.

The computer model HSPF was used to develop a simulation of hydrology and sediment transport in the Northwest Branch, Northeast Branch, Lower Beaverdam Creek, and Watts Branch watersheds for the period 1995-2004. The model builds on earlier HSPF models for the Anacostia watershed, but incorporates monitoring data recently collected by the USGS at their gages on the Northeast and Northwest Branches. Monthly sediment loads from ESTIMATOR were used as sediment calibration targets for the Northeast and Northwest Branches. Sediment calibration targets for Lower Beaverdam Creek, Watts Branch, and subwatersheds of the Northeast and Northwest Branches were determined from the Northwest and Northeast Branch ESTIMATOR loads with the help of the Penn State streambank erosion algorithm. In general, the watershed models match their calibration targets on an average annual basis and capture much of the monthly variation in sediment loads.

The TAM/WASP water clarity model is a coupled set of hydrodynamic and water quality models that simulate daily concentrations of TSS, phytoplankton (algae), and other water quality constituents, as well as Secchi disk depth, a common measure of water clarity. The model captures a portion of the interaction between water clarity and phytoplankton growth by computing the phytoplankton growth rate based on the model's estimates of daily suspended sediment concentrations. The model tends to over-predict the high-percentile values of TSS concentrations, likely to occur during periods of wet weather, but does a reasonable in predicting both median values of TSS and Secchi depths along the length of the tidal river.

5 REFERENCES

Ambrose, R.B. Jr., T.A. Wool, and J.L. Martin. 1993. The Water Quality Analysis Simulation Program, WASP5. U.S. Environmental Protection Agency Research Laboratory. Athens, GA.

Bicknell, B.R., J.C. Imhoff, J.L. Kittle, Jr., and A.S. Donigian, Jr. 2000. Hydrological Simulation Program - Fortran (HSPF): User's Manual for Release 12.

Biological Systems Engineering Department, Virginia Polytechnic Institute and State University. 2003. Opequon Watershed TMDLs for Benthic Impairments: Abrams Creek and Lower Opequon Creek, Frederick and Clarke Counties, Virginia. Blacksburg, VA.
<http://www.deq.virginia.gov/tmdl/apptmdls/shenrvr/abropebc.pdf>

Biological Systems Engineering Department, Virginia Polytechnic Institute and State University. 2005. Using GWLF for TMDL Development. American Society for Agricultural Engineers. Third Conference on Watershed Management to Meet Water Quality Standards and Emerging TMDL. Atlanta, GA. March 6 2005.

Cerco, C. F., M. R. Noel, and L. Linker. 2004. Managing for Water Clarity in Chesapeake Bay. Journal of Environmental Engineering, June 2004 (631 – 642).

Chesapeake Bay Program Office. 2006. CBP Watershed Model Scenario Output Database, Phase 4.3. <http://www.chesapeakebay.net/data/index.htm>

DCDOH. 2001. Total Maximum Daily Loads Upper Anacostia River Lower Anacostia River District of Columbia Biochemical Oxygen Demand. District of Columbia Department of Health, Environmental Health Administration, Bureau of Environmental Quality, Water Quality Division, Water Quality Control Branch, May 2001.

DCDOH. 2002. Total Maximum Daily Loads Upper Anacostia River Lower Anacostia River District of Columbia Total Suspended Solids. District of Columbia Department of Health, Environmental Health Administration, Bureau of Environmental Quality, Water Quality Division, Water Quality Control Branch, Draft - January 4, 2002.

DCWASA. 1986. Map - Sewerage System. District of Columbia Government, Department of Public Works, Water and Sewer Utility Administration, November 1986.

DC WASA. 2001. Study Memorandum LTCP-6-4: Anacostia River Model Documentation - Draft. District of Columbia Water and Sewer Authority EPMC III - Sewer Systems. Program Manager - Greeley and Hansen. August 2001.

DCWASA. 2002. Combined Sewer System Long Term Control Plan – Final Report. District of Columbia Water and Sewer Authority, Washington, DC, July 2002.

Doherty, J. 2001. PEST: Model independent parameter estimation - User's Manual. Watermark Numerical Computing.

Evans, B.M., D.W. Lehning, K.J. Corradini, G.W. Petersen, E. Nizeyimana, J.M. Hamlett, P.D. Robillard, and R.L. Day, 2002. A Comprehensive GIS-Based Modeling Approach for Predicting Nutrient Loads in Watersheds. *J. Spatial Hydrology*, Vol. 2, No. 2.

Evans, B. M., S. A. Sheeder, and D. W. Lehning. 2003. A Spatial Technique For Estimating Streambank Rosion Based On Watershed Characteristics. *Journal of Spatial Hydrology*, Vol. 3, No. 1.

Gruessner, B., D.J. Velinsky, G.D. Foster, R.P. Mason, and J. Scudlark. 1997. Dissolved and particulate transport of chemical contaminants in the Northeast and Northwest Branches of the Anacostia River. Interstate Commission on the Potomac River Basin, Report 97-10. ICPRB, Rockville, Maryland.

Hill, S., and P. McLaren. 2000. A sediment trend analysis (STA[®]) of the Anacostia River. GeoSea[®] Consulting (Canada) Ltd. Brentwood Bay, British Columbia, Canada, December 2000.

Katz, C.N., A.R. Carlson, and D.B. Chadwick. 2000. Anacostia River water quality assessment – draft report to the Anacostia Watershed Toxics Alliance, SPAWAR Systems Center, Marine Environmental Quality Branch, San Diego, CA, December 2000.

Krone, R. B. 1962. Flume Studies of the Transport of Sediment in Estuarial Shoaling Processes. Hydraulic Engineering Laboratory and Sanitary Engineering Research Laboratory, University of California. Berkeley, CA.

LTI. 1995. Documentation Report District of Columbia NPDES Part II Storm Water Permit Application GIS Coverages. Prepared by Limno-Tech, Inc., Washington, DC for Peer Consultants, Rockville, MD, 7/14/95.

LTI. 2000. Dye Study for the Tidal Anacostia River - Final Report. Prepared for U.S. EPA Region 3 by Limno-Tech, Inc., Washington DC. September 30, 2000.

LTI. 2007. Personal communication.

Mandel, R. and C.L. Schultz. 2000. The TAM/WASP Model: a modeling framework for the Total Maximum Daily Load allocation in the tidal Anacostia River – Final Report. Prepared by the Interstate Commission on the Potomac River Basin for the District of Columbia, Department of Health, Environmental Health Administration. Washington, DC.

Manchester, M. and R. Mandel. 2001. Technical Memo: A Preliminary Calibration of the Simulation of Hydrology, Sediment Transport, and Nutrient Dynamics in the HSPF Model of the Non-Tidal Anacostia River. Draft. The Interstate Commission on the Potomac River Basin. Rockville, MD.

Mandel, R. and C. Schultz. 2000. The TAM/WASP Model: A Modeling Framework for the Total Maximum Daily Load Allocation in the Tidal Anacostia River. District of Columbia Department of Health. Washington, DC.

Mandel, R., R. Shi, and D. Vann. 2003. The Development of an HSPF Model of the Non-tidal Anacostia River Watershed, Phase II. The Interstate Commission on the Potomac River Basin. Rockville, MD.

Maryland Department of State Planning. 1973. Natural Soil Groups Technical Report. .
http://www.mdp.state.md.us/zip_downloads.htm

Maryland Department of State Planning. 2002. Land Use Land Cover.
http://www.mdp.state.md.us/zip_downloads.htm

MWCOG. 2001a. Study Memorandum LTCP 6-2c: District of Columbia CSO Long Term Control Plan Wet Weather Surveys Report. Prepared for the District of Columbia Water and Sewer Authority by the Metropolitan Washington Council of Governments and the US Naval Research Laboratory, September 2001.

MWCOG. 2001b. Technical Memorandum LTCP 6-4: Anacostia River Model Documentation, Draft. Prepared for the District of Columbia Water and Sewer Authority EPMC III – Sewer Systems Engineering Program Management Consultant III Greeley and Hansen – Program Manager, by the Metropolitan Washington Council of Governments, August 2001.

Natural Resources Conservation Service. 1995. Soil Survey of Montgomery County, Maryland. Department of Agriculture. Washington, DC.

Partheniades, E. 1962. A Study of Erosion and Deposition of Cohesive Soils in Salt Water. Ph. D. Thesis, University of California. Berkeley, CA.

Schultz, C.L. 2003. Calibration of the TAM/WASP sediment transport model – Final Report. Interstate Commission on the Potomac River Basin, Rockville, Maryland, October 2001, Revised April 2003, ICPRB Report No. 03-01.

Schultz, C.L., and D.V. Velinsky. 2001. Collection of Field Data for the Transport of Sediments in the Anacostia River - Draft Report. Prepared for the District of Columbia, Department of Health, Environmental Health Administration by the Interstate Commission on the Potomac River Basin, Rockville, Maryland, May 3, 2001.

Shepp, D.L., C. Clarkson, and T.J. Murphy. 2000. Estimation of Nonpoint Source Loads to the Anacostia River in the District of Columbia for the Total Maximum Daily Load Process. Prepared by the Metropolitan Washington Council of Governments for the District of Columbia Department of Health, Environmental Health Administration, Water Quality Management Division, March 2000.

- Soil Conservation Service. 1967. Soil Survey Prince George's County Maryland.. U.S. Government Printing Office. Washington, DC.
- Soil Conservation Service. 1983. National Engineering Handbook. Section 3: Sedimentation. Water Resources Publications. Littleton, CO.
- Sullivan, M.P. and W.E. Brown. 1988. The Tidal Anacostia Model. Metropolitan Washington Council of Governments. Washington, DC.
- Tetra Tech.2000. Lower Beaverdam Creek HSPF Modeling. Fairfax, VA.
- Trieu, P., J. Galli, K. Levensky, and C. Vatoec. 2004. Technical Memorandum: Anacostia Tributary Streambank Erosion Pilot Study. Phase I. Upper Beaverdam Creek Subwatershed. Metropolitan Washington Council of Governments. Washington, DC.
- US ACE. 1999. Kingman Lake Wetland Restoration Project Anacostia River (set of 17 sheets), Washington, DC", U.S. Army Engineer District, Baltimore, Corps of Engineers, Baltimore, Maryland, File: B433, June 1999.
- USEPA. 2002a. Total Maximum Daily Loads Upper Anacostia River Lower Anacostia River District of Columbia Total Suspended Solids. U.S. Environmental Protection Agency Region 3, Philadelphia, PA, March 1, 2002.
- USEPA. 2002b. Decision Rationale Total Maximum Daily Loads Total Suspended Solids Upper Anacostia River Lower Anacostia River District of Columbia, U.S. Environmental Protection Agency Region 3, Philadelphia, PA, March 1, 2002.
- USDA. 1986. Urban Hydrology for Small Watersheds, Technical Release 55. United States Department of Agriculture.
- USGS. 1997. National Hydrologic Database, U.S. Geological Survey, <http://nhd.usgs.gov>
- Velinsky, D.V., B. Gruessner, H.C. Haywood, J. Cornwall, R. Gammisch, and T.L. Wade. 1997. Determination of the volume of contaminated sediments in the Anacostia River, District of Columbia. Prepared by ICPRB for the DC Environmental Regulation Administration, Washington, DC.
- Velinsky, D.V., G.F. Riedel, G. Foster. 1999. Effects of stormwater runoff on the water quality of the tidal Anacostia River. Prepared for the US EPA, Region III by the Academy of Natural Sciences, Patrick Center for Environmental Research, Philadelphia, PA, Report No. 99-6.
- Walker, T. 1982. Use of Secchi disk to measure attenuation of underwater light for photosynthesis. *J. Appl. Ecology*, 19, 539-544
- Warner, A., D. Shepp, K. Corish, and J. Galli. 1997. An existing source assessment of pollutants to the Anacostia watershed. Prepared for the DC Department of Consumer and

Regulatory Affairs, Environmental Regulation Administration, by the Metropolitan Washington Council of Governments, Washington, DC.

Appendix A – ESTIMATOR Results

Introduction

The U. S. Geological Survey (USGS) ESTIMATOR model (Cohn *et al.*, 1989; 1992) was used to estimate suspended solids loads for the Northeast Branch (NEB) and Northwest Branch (NWB) tributaries of the Anacostia. ESTIMATOR is a multiple regression model that predicts average daily concentration and load based on independent variables representing flow, season, and time. ESTIMATOR regression results and the daily average flow records for the time period of interest, 1995 through 2004, were used to compute time series of daily, monthly, and annual sediment loads for both tributaries. The daily load time series were used as inputs for the TAM/WASP model of suspended solids and water clarity in the tidal Anacostia. The monthly load time series were used to calibrate the HSPF watershed model (Phase 3) for the non-tidal Anacostia.

Summary of Data

Average daily flow data is available from the USGS gage stations, 01649500 on the NEB and 01651000 on the NWB. Suspended solids concentration data for the study period, 1995 through 2004, was available from a number of programs and special studies, listed in Table 1 and described below:

USGS/MDE 2003-2004 storm water monitoring study of the NEB and NWB:

The USGS, with funding from MDE, and additional funding from Prince George's County, has installed automated sampling devices at its gage stations on the NEB (station 01649500) and the NWB (station 01651000), and has collected samples since July of 2003. Each storm flow sample collected by the automatic sampling devices represents water quality at a single point in time, and is analyzed for SSC. Data for the time period, July 2003 through September 2004, were available for use in this project (Brenda Majedi, private communication).

MDE 2003 water quality monitoring: In 2003, MDE collected water quality data at the USGS gage stations on the NEB (station 01649500) and the NWB (station 01651000) in support of its TMDL program. At the time of this study, provisional data was available (private communication, Elinor Zetina).

Academy of Natural Sciences – Patrick Center for Environmental Research (ANS-PCER) 1998 stormwater runoff study: The ANS-PCER stormwater runoff study included data from samples collected at the USGS gage stations on the NEB (station 01649500) and NWB (station 01651000) (Velinsky *et al.*, 1999).

ICPRB NEB and NWB 1995-1996 storm water monitoring project: A year-long study of toxics contaminants in the NEB and NWB was conducted by ICPRB in 1995-96. Analyses for six base flow and twelve storm flow samples are available for TSS (Gruessner *et al.*, 1997).

LTCP 1999-2000 monitoring of the NEB and NWB: As part of the DCWASA LTCP study, the Occoquan Water Monitoring Laboratory (OWML) installed automatic sampling devices at the USGS gage stations on the NEB (station

01649500) and the NWB (station 01651000) to provide data for load estimates of constituents of interest for that project, including TSS (MWCOG, 2001). During storm flow conditions, composite samples were collected at equal-flow intervals over periods of time ranging from 0.3 to 1.2 days.

ANS-PCER 2002 toxic chemicals monitoring study: The ANS-PCER study of toxic chemicals in the Anacostia main channel for the DCDOH included samples collected adjacent to the USGS gage station on the NEB (station 01649500) and at a location on the NWB, at US Highway 1, that was above head-of-tide during all sampled storm events. Water quality data, including total suspended solids and organic carbon, were collected on four separate dates in May, June, August, and October of 2002 and post-storm time series data were collected in October, 2002 (private communication, David Velinsky).

Table 1. Tributary monitoring data sets - solids and water clarity-related parameter values

| Study | Study ID | Time Period | Parameter | Sample Type | Sampling Method | No. Samples NEB/NWB |
|---------------------------------------|--------------|---------------------|-----------|---------------|---------------------------|---------------------|
| USGS/MDE automated sampler monitoring | USGS/MDE | Jul 2003 – Sep 2004 | SSC | Discrete grab | Automated sampling device | 40/40 |
| MDE water quality monitoring | MDE | 2003 | TSS | Discrete grab | Manual | 17/18 |
| ANS-PCER stormwater runoff study | ANS/EPA | 1998 | TSS | Discrete grab | Manual | 9/9 |
| ICPRB study | ICPRB/DC | 1995 - 1996 | TSS | Discrete grab | Manual | 17/17 |
| LTCP upstream boundary conditions | OWML/DC WASA | 1999 - 2000 | TSS | Composite | Automated sampling device | 40/38 |
| ANS-PCER toxics study | ANS/DC | 2002 | TSS | Discrete grab | Manual | 9/10 |

The data from the six studies listed in Table 1 were judged to be sufficiently comparable to be combined into single data sets: a set of 132 suspended solids observations for the NEB and a set of 132 suspended solids observations for the NWB. These data sets are plotted in Figures A-1 and A-2 and tabulated in Tables 3 and 4. Though the LTCP data were derived from composite rather than discrete samples, they were judged to be acceptable because the time period of the composites, 0.3 to 1.2 days, was comparable to the averaging time period for the daily flows values used in the ESTIMATOR analysis. SSC data and TSS data are based on two different laboratory analytical methods that have been found to produce slightly different results (Gray *et al.*, 2000), with SSC data considered to be more reliable. SSC data are obtained from a measurement of the mass of all sediment contained in the volume of water comprising the sample, whereas TSS is commonly a measurement of the mass of sediment contained in a sub-sample of the original sample. SSC measurements have been found to be higher than paired TSS measurements in cases where there is a significant amount of sand in the sample (25%

sand or greater). Thus, the SSC measurements from the USGS/MDE study would be expected to be higher than corresponding TSS measurements might have been, especially in the case of high-flow samples.

ESTIMATOR Model

Suspended solids loads were calculated from available data for the time period, 1995-2004, using the USGS ESTIMATOR computer program developed by Tim Cohn and others. ESTIMATOR is a 7-parameter, log-linear regression model that uses stream discharge, time, and season to predict daily, monthly, and annual in-stream constituent concentrations using the following equation:

$$\ln[C] = \beta_0 + \beta_1 \ln[Q/Q_c] + \beta_2 (\ln[Q/Q_c])^2 + \beta_3 [T - T_c] + \beta_4 [T - T_c]^2 + \beta_5 \sin[2*\pi T] + \beta_6 \cos[2*\pi T] + \varepsilon$$

where

- $\ln[]$ = natural logarithm function;
- C = measured constituent concentration (mg/L);
- $\beta_0 - \beta_6$ = coefficients of the regression model;
- Q = mean daily discharge on the day the sample was taken (ft³/sec);
- Q_c = centering variable defined such that β_1 and β_2 are statistically independent;
- T = decimal time (year);
- T_c = centering variable defined such that β_3 and β_4 are statistically independent;
- π = 3.14169;
- ε = independent random error.

The coefficients of the regression model, β_0 through β_6 , are computed from the observed concentration data by ordinary least squares (or by minimum variance, in the case of censored data). β_0 is a constant, β_1 and β_2 describe the relation between discharge and concentration, β_3 and β_4 describe long-term time trends in concentration, and β_5 and β_6 describe seasonal variations in concentration (Cohn *et al.*, 1992). The centering variables, Q_c and T_c , are used to reduce covariance among the independent parameters and to enhance the precision of the load estimates. It is assumed that model errors, ε , are independent and normally distributed, with zero mean and variance and that constituent concentrations fit the specified log-linear model.

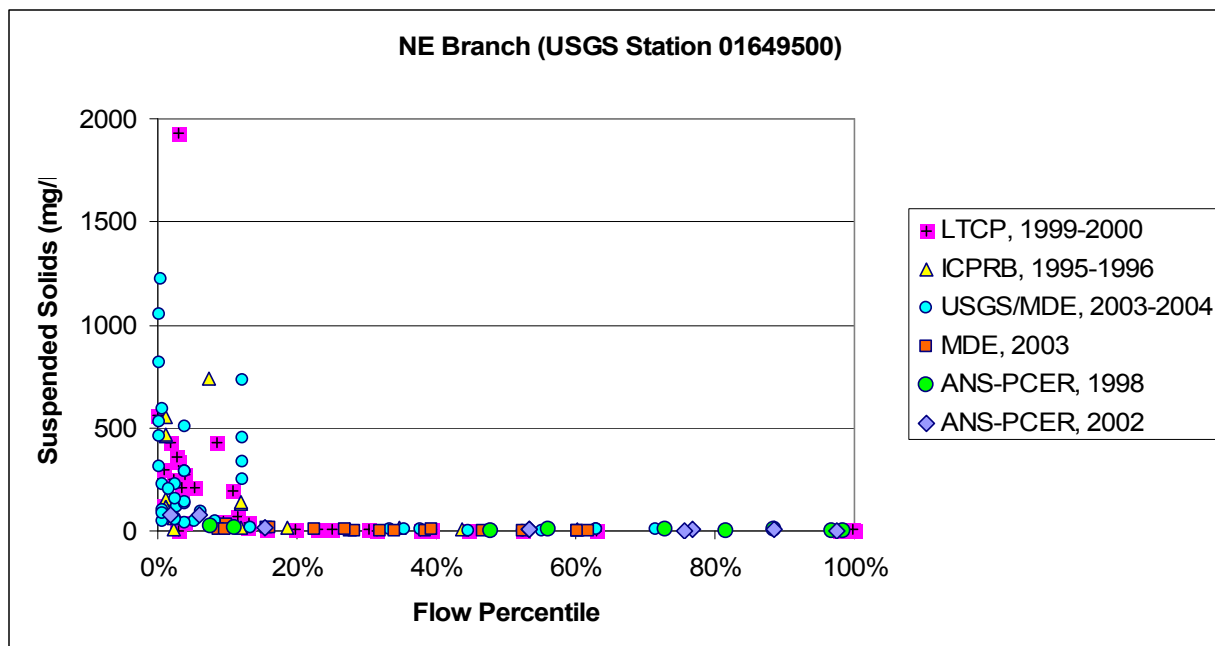


Figure A-1. Available suspended solids data for the Northeast Branch of the Anacostia, 1995-2004

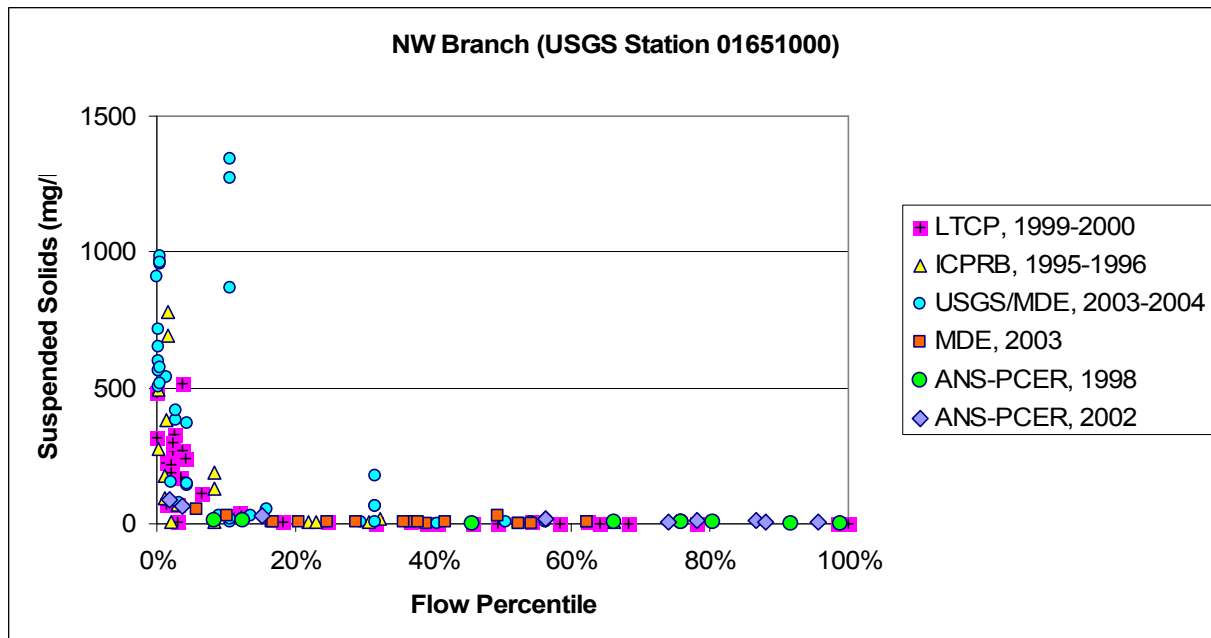


Figure A-1. Available suspended solids data for the Northwest Branch of the Anacostia, 1995-2004

ESTIMATOR requires a complete record of daily discharge that covers at least the time period of the calibration dataset and the time period selected by the user over which loads are to be estimated. It is also important to obtain a sufficient number of water quality samples that thoroughly characterize the relationship between constituent concentration and flow. The more data available, the more accurate the load estimates, but a minimum of 10 observations are recommended for each regression coefficient used, and 20 percent of the observations should be above the minimum detection limit (Baier *et al.*, 1995; Cohn, 2002). This translates into a minimum of 70 observations for a 7-parameter analysis. Ideally, half of the samples should be obtained during high flow, and the rest should be distributed uniformly throughout the year because constituent concentrations can be greatly affected by the amount of discharge at the time of sampling.

Results

The ESTIMATOR model was used to estimate daily, monthly, and annual suspended sediment loads for both the NEB and NWB tributaries for the time period, January 1995 through September 2004. Input data consisted of daily average flow data from the two most downstream USGS gage stations, 01649500 on the NEB and 01651000 on the NWB, and available suspended solids data, given in Tables 3 and 4. A graph of the average of monthly values appears in Figure A-3. The month with the highest average load is September, due to the very high storm flows that occur during hurricanes that reach the Washington, DC area. Results for annual loads, reported by Water Year (Oct 1 of previous year through Sep 30) are given in Table 2 and shown graphically in Figure A-4. The highest annual loads occurred in 2003, which was the year with high annual flow for the period of record at the two gage stations, 1939 – present.

Table 2. ESTIMATOR Predictions of Annual Sediment Loads

| WaterYear | NEB Annual Load (kg) | | | NWB Annual Load (kg) | | |
|-----------|----------------------|-------------------------|-------------|----------------------|-------------------------|-------------|
| | Predicted | 95% Confidence Interval | | Predicted | 95% Confidence Interval | |
| 1995 | 6,338,539 | 1,593,209 | 17,388,403 | 3,479,610 | 999,993 | 8,877,875 |
| 1996 | 34,537,867 | 6,150,482 | 112,084,750 | 24,684,290 | 4,850,116 | 76,552,058 |
| 1997 | 25,418,851 | 7,144,201 | 65,659,418 | 10,006,885 | 3,169,562 | 24,155,926 |
| 1998 | 26,530,366 | 6,074,560 | 76,360,874 | 10,229,528 | 3,442,918 | 23,824,735 |
| 1999 | 43,474,572 | 2,410,938 | 212,486,341 | 24,177,984 | 1,447,969 | 115,757,500 |
| 2000 | 6,701,643 | 2,801,615 | 13,622,658 | 4,386,215 | 1,740,173 | 9,224,904 |
| 2001 | 12,036,738 | 2,442,574 | 36,761,433 | 9,536,887 | 2,022,189 | 28,515,258 |
| 2002 | 2,371,110 | 454,510 | 7,439,183 | 1,822,468 | 437,806 | 5,118,700 |
| 2003 | 73,180,591 | 16,737,498 | 210,748,294 | 54,431,200 | 10,093,077 | 173,419,145 |
| 2004 | 37,390,943 | 7,766,266 | 112,925,253 | 32,362,242 | 7,618,951 | 91,840,369 |
| Mean | 267,981,220 | | | 175,117,309 | | |

ESTIMATOR gives values and measures of statistical significance for all of the 7 coefficients of the regression equation, β_0 through β_6 . For both tributaries, one or both coefficients for flow and seasonality variables were statistically significant, showing that suspended solids concentrations are dependent on stream flow (*i.e.* daily discharge) and on season. For the NEB, neither of the coefficients, β_3 and β_4 , representing the effects of

long-term trends in time, were statistically significant. For the NWB, β_3 was determined by ESTIMATOR to be significant, suggesting that suspended solids concentrations increased over the time period, 1995 through 2004. However, it was decided that this results was more likely due to the inclusion of both TSS and SSC data in the sample sets, rather than actual changes in watershed loads in this time period. Because the SSC data was collected during the end of the study period, 2003-2004, it likely biased the later years of the sample set toward higher suspended solids values (see discussion above). To check this hypothesis, the NWB ESTIMATOR run was re-done without the SSC data, and the significance of β_3 was found to disappear. Therefore, it was concluded that the NEB and NWB sample sets were not of sufficient quality to determine long-term time trends. The final ESTIMATOR runs for both the NEB and the NWB were done without inclusion of the coefficients, β_3 and β_4 .

Coefficients of determination for the final ESTIMATOR runs (dropping coefficients representing long-term trends in time) were $R^2 = 68.4$ for the NEB and $R^2 = 73.5$ for the NWB. Comparisons of ESTIMATOR results with observed data are shown in Figures A-5 and A-6. The solid curves are plots of predicted suspended solids concentrations as a function of flow only, neglecting the effects of seasonality. The circles are plots of predicted suspended solids concentrations as a function of both flow and seasonality. Clearly the ESTIMATOR is too simple a model to fully capture the flow dependence of suspended solids concentrations. For both the NEB and the NWB, ESTIMATOR somewhat over-predicts suspended solids concentrations for mid-flows of 10 to 100 mg/L, and somewhat under-predicts suspended solids concentrations for the highest flows, of > 1000 mg/L.

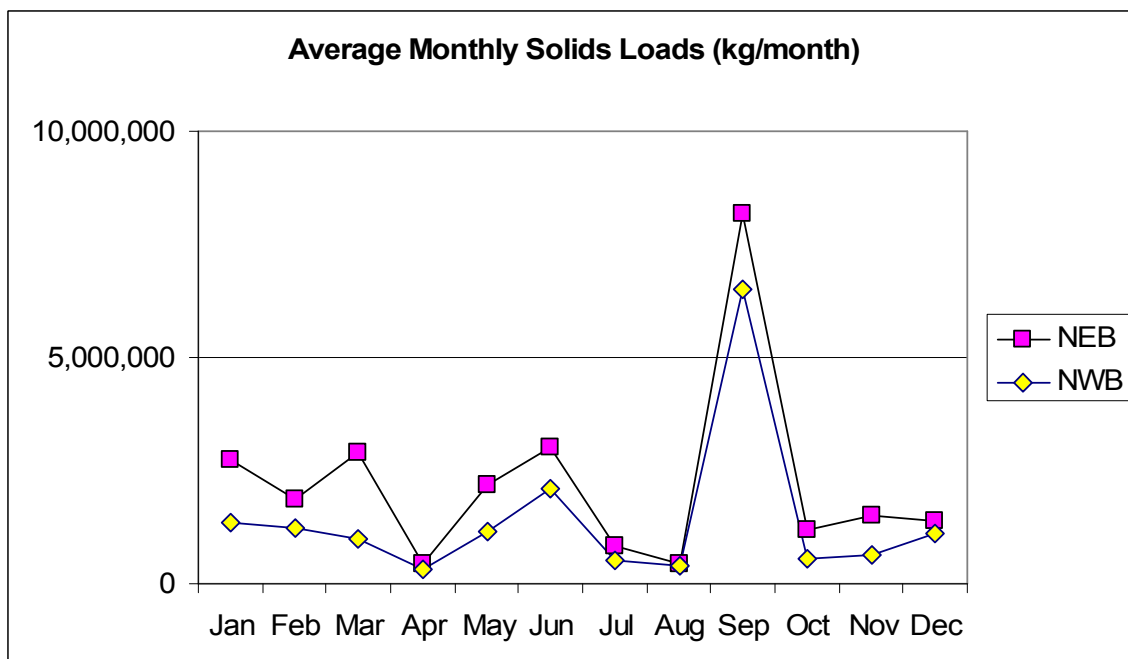


Figure A-3. Average monthly suspended sediment loads, 1995-2004

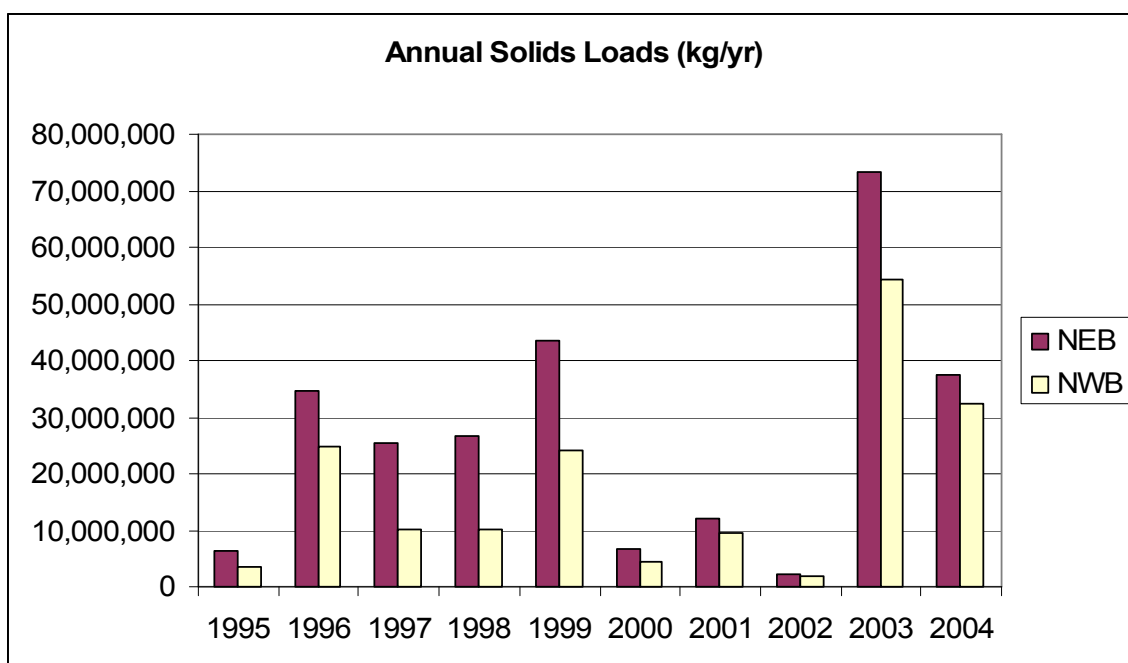


Figure A-4. Annual suspended sediment loads, Water Year 1995-2004

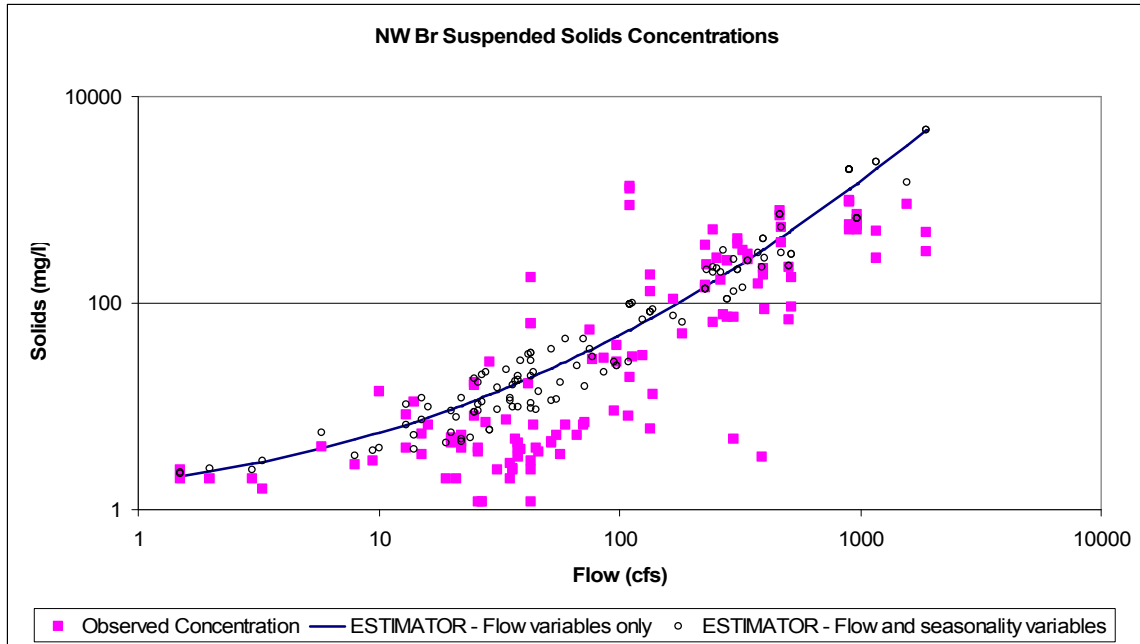


Figure A-5. Comparison of observations with ESTIMATOR predictions, Northwest Branch

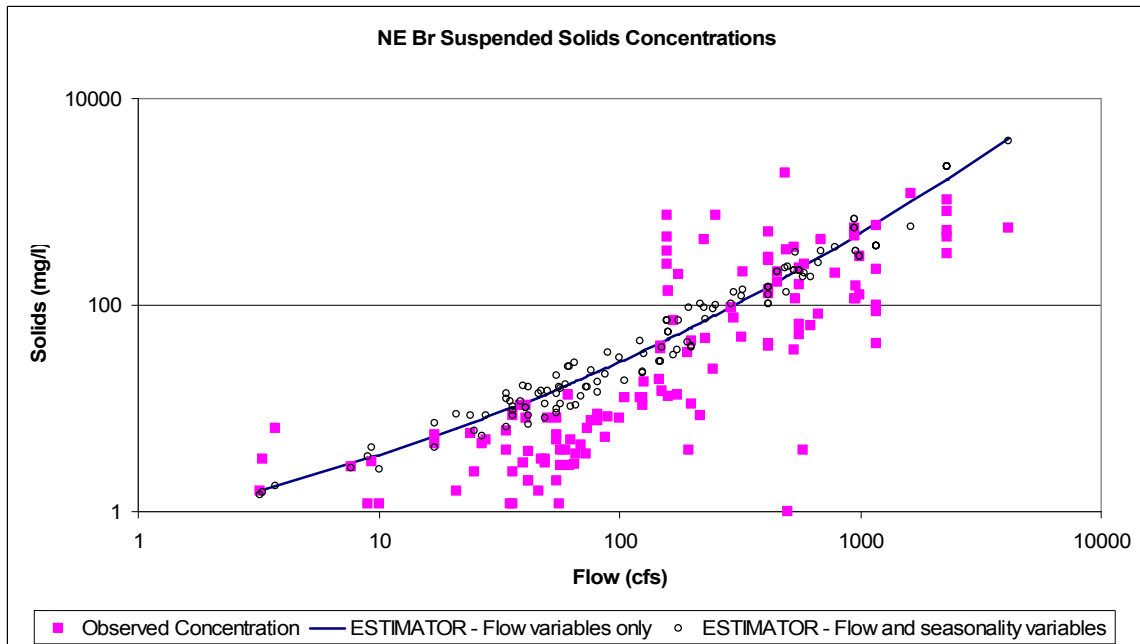


Figure A-6 Comparison of observations with ESTIMATOR predictions, Northeast Branch

Table 3. Northeast Branch Suspended Solids Data Use in ESTIMATOR Model

| LocationID | StudyID | SampleDate | SampleTime | Daily Flow Average (cfs) | Suspended Solids (mg/l) | Qualifier |
|------------|----------|------------|------------|--------------------------------|----------------------------|-----------|
| 01649500 | ICPRB/DC | 9/27/1995 | 10:00 AM | 36 | 8.5 | |
| 01649500 | ICPRB/DC | 11/7/1995 | 10:45 AM | 74 | 6.4 | |
| 01649500 | ICPRB/DC | 1/23/1996 | 10:15 AM | 105 | 12.8 | |
| 01649500 | ICPRB/DC | 3/19/1996 | 10:00 AM | 576 | 4 | |
| 01649500 | ICPRB/DC | 4/26/1996 | 3:00 PM | 50 | 8 | |
| 01649500 | ICPRB/DC | 11/14/1995 | 1:15 PM | 958 | 154 | |
| 01649500 | ICPRB/DC | 11/14/1995 | 7:30 PM | 958 | 114 | |
| 01649500 | ICPRB/DC | 11/15/1995 | 9:30 AM | 626 | 64 | |
| 01649500 | ICPRB/DC | 4/30/1996 | 12:45 PM | 160 | 13 | |
| 01649500 | ICPRB/DC | 4/30/1996 | 4:15 PM | 160 | 138 | |
| 01649500 | ICPRB/DC | 4/30/1996 | 7:30 PM | 160 | 136 | |
| 01649500 | ICPRB/DC | 7/13/1996 | 8:30 AM | 942 | 462 | |
| 01649500 | ICPRB/DC | 7/13/1996 | 11:15 AM | 942 | 468 | |
| 01649500 | ICPRB/DC | 7/12/1996 | 8:00 PM | 61 | 13.6 | |
| 01649500 | ICPRB/DC | 9/6/1996 | 1:00 PM | 949 | 552 | |
| 01649500 | ICPRB/DC | 9/6/1996 | 6:45 PM | 949 | 114 | |
| 01649500 | ICPRB/DC | 9/7/1996 | 11:15 AM | 250 | 740 | |
| 01649500 | MDE | 1/6/2003 | 11:20 AM | 125 | 12.8 | |
| 01649500 | MDE | 2/3/2003 | 10:35 AM | 42 | 3.8 | |
| 01649500 | MDE | 3/3/2003 | 11:15 AM | 192 | 34.7 | |
| 01649500 | MDE | 3/17/2003 | 10:55 AM | 73 | 3.6 | |
| 01649500 | MDE | 4/21/2003 | 10:15 AM | 56 | 2.4 | < |
| 01649500 | MDE | 5/5/2003 | 10:30 AM | 47 | 3.2 | |
| 01649500 | MDE | 5/19/2003 | 10:25 AM | 122 | 12.6 | |
| 01649500 | MDE | 6/2/2003 | 10:40 AM | 89 | 8.4 | |
| 01649500 | MDE | 6/16/2003 | 11:10 AM | 217 | 8.6 | |
| 01649500 | MDE | 7/7/2003 | 9:40 AM | 195 | 4.0 | |
| 01649500 | MDE | 7/21/2003 | 11:10 AM | 65 | 2.9 | |
| 01649500 | MDE | 8/4/2003 | 10:20 AM | 62 | 2.8 | |
| 01649500 | MDE | 8/18/2003 | 10:46 AM | 55 | 5.0 | |
| 01649500 | MDE | 9/8/2003 | 11:00 AM | 35 | 2.4 | < |
| 01649500 | MDE | 9/22/2003 | 12:35 PM | 76 | 7.6 | |
| 01649500 | MDE | 10/6/2003 | 10:25 AM | 36 | 2.4 | < |
| 01649500 | MDE | 10/20/2003 | 10:30 AM | 36 | 2.4 | |
| 01649500 | USGS/MDE | 7/23/2003 | 9:15 AM | 540 | 115 | |
| 01649500 | USGS/MDE | 8/19/2003 | 10:30 AM | 42 | 2.0 | |
| 01649500 | USGS/MDE | 9/24/2003 | 8:00 AM | 320 | 49 | |
| 01649500 | USGS/MDE | 10/28/2003 | 11:30 AM | 415 | 42 | |
| 01649500 | USGS/MDE | 11/18/2003 | 10:00 AM | 57 | 4.0 | |
| 01649500 | USGS/MDE | 12/11/2003 | 9:00 AM | 1620 | 1220 | |
| 01649500 | USGS/MDE | 12/16/2003 | 9:45 AM | 198 | 11 | |
| 01649500 | USGS/MDE | 1/13/2004 | 11:30 AM | 63 | 5.0 | |
| 01649500 | USGS/MDE | 2/6/2004 | 9:15 AM | 1170 | 43 | |
| 01649500 | USGS/MDE | 2/6/2004 | 9:45 AM | 1170 | 87 | |
| 01649500 | USGS/MDE | 2/6/2004 | 10:15 AM | 1170 | 101 | |
| 01649500 | USGS/MDE | 2/6/2004 | 11:45 AM | 1170 | 225 | |
| 01649500 | USGS/MDE | 2/6/2004 | 1:15 PM | 1170 | 591 | |

| LocationID | StudyID | SampleDate | SampleTime | Daily Flow Average (cfs) | Suspended Solids (mg/l) | Qualifier |
|------------|-------------|------------|------------|--------------------------------|----------------------------|-----------|
| 01649500 | USGS/MDE | 2/11/2004 | 10:30 AM | 146 | 19 | |
| 01649500 | USGS/MDE | 3/24/2004 | 9:30 AM | 49 | 3 | |
| 01649500 | USGS/MDE | 4/12/2004 | 1:45 PM | 416 | 131 | |
| 01649500 | USGS/MDE | 4/12/2004 | 3:45 PM | 416 | 139 | |
| 01649500 | USGS/MDE | 4/12/2004 | 5:45 PM | 416 | 291 | |
| 01649500 | USGS/MDE | 4/12/2004 | 7:45 PM | 416 | 285 | |
| 01649500 | USGS/MDE | 4/12/2004 | 11:45 PM | 416 | 508 | |
| 01649500 | USGS/MDE | 4/13/2004 | 3:45 AM | 557 | 228 | |
| 01649500 | USGS/MDE | 4/13/2004 | 8:00 AM | 557 | 158 | |
| 01649500 | USGS/MDE | 4/13/2004 | 4:15 PM | 557 | 52 | |
| 01649500 | USGS/MDE | 4/13/2004 | 8:15 PM | 557 | 66 | |
| 01649500 | USGS/MDE | 4/14/2004 | 12:15 AM | 228 | 48 | |
| 01649500 | USGS/MDE | 4/20/2004 | 9:00 AM | 60 | 4 | |
| 01649500 | USGS/MDE | 5/25/2004 | 10:00 AM | 34 | 4 | |
| 01649500 | USGS/MDE | 6/23/2004 | 8:45 AM | 34 | 6 | |
| 01649500 | USGS/MDE | 6/25/2004 | 4:30 PM | 158 | 249 | |
| 01649500 | USGS/MDE | 6/25/2004 | 5:30 PM | 158 | 732 | |
| 01649500 | USGS/MDE | 6/25/2004 | 6:30 PM | 158 | 452 | |
| 01649500 | USGS/MDE | 6/25/2004 | 7:30 PM | 158 | 331 | |
| 01649500 | USGS/MDE | 7/13/2004 | 8:30 AM | 40 | 3 | |
| 01649500 | USGS/MDE | 7/28/2004 | 10:45 AM | 2280 | 1050 | |
| 01649500 | USGS/MDE | 7/28/2004 | 11:15 AM | 2280 | 818 | |
| 01649500 | USGS/MDE | 7/28/2004 | 12:30 PM | 2280 | 532 | |
| 01649500 | USGS/MDE | 7/28/2004 | 1:00 PM | 2280 | 457 | |
| 01649500 | USGS/MDE | 7/28/2004 | 2:30 PM | 2280 | 311 | |
| 01649500 | USGS/MDE | 9/21/2004 | 1:00 PM | 28 | 5.0 | |
| 01649500 | USGS/MDE | 9/28/2004 | 1:15 PM | 783 | 202 | |
| 01649500 | USGS/MDE | 9/29/2004 | 9:45 AM | 291 | 94 | |
| 01649500 | ANS/DC | 6/24/2002 | 12:00 PM | 9.4 | 3.1 | |
| 01649500 | ANS/DC | 8/30/2002 | 12:00 PM | 24 | 5.7 | |
| 01649500 | ANS/DC | 8/28/2002 | 12:00 PM | 299 | 74.2 | |
| 01649500 | ANS/DC | 10/16/2002 | 12:00 PM | 674 | 81.4 | |
| 01649500 | ANS/DC | 10/17/2002 | 5:00 PM | 127 | 17.8 | |
| 01649500 | ANS/DC | 10/18/2002 | 8:30 AM | 41 | 10.8 | |
| 01649500 | ANS/DC | 10/18/2002 | 7:30 PM | 41 | 8.0 | |
| 01649500 | ANS/DC | 10/19/2002 | 9:00 AM | 25 | 2.4 | |
| 01649500 | ANS/DC | 10/21/2002 | 11:15 AM | 17 | 4.6 | |
| 01649500 | ANS/EPA | 2/25/1998 | 12:00 PM | 173 | 13.5 | |
| 01649500 | ANS/EPA | 4/30/1998 | 12:00 PM | 46 | 1.6 | |
| 01649500 | ANS/EPA | 5/4/1998 | 12:00 PM | 246 | 24 | |
| 01649500 | ANS/EPA | 7/14/1998 | 12:00 PM | 21 | 1.6 | |
| 01649500 | ANS/EPA | 7/24/1998 | 12:00 PM | 17 | 5.6 | |
| 01649500 | ANS/EPA | 9/16/1998 | 12:00 PM | 7.7 | 2.8 | |
| 01649500 | ANS/EPA | 9/23/1998 | 12:00 PM | 39 | 10.6 | |
| 01649500 | ANS/EPA | 10/19/1998 | 12:00 PM | 10 | 1.2 | |
| 01649500 | ANS/EPA | 11/12/1998 | 12:00 PM | 27 | 4.5 | |
| 01649500 | OWML/DCWASA | 8/5/1999 | 10:45 AM | 3.7 | 6.4 | |
| 01649500 | OWML/DCWASA | 8/12/1999 | 10:30 AM | 3.3 | 3.2 | |

| LocationID | StudyID | SampleDate | SampleTime | Daily Flow Average (cfs) | Suspended Solids (mg/l) | Qualifier |
|------------|-------------|------------|------------|--------------------------------|----------------------------|-----------|
| 01649500 | OWML/DCWASA | 8/19/1999 | 8:55 AM | 3.2 | 1.6 | |
| 01649500 | OWML/DCWASA | 8/26/1999 | 1:03 AM | 224 | 426 | |
| 01649500 | OWML/DCWASA | 8/27/1999 | 4:09 AM | 175 | 198 | |
| 01649500 | OWML/DCWASA | 9/2/1999 | 9:34 AM | 9 | 1.2 | |
| 01649500 | OWML/DCWASA | 9/5/1999 | 1:50 AM | 452 | 209 | |
| 01649500 | OWML/DCWASA | 9/5/1999 | 10:30 PM | 452 | 169 | |
| 01649500 | OWML/DCWASA | 9/7/1999 | 3:05 AM | 325 | 211 | |
| 01649500 | OWML/DCWASA | 9/10/1999 | 2:40 AM | 488 | 1930 | |
| 01649500 | OWML/DCWASA | 9/9/1999 | 1:00 PM | 502 | 1.0 | |
| 01649500 | OWML/DCWASA | 9/16/1999 | 9:54 PM | 4130 | 558 | |
| 01649500 | OWML/DCWASA | 9/17/1999 | 3:38 PM | 689 | 430 | |
| 01649500 | OWML/DCWASA | 9/23/1999 | 9:00 AM | 100 | 8.0 | |
| 01649500 | OWML/DCWASA | 9/30/1999 | 3:52 AM | 529 | 360 | |
| 01649500 | OWML/DCWASA | 9/30/1999 | 5:08 PM | 529 | 37 | |
| 01649500 | OWML/DCWASA | 10/7/1999 | 11:05 AM | 57 | 2.8 | |
| 01649500 | OWML/DCWASA | 10/14/1999 | 9:55 AM | 55 | 5.6 | |
| 01649500 | OWML/DCWASA | 10/21/1999 | 12:10 PM | 87 | 5.2 | |
| 01649500 | OWML/DCWASA | 11/3/1999 | 11:00 AM | 81 | 7.6 | |
| 01649500 | OWML/DCWASA | 11/16/1999 | 1:50 PM | 34 | 0.5 | |
| 01649500 | OWML/DCWASA | 11/27/1999 | 12:33 AM | 414 | 272 | |
| 01649500 | OWML/DCWASA | 11/27/1999 | 1:51 PM | 414 | 40 | |
| 01649500 | OWML/DCWASA | 12/1/1999 | 11:51 AM | 55 | 2.0 | |
| 01649500 | OWML/DCWASA | 12/6/1999 | 8:20 AM | 148 | 40 | |
| 01649500 | OWML/DCWASA | 12/6/1999 | 6:28 PM | 148 | 38 | |
| 01649500 | OWML/DCWASA | 12/10/1999 | 8:02 PM | 167 | 71 | |
| 01649500 | OWML/DCWASA | 12/14/1999 | 1:10 AM | 994 | 127 | |
| 01649500 | OWML/DCWASA | 12/14/1999 | 11:07 PM | 994 | 298 | |
| 01649500 | OWML/DCWASA | 12/16/1999 | 10:35 AM | 125 | 10.8 | |
| 01649500 | OWML/DCWASA | 12/28/1999 | 11:00 AM | 49 | 3.2 | |
| 01649500 | OWML/DCWASA | 1/13/2000 | 11:50 AM | 66 | 3.6 | |
| 01649500 | OWML/DCWASA | 1/27/2000 | 11:47 AM | 55 | 8.0 | |
| 01649500 | OWML/DCWASA | 2/9/2000 | 11:00 AM | 81 | 8.8 | |
| 01649500 | OWML/DCWASA | 2/11/2000 | 12:34 AM | 200 | 45 | |
| 01649500 | OWML/DCWASA | 2/23/2000 | 11:20 AM | 69 | 4.4 | |
| 01649500 | OWML/DCWASA | 2/28/2000 | 9:15 AM | 496 | 338 | |
| 01649500 | OWML/DCWASA | 3/8/2000 | 12:05 PM | 42 | 2.0 | |
| 01649500 | OWML/DCWASA | 3/28/2000 | 1:55 AM | 588 | 250 | |
| 01649500 | OWML/DCWASA | 3/29/2000 | 11:38 AM | 150 | 14.8 | |

Table 4. Northwest Branch Suspended Solids Data Used in ESTIMATOR

| LocationID | StudyID | SampleDate | SampleTime | Daily Flow Average (cfs) | Suspended Solids (mg/l) | Qualifier |
|------------|----------|------------|------------|-----------------------------------|----------------------------|-----------|
| 01651000 | ICPRB/DC | 9/27/1995 | 11:30 AM | 20 | 5 | |
| 01651000 | ICPRB/DC | 11/7/1995 | 11:45 AM | 57 | 3.4 | |
| 01651000 | ICPRB/DC | 1/23/1996 | 11:45 AM | 55 | 5.2 | |
| 01651000 | ICPRB/DC | 3/19/1996 | 11:00 AM | 391 | 3.2 | |
| 01651000 | ICPRB/DC | 4/26/1996 | 1:30 PM | 44 | 6.7 | |
| 01651000 | ICPRB/DC | 11/14/1995 | 12:30 PM | 518 | 176 | |
| 01651000 | ICPRB/DC | 11/14/1995 | 8:00 PM | 518 | 92 | |
| 01651000 | ICPRB/DC | 11/15/1995 | 10:15 AM | 300 | 72 | |
| 01651000 | ICPRB/DC | 4/30/1996 | 12:00 PM | 135 | 6 | |
| 01651000 | ICPRB/DC | 4/30/1996 | 5:00 PM | 135 | 186 | |
| 01651000 | ICPRB/DC | 4/30/1996 | 6:40 PM | 135 | 128 | |
| 01651000 | ICPRB/DC | 7/13/1996 | 9:20 AM | 467 | 694 | |
| 01651000 | ICPRB/DC | 7/13/1996 | 12:00 PM | 467 | 780 | |
| 01651000 | ICPRB/DC | 7/12/1996 | 9:00 PM | 42 | 16.4 | |
| 01651000 | ICPRB/DC | 9/6/1996 | 2:00 PM | 1170 | 494 | |
| 01651000 | ICPRB/DC | 9/6/1996 | 7:45 PM | 1170 | 276 | |
| 01651000 | ICPRB/DC | 9/7/1996 | 12:00 PM | 471 | 380 | |
| 01651000 | MDE | 1/6/2003 | 10:00 AM | 72 | 7 | |
| 01651000 | MDE | 1/21/2003 | 10:50 AM | 29 | 27 | |
| 01651000 | MDE | 2/3/2003 | 10:20 AM | 22 | 4 | |
| 01651000 | MDE | 3/3/2003 | 10:40 AM | 182 | 50 | |
| 01651000 | MDE | 3/17/2003 | 10:20 AM | 46 | 3.6 | |
| 01651000 | MDE | 4/21/2003 | 9:50 AM | 36 | 2.5 | |
| 01651000 | MDE | 5/5/2003 | 10:15 AM | 38 | 3.2 | |
| 01651000 | MDE | 5/19/2003 | 10:00 AM | 71 | 6.6 | |
| 01651000 | MDE | 6/2/2003 | 10:10 AM | 52 | 4.6 | |
| 01651000 | MDE | 6/16/2003 | 10:45 AM | 60 | 6.6 | |
| 01651000 | MDE | 7/7/2003 | 9:20 AM | 113 | 30 | |
| 01651000 | MDE | 7/21/2003 | 10:50 AM | 27 | 2.4 | < |
| 01651000 | MDE | 8/4/2003 | 10:05 AM | 39 | 3.8 | |
| 01651000 | MDE | 8/18/2003 | 10:10 AM | 34 | 7.5 | |
| 01651000 | MDE | 9/8/2003 | 10:45 AM | 22 | 4.6 | |
| 01651000 | MDE | 9/22/2003 | 11:45 AM | 37 | 4.8 | |
| 01651000 | MDE | 10/6/2003 | 10:45 AM | 27 | 2.4 | < |
| 01651000 | MDE | 10/20/2003 | 9:45 AM | 26 | 2.4 | < |
| 01651000 | USGS/MDE | 7/23/2003 | 12:00 PM | 272 | 77 | |
| 01651000 | USGS/MDE | 8/19/2003 | 9:00 AM | 26 | 4 | |
| 01651000 | USGS/MDE | 9/24/2003 | 10:30 AM | 125 | 31 | |
| 01651000 | USGS/MDE | 10/29/2003 | 12:15 PM | 472 | 538 | |
| 01651000 | USGS/MDE | 11/18/2003 | 1:15 PM | 38 | 4 | |
| 01651000 | USGS/MDE | 12/11/2003 | 1:00 PM | 1570 | 906 | |
| 01651000 | USGS/MDE | 12/16/2003 | 12:15 PM | 109 | 8 | |
| 01651000 | USGS/MDE | 1/13/2004 | 9:15 AM | 45 | 4 | |
| 01651000 | USGS/MDE | 2/6/2004 | 12:45 PM | 967 | 648 | |
| 01651000 | USGS/MDE | 2/6/2004 | 1:45 PM | 967 | 564 | |
| 01651000 | USGS/MDE | 2/6/2004 | 2:45 PM | 967 | 596 | |

| LocationID | StudyID | SampleDate | SampleTime | Daily Flow Average (cfs) | Suspended Solids (mg/l) | Qualifier |
|------------|----------|------------|------------|-----------------------------------|----------------------------|-----------|
| 01651000 | USGS/MDE | 2/6/2004 | 7:45 PM | 967 | 713 | |
| 01651000 | USGS/MDE | 2/6/2004 | 11:45 PM | 967 | 504 | |
| 01651000 | USGS/MDE | 2/11/2004 | 1:15 PM | 86 | 29 | |
| 01651000 | USGS/MDE | 3/23/2004 | 10:45 AM | 35 | 2 | |
| 01651000 | USGS/MDE | 4/12/2004 | 2:45 PM | 229 | 141 | |
| 01651000 | USGS/MDE | 4/12/2004 | 5:45 PM | 229 | 149 | |
| 01651000 | USGS/MDE | 4/12/2004 | 8:45 PM | 229 | 144 | |
| 01651000 | USGS/MDE | 4/12/2004 | 11:45 PM | 229 | 367 | |
| 01651000 | USGS/MDE | 4/13/2004 | 5:45 AM | 310 | 416 | |
| 01651000 | USGS/MDE | 4/13/2004 | 9:30 AM | 310 | 378 | |
| 01651000 | USGS/MDE | 4/21/2004 | 8:45 AM | 43 | 3 | |
| 01651000 | USGS/MDE | 5/26/2004 | 8:45 AM | 43 | 64 | |
| 01651000 | USGS/MDE | 6/22/2004 | 8:15 AM | 25 | 8 | |
| 01651000 | USGS/MDE | 7/1/2004 | 6:00 PM | 110 | 19 | |
| 01651000 | USGS/MDE | 7/1/2004 | 7:00 PM | 110 | 1340 | |
| 01651000 | USGS/MDE | 7/1/2004 | 8:00 PM | 110 | 1270 | |
| 01651000 | USGS/MDE | 7/1/2004 | 9:00 PM | 110 | 868 | |
| 01651000 | USGS/MDE | 7/2/2004 | 1:00 AM | 43 | 178 | |
| 01651000 | USGS/MDE | 7/2/2004 | 5:00 AM | 43 | 64 | |
| 01651000 | USGS/MDE | 7/14/2004 | 9:45 AM | 28 | 7 | |
| 01651000 | USGS/MDE | 7/28/2004 | 12:00 PM | 899 | 953 | |
| 01651000 | USGS/MDE | 7/28/2004 | 12:15 PM | 899 | 967 | |
| 01651000 | USGS/MDE | 7/28/2004 | 12:30 PM | 899 | 982 | |
| 01651000 | USGS/MDE | 7/28/2004 | 12:45 PM | 899 | 962 | |
| 01651000 | USGS/MDE | 7/28/2004 | 2:45 PM | 899 | 576 | |
| 01651000 | USGS/MDE | 7/28/2004 | 4:45 PM | 899 | 514 | |
| 01651000 | USGS/MDE | 9/22/2004 | 12:30 PM | 13 | 4 | |
| 01651000 | USGS/MDE | 9/28/2004 | 1:00 PM | 375 | 155 | |
| 01651000 | USGS/MDE | 9/29/2004 | 9:00 AM | 75 | 55 | |
| 01651000 | ANS/DC | 6/24/2002 | 12:00 PM | 5.8 | 4.1 | |
| 01651000 | ANS/DC | 8/30/2002 | 12:00 PM | 16 | 6.7 | |
| 01651000 | ANS/DC | 8/28/2002 | 12:00 PM | 244 | 65.6 | |
| 01651000 | ANS/DC | 10/16/2002 | 12:00 PM | 401 | 86.4 | |
| 01651000 | ANS/DC | 10/17/2002 | 5:30 PM | 77 | 28.4 | |
| 01651000 | ANS/DC | 10/18/2002 | 8:30 AM | 25 | 16.8 | |
| 01651000 | ANS/DC | 10/18/2002 | 6:30 PM | 25 | 16 | |
| 01651000 | ANS/DC | 10/19/2002 | 8:00 AM | 14 | 11 | |
| 01651000 | ANS/DC | 10/20/2002 | 9:00 AM | 10 | 13.8 | |
| 01651000 | ANS/DC | 10/21/2002 | 10:30 AM | 9.5 | 3 | |
| 01651000 | ANS/EPA | 2/25/1998 | 12:00 PM | 95 | 9 | |
| 01651000 | ANS/EPA | 4/30/1998 | 12:00 PM | 31 | 0.8 | |
| 01651000 | ANS/EPA | 5/4/1998 | 12:00 PM | 137 | 13 | |
| 01651000 | ANS/EPA | 7/14/1998 | 12:00 PM | 15 | 5.4 | |
| 01651000 | ANS/EPA | 7/24/1998 | 12:00 PM | 13 | 8.2 | |
| 01651000 | ANS/EPA | 9/16/1998 | 12:00 PM | 3 | 2 | |
| 01651000 | ANS/EPA | 9/23/1998 | 12:00 PM | 15 | 3.4 | |
| 01651000 | ANS/EPA | 10/19/1998 | 12:00 PM | 8 | 2.7 | |

| LocationID | StudyID | SampleDate | SampleTime | Daily Flow Average (cfs) | Suspended Solids (mg/l) | Qualifier |
|------------|-------------|------------|------------|-----------------------------------|----------------------------|-----------|
| 01651000 | ANS/EPA | 11/12/1998 | 12:00 PM | 20 | 4.4 | |
| 01651000 | OWML/DCWASA | 8/5/1999 | 12:19 PM | 1.5 | 2 | |
| 01651000 | OWML/DCWASA | 8/12/1999 | 11:48 AM | 1.5 | 2.4 | |
| 01651000 | OWML/DCWASA | 8/19/1999 | 9:44 AM | 2 | 2 | |
| 01651000 | OWML/DCWASA | 8/25/1999 | 9:45 PM | 230 | 238 | |
| 01651000 | OWML/DCWASA | 9/2/1999 | 10:19 AM | 3.3 | 1.6 | |
| 01651000 | OWML/DCWASA | 9/5/1999 | 2:25 AM | 397 | 185 | |
| 01651000 | OWML/DCWASA | 9/5/1999 | 11:20 PM | 397 | 218 | |
| 01651000 | OWML/DCWASA | 9/7/1999 | 2:40 AM | 253 | 272 | |
| 01651000 | OWML/DCWASA | 9/10/1999 | 2:45 AM | 245 | 517 | |
| 01651000 | OWML/DCWASA | 9/9/1999 | 12:20 PM | 298 | 4.8 | |
| 01651000 | OWML/DCWASA | 9/16/1999 | 10:35 AM | 1880 | 318 | |
| 01651000 | OWML/DCWASA | 9/16/1999 | 9:37 PM | 1880 | 478 | |
| 01651000 | OWML/DCWASA | 9/21/1999 | 7:27 PM | 264 | 168 | |
| 01651000 | OWML/DCWASA | 9/23/1999 | 9:46 AM | 38 | 4.4 | |
| 01651000 | OWML/DCWASA | 9/30/1999 | 3:55 AM | 340 | 300 | |
| 01651000 | OWML/DCWASA | 9/30/1999 | 4:02 PM | 340 | 268 | |
| 01651000 | OWML/DCWASA | 10/7/1999 | 11:40 AM | 26 | 3.6 | |
| 01651000 | OWML/DCWASA | 10/14/1999 | 9:25 AM | 21 | 2 | |
| 01651000 | OWML/DCWASA | 10/21/1999 | 1:00 PM | 35 | 2.8 | |
| 01651000 | OWML/DCWASA | 11/3/1999 | 11:50 AM | 31 | 2.4 | |
| 01651000 | OWML/DCWASA | 11/16/1999 | 2:30 PM | 14 | 0.5 | |
| 01651000 | OWML/DCWASA | 11/27/1999 | 12:44 AM | 282 | 257 | |
| 01651000 | OWML/DCWASA | 11/27/1999 | 3:54 PM | 282 | 72 | |
| 01651000 | OWML/DCWASA | 12/1/1999 | 11:25 AM | 19 | 2 | |
| 01651000 | OWML/DCWASA | 12/6/1999 | 3:26 PM | 97 | 27 | |
| 01651000 | OWML/DCWASA | 12/10/1999 | 11:26 PM | 98 | 39 | |
| 01651000 | OWML/DCWASA | 12/14/1999 | 12:12 AM | 504 | 68 | |
| 01651000 | OWML/DCWASA | 12/14/1999 | 11:11 PM | 504 | 221 | |
| 01651000 | OWML/DCWASA | 12/16/1999 | 11:30 AM | 52 | 4.4 | |
| 01651000 | OWML/DCWASA | 12/28/1999 | 11:40 AM | 24 | 0.5 | |
| 01651000 | OWML/DCWASA | 1/13/2000 | 12:20 PM | 29 | 0.5 | |
| 01651000 | OWML/DCWASA | 1/27/2000 | 11:02 AM | 22 | 5.2 | |
| 01651000 | OWML/DCWASA | 2/9/2000 | 10:22 AM | 43 | 2.4 | |
| 01651000 | OWML/DCWASA | 2/23/2000 | 11:50 AM | 43 | 1.2 | |
| 01651000 | OWML/DCWASA | 2/28/2000 | 10:52 AM | 325 | 326 | |
| 01651000 | OWML/DCWASA | 3/8/2000 | 11:41 AM | 36 | 2.4 | |
| 01651000 | OWML/DCWASA | 3/28/2000 | 2:10 AM | 168 | 109 | |
| 01651000 | OWML/DCWASA | 3/29/2000 | 10:42 AM | 67 | 5.2 | |

REFERENCES

- Cohn, T., L.L. DeLong, E.J. Gilroy, R.M. Hirsch, and D.K. Wells. 1989. Estimating Constituent Loads. *Water Resources Research*, 25(5): 937-942.
- Cohn, T., D.L. Caulder, E.J. Gilroy, L.D. Zynjuk, and R.M. Summers. 1992. The Validity of a Simple Statistical Model for Estimating Fluvial Constituent Loads: An Empirical Study Involving Nutrient Loads Entering Chesapeake Bay. *Water Resources Research*, 28(9): 2353-2364.
- Gray, J.R., G.D. Glysson, L.M. Turcios, G.E. Schwartz. 2000. Comparability of suspended-sediment concentration and total suspended solids data. WRIR 00-4191. U.S. Geological Survey, Reston, VA, August 2000.
- Gruessner, B., D.J. Velinsky, G.D. Foster, J. Scudlark, R. Mason. 1998. Dissolved and Particulate Transport of Chemical Contaminants in the Northeast and Northwest Branches of the Anacostia River. Revised April 1998. Interstate Commission on the Potomac River Basin Report 97-10. ICPRB, Rockville, MD.
- MWCOG. 2001. Technical Memorandum LTCP 6-2d: District of Columbia CSO Long Term Control Plan Upstream Boundary Conditions. Prepared for the District of Columbia Water and Sewer Authority by the Metropolitan Washington Council of Governments and the Occoquan Watershed Monitoring Laboratory, September 2001.
- Velinsky, D.J., G.F. Riedel and G.Foster. 1999. Effects of Stormwater Runoff on the Water Quality of the Tidal Anacostia River. PCER Report #99-6. Submitted to U.S. EPA Region III. The Academy of Natural Sciences, Patrick Center for Environmental Research, Philadelphia, PA.

